Universidad de Santiago de Compostela
Facultad de Medicina y Odontología
Departamento de Bioquímica y Biología Molecular

Neurotoxicity Induced by Oxidative Stress and Aluminium in Relation to Parkinson's Disease: A Mitochondrial Bioenergetic Approach by High-Resolution Respirometry

Neurotoxicidad Inducida por Estrés Oxidativo y Aluminio en Relación con la Enfermedad de Parkinson: Un estudio de la Bioenergética Mitocondrial por Respirometría de Alta Resolución

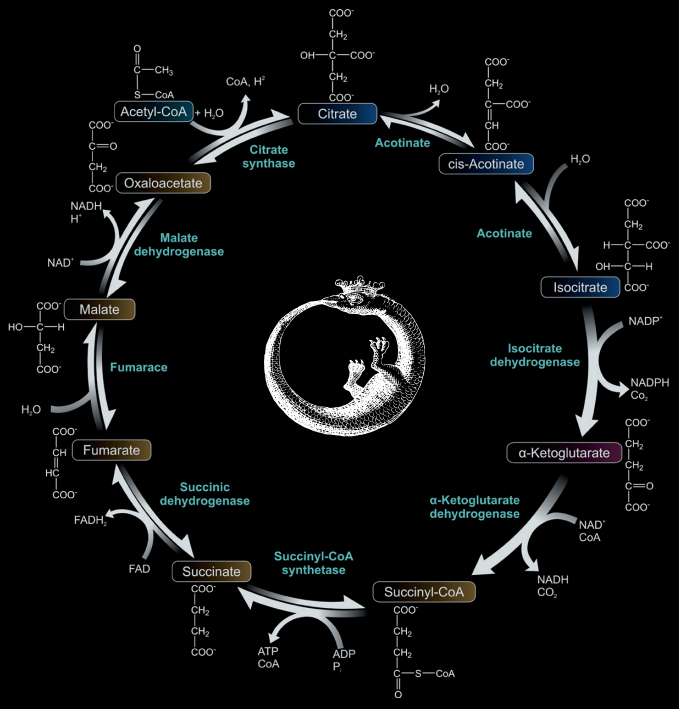

Tesis Doctoral

Javier Iglesias González

2014

USC
UNIVERSIDADE
DE SANTIAGO
DE COMPOSTELA

Universidad de Santiago de Compostela
Facultad de Medicina
Departamento de Bioquímica y Biología Molecular

Neurotoxicity Induced by Oxidative Stress and Aluminium in Relation to Parkinson's Disease: A Mitochondrial Bioenergetic Approach by High-Resolution Respirometry

Tesis doctoral

Javier Iglesias González

2014

USC
UNIVERSIDADE
DE SANTIAGO
DE COMPOSTELA

Neurotoxicity Induced by Oxidative Stress and Aluminium in Relation to Parkinson's Disease: A Mitochondrial Bioenergetic Approach by High-Resolution Respirometry

Tesis doctoral presentada por
Javier Iglesias González

Directores:
Ramón Soto Otero
Catedrático de Bioquímica

Estefanía María Salomé Méndez Álvarez
Catedrática de Bioquímica

Departamento de Bioquímica y Biología Molecular
Facultad de Medicina
Universidad de Santiago de Compostela

Santiago de Compostela, 2014

USC
UNIVERSIDADE
DE SANTIAGO
DE COMPOSTELA

D. Ramón Soto Otero, Catedrático de Bioquímica de la Facultad de Medicina de la Universidad de Santiago de Compostela y ***Dña. Estefanía María Salomé Méndez Álvarez***, Catedrática de Bioquímica de la Universidad de Santiago de Compostela,

INFORMAN,

Que la presente memoria titulada: "***Neurotoxicity Induced by Oxidative Stress and Aluminium in Relation to Parkinson's disease: A Mitochondrial Bioenergetic Approach by High-Resolution Respirometry***", presentada por **D. Javier Iglesias González** para optar al grado de Doctor en Biología, ha sido realizada bajo nuestra dirección, y considerando que constituye trabajo de Tesis y reúne todas las condiciones necesarias para ser presentada para su valoración por el tribunal correspondiente, autorizamos su presentación al Consejo del Departamento de Bioquímica y Biología Molecular de la Universidad de Santiago de Compostela.

Y para que así conste y surta los efectos oportunos, firmamos el presente informe en Santiago de Compostela a 15 de Mayo de 2014.

Ramón Soto Otero
Catedrático
Dpto. Bioquímica y Biología Molecular

Estefanía M.S. Méndez Álvarez
Catedrática
Dpto. Bioquímica y Biología Molecular

El Doctorando

Javier Iglesias González

USC
UNIVERSIDADE
DE SANTIAGO
DE COMPOSTELA

A mi familia y a María

USC
UNIVERSIDADE
DE SANTIAGO
DE COMPOSTELA

Agradecimientos

El trabajo en un laboratorio nos abre las puertas al cosmos de lo desconocido. Cuando realizamos un experimento, cuando nos asomamos a una hipótesis y comprobamos su validez, ese es el instante en el que uno debe abrir los ojos con curiosidad. En esos momentos somos uno de los primeros privilegiados en ver procesos que nadie antes ha descrito ¿Os habéis parado a pensar en ello? Los primeros seres humanos en ver el mecanismo oculto hasta el momento. Da vértigo. Sin embargo, hacer ciencia en este país es una actividad que exige el mayor de los esfuerzos y sacrificios. Un camino que, sin el apoyo preciso, es imposible que nadie lo recorra. Han sido años difíciles que han implicado un master y dos años en otro laboratorio para conseguir la financiación necesaria para sobrevivir en el día a día. Se que muchos os preguntabais si esto acabaría algún día pero, como todo, ha llegado el momento de poner el punto final. Es por ello que quiero agradecer a todo el mundo su enorme cariño y apoyo durante este tiempo. Si, me detendré en algunos de vosotros, pero por si acaso no os encontráis en estas líneas sentíos representados en este sincero agradecimiento.

En primer lugar a ti, María, mi compañera de viaje, amiga y pareja. Sin tu ayuda todo esto habría sido imposible. Sin tus consejos, tu apoyo, tu cariño, tu comprensión… ¿Cuántas decisiones hemos tomado en todo este tiempo? Cuantos números, esfuerzos y requiebros para sacar adelante ambas carreras científicas. El camino juntos comenzó en Madrid durante la carrera, pero hemos forjado una vida a partir de ahí en la que buscamos ahondar en el mundo de la ciencia. Que gran pasión compartida, que fortuna el disfrutarla juntos. Lo hemos hablado cientos de veces, pertenecer ambos a este mundo nos ha ayudado a apoyarnos el uno en el otro. A comprendernos. Admiro tu gran perseverancia, alegría, tesón e inteligencia. Nuestro proyecto juntos es un reflejo de lo complicado que es este mundo, de cómo nos obliga a migrar de uno a otro sitio para encontrar un lugar en el que desempeñar nuestra pasión que es la ciencia. Gracias por tu valentía y fuerza durante todo este tiempo, el tiempo hará justicia a nuestro esfuerzo. Gracias y mil veces gracias, nunca seré capaz de devolverte todo lo que me has dado durante estos años. Te quiero.

En segundo lugar a mi familia, mis padres y hermana. Qué puedo decir, no encuentro las palabras adecuadas para expresar mi enorme gratitud por todo lo que habéis hecho por mí durante tantos años. Desde la infancia hasta el presente, siempre habéis estado a mi lado. Aún recuerdo mis quejas y protestas por ir a las clases de inglés. Las muchas veces que os habéis sentado junto a mí y me habéis

contado cosas que me hacían soñar con lo desconocido, con lo oculto en el conocimiento, con la diversión que reside en el aprendizaje. La elección de mi carrera y el esfuerzo hecho en conjunto. Mi traslado a Santiago y vuestro apoyo en todo el proyecto. Gracias por todas vuestras visitas y apoyo durante este tiempo. Sin vosotros, el recorrido de este camino académico no habría sido lo mismo. Es más, probablemente no habría sido. Lo logramos, porque esta Tesis es también en parte vuestra. Espero ser digno de que os sintáis orgullosos por todos los logros alcanzados. Os quiero. A mi hermana Alicia, por todos sus comentarios irónicos y divertidos. Porque siempre que estoy con ella me hace disfrutar al máximo del tiempo y pasarlo tan bien que nunca quiero que acaben sus visitas. Siempre hemos tenido una relación especial, gracias por todo tu cariño durante este tiempo, siempre me tendrás para lo que necesites. Y por último, quisiera recordar a mi abuelo. A aquellos días en los que me mostraba muestras al microscopio y me enseñaba sobre patología. Siempre te echaré de menos.

A mi familia política. Es un placer contar también con vosotros en mi vida. Por todas las veces que te has preocupado por mi Tesis y que me has preguntado con sincero cariño por ella, gracias Ana. Y también a Pachi, David, Vero, James y Marta por vuestra compañía y amistad. Y como no, al pequeño de la familia. A ese duende, Ethan, que se ha colado hace pocos años en nuestras vidas. Gracias por haberme dado vuestro cariño durante todo este tiempo.

Volviendo al punto en el que elegí hacer el doctorado quiero agradecer a mis directores, el Prof. Ramón Soto y la Profa. Estefanía Méndez, la oportunidad que me dieron de entrar a trabajar en su grupo de investigación. Muchas gracias por las incontables horas de trabajo, charlas, consejos y esfuerzos compartidos ¿Cuántas veces nos hemos sentado a discutir una misma idea? Ha sido un esfuerzo titánico y habéis estado a mi lado para recorrerlo, os estoy profundamente agradecido por ello. Y hablando del mundo profesional no puedo dejar de recordar los buenos años trabajando contigo, Sofía. Ha sido un verdadero privilegio tenerte a mi lado durante parte del viaje, siempre tendrás en mí a un amigo. ¿Te acuerdas de mi primer día de laboratorio? Tuvimos un eclipse de sol y todo. También quiero recordar a todos aquellos que han compartido conmigo parte del tiempo transcurrido como Alicia, Alba y Antón. Os deseo mucha suerte en vuestros proyectos. Al mismo tiempo no puedo evitar recordar la estancia realizada en el King's College, supervisada por el Prof. Peter Jenner y la Profa. Sara Salvage. Fue una gran oportunidad que me abrierais las puertas de vuestro laboratorio y que me permitierais trabajar con grandes compañeros como Atsuko Hikima, Sarah, John, Mammouth, Susana, Kayhan, Peter… También me gustaría recordar a una persona

que decidió apostar por mí pero cuyo nombre siempre he desconocido. Al presidente del tribunal de la beca LaCaixa, que me dio su apoyo y palabras de aliento para que perseverara en la ciencia y que acabara mi doctorado tras el Máster. Una persona que empatizó conmigo al 100% y me ayudó en la concesión de la beca LaCaixa. Muchísimas gracias por creer en mí. Por supuesto a la Obra Social LaCaixa también, la única entidad que ha decidido financiar parte de este trabajo. Por último, al Prof. Labandeira, por darme la oportunidad de trabajar en su equipo y estudiar nuevos campos apasionantes.

A mis amigos, Juan y María ¿Cómo hacéis para ser tan buenos amigos? Creo que habéis sido uno de los mejores descubrimientos en este recorrido. Lo hemos pasado en grande durante todo este tiempo y espero que, aunque nuestros trabajos nos lleven por mil sitios distintos sigamos encontrándonos como hasta ahora. La verdad es que es complicado encontrar amigos tan afines, vosotros sois unos de los mejores. Os llevaré conmigo allí donde vaya. Genji también. A mi amiga Esther que ahora se encuentra lejos en Austria pero que siempre fue un apoyo en Santiago. Se te echa de menos en nuestras vidas. A Mario, que tío más genial eres. Muchísimas gracias por tu ayuda en las portadillas de la tesis, como ves no te he hecho justicia con la portada. Es una alegría tenerte como amigo, cuantas veces nos hemos reído juntos, lo seguiremos haciendo en el futuro. A Jorge, otro grandísimo amigo. Que buenos viajes Roma, que tardes mas magníficas. A Álvaro y Belén (¡A la peque/s también!), mis buenos amigos desde la carrera. Y para finalizar a todos aquellos que he conocido en esta vieja y magnífica ciudad que es Santiago de Compostela. A José por sus charlas y cafés. A Iago, Dani, Toni, José y María, que momentos más geniales hemos compartido, espero que nuestra amistad no tenga fin. Gracias por todo vuestro apoyo durante estos largos y difíciles últimos meses, en los que sin vuestra amistad no habría conservado la cordura ¿Nos tomamos un café? A todos mis compañeros de la SCEA: Andrés, Laura, Laksmy, Denis, Manuel, Miguel… A todos mis compañeros de esgrima deportiva, en especial a Santi y a Pi. A todos aquellos que he conocido en esta ciudad, que sois incontables. A mis amigos y conocidos de Comunidad Umbría. En especial a Blag, Unanada, Akin, Chemo, Khalos, Xoel y al pequeño Andrés. Siempre es una alegría veros y compartir una cerveza con vosotros. Cómo no recordar a mis compañeros y amigos del Máster de Neurociencia: Dudi, Blanca, Cris, Tati, Dani, Toño… sois simplemente geniales.

Y por último, a todos aquellos que he conocido durante los congresos y con los que he tenido el privilegio de compartir ideas. En especial recordar los últimos días en Bath con el Prof. Juan Pedro Bolaños, la Prof. Mª Ángeles Almeida y vuestro equipo de investigación, fue un placer conoceros.

USC
UNIVERSIDADE
DE SANTIAGO
DE COMPOSTELA

Contents

Publicaciones y colaboraciones realizadas durante el desarrollo de la presente Tesis

1. Iglesias-González, J.; Sánchez-Iglesias, S.; Beiras-Iglesias, A.; Méndez-Álvarez, E.; Soto-Otero, R.; "Effects caused by aluminium on rat brain mitochondria bioenergetics: an *in vitro* and *in vivo* study", *In Review*.
2. Iglesias-González, J.; Sánchez-Iglesias, S.; Beiras-Iglesias, A.; Soto-Otero, R.; Méndez-Álvarez, E.; "A simple method for isolating rat brain mitochondria with high metabolic activity: effects of EDTA and EGTA". *Journal of Neuroscience Methods*, **213:** 39-42. DOI: 10.1016/j.jneumeth.2012.12.005. 2013.
3. Iglesias-González, J.; Sánchez-Iglesias, S.; Méndez-Álvarez, E.; Rose, S.; Hikima, A.; Jenner, P.; Soto-Otero, R.; "Differential toxicity of 6-hydroxydopamine in SH-SY5Y human neuroblastoma cells and rat brain mitochondria: protective role of catalase and superoxide dismutase". *Neurochemistry International*, **37(10):** 2150-60. 2012.
4. Sofía Sánchez-Iglesias; Estefanía Méndez-Álvarez; Javier Iglesias-González; Ana Muñoz-Patiño, Inés Sánchez-Sellero; José Luis Labandeira-García; Ramón Soto-Otero; "Brain oxidative stress and selective behaviour of aluminium in specific areas of rat brain: potential effects in a 6-OHDA-induced model of Parkinson's disease". *Journal of Neurochemistry*, **109:** 879-888. 2009.
5. Sánchez-Iglesias, S.; Soto-Otero, R.; Iglesias-González, J.; Barciela-Alonso, M.C.; Bermejo-Barrera, M.; Méndez-Álvarez, E.; "Analysis of brain regional distribution of aluminium in rats via oral and intraperitoneal administration". *Journal of Trace Elements in Medicine and Biology*, **21 (S1):** 31-34, 2007.

USC
UNIVERSIDADE
DE SANTIAGO
DE COMPOSTELA

Chapter 1

Introduction

USC
UNIVERSIDADE
DE SANTIAGO
DE COMPOSTELA

1.1 Parkinson's disease

Parkinson's disease (PD) was described in 1817 by James Parkinson (Fig. 1.1) as a shaking palsy with cardinal symptoms such as rigidity, postural instability, bradykinesia, and tremor (Parkinson, 1817). The characteristic hallmarks of the disease are a progressive degeneration of dopaminergic neurons in *substantia nigra pars compacta* (SN*pc*) and the appearance of protein inclusions denominated Lewy bodies (LBs). As consequence of the neuronal death, the *striatum* presents a considerable deficit of dopamine that triggers the motor symptoms of PD. Additionally, the onset and progression of the cardinal motor symptoms is unpredictable making the early detection of the disease very difficult. PD has been studied during the last two centuries, but the mechanism that triggers the disease still remains unclear. For this reason, the diagnosis of the syndrome is usually delayed several years after the onset of the disease (Gaig & Tolosa, 2009). Commonly, the tremor shows up when the

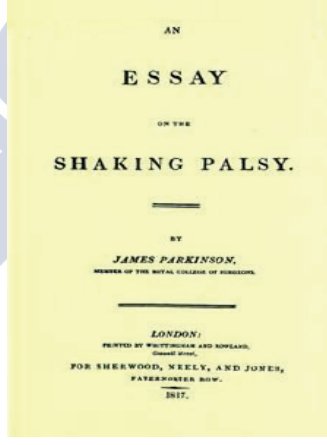
AN

ESSAY

ON THE

SHAKING PALSY.

BY

JAMES PARKINSON,

LONDON:

FOR SHERWOOD, NEELY, AND JONES,

1817.

Fig. 1.1 First publication about PD by James Parkinson in 1817.

patients are not developing voluntary movements, presenting a characteristic frequency of 4-6 Hz that involves arms, legs, jaw and head. Epidemiologically, the rate of prevalence for PD is estimated in 8-18 for each 100,000 people per year, affecting more than 1% of population over 60's and a 4% of population over 80's (De Lau & Breteler, 2006; Gaig & Tolosa, 2009). This rate of prevalence makes PD into the second neuro-degenerative disorder after Alzheimer's disease.

1.1.1 Dopaminergic system

The most altered neurochemical pathway in PD is the dopaminergic and, in less magnitude, other catecholaminergic systems. Dopamine is a catecholaminergic neurotransmitter synthesized from L-tyrosine by the enzymes tyrosine hydroxylase (TH) and DOPA descarboxylase (Fig. 1.2). The allosteric enzyme in the synthesis of

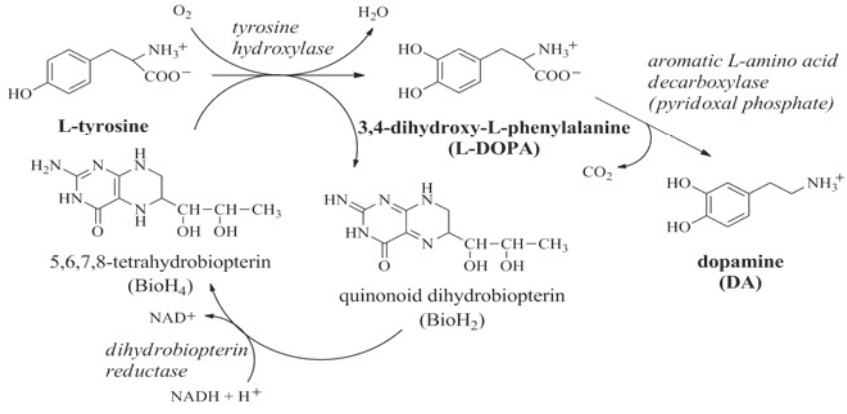

Fig. 1.2 Biosynthesis of dopamine from L-tyrosine (Méndez-Álvarez & Soto-Otero, 2004).

the catecholamines (i.e. dopamine, noradrenaline, and adrenaline) is the TH, being the initial and rate-limiting step of the reaction. TH is modulated by phosphorylation of the N-terminal sites, at transcriptional and post-translational levels, and with the local concentration of the catecholamine itself (Brady *et al.*, 2012).

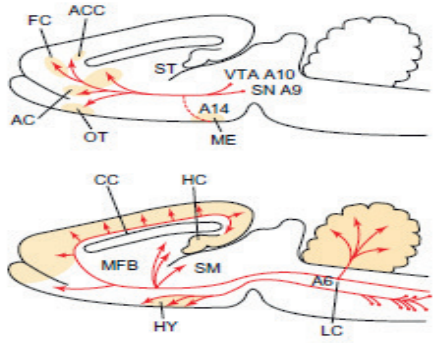

Fig. 1.3 Catecholaminergic neuronal pathways in the rat brain (Brady *et al.*, 2012).

In mammals, brain dopaminergic neurons are mainly found in midbrain (i.e. groups A8 to A10), diencephalon, olfactory bulb and retina (Fig. 1.3) (Brady *et al.*, 2012). The midbrain groups comprise long projection systems, linking the *substantia nigra* and the ventral tegmental area with neostriatum (i.e. putamen and caudate nucleus), limbic cortex and other limbic structures (i.e. accumbens, amygdala and piriform cortex) (Carlsson *et al.*, 1962). The principal role of this neurotransmitter is the neuromodulation of some physiological functions implicated in voluntary movement, motivational processes,

affective behaviour, learning, cognition, and hormone regulation (Brady *et al.*, 2012). A lack of dopamine would alter these functions in more or less magnitude depending on the lesion degree.

1.1.2 Hallmarks and onset of the neurodegeneration

Parkinson's disease is considered as a multifactorial syndrome in which dopaminergic neurons of SN*pc* degenerate in concomitant with the appearance of the inclusion body pathology (i.e. Lewy neuritis and Lewy bodies) (Braak *et al.*, 2006). Pathological and neuroimaging studies have shown that when motor symptoms are evident, a significant cell loss in the SN*pc* has already occurred (Gaig & Tolosa, 2009). At neuropathological examination, some studies demonstrate that motor symptoms only take place when patients present a reduction of 80% in the striatal dopamine content and a loss of about 60% of dopaminergic neurons in the SN*pc* (Hornykiewicz & Kish, 1987; Gaig & Tolosa, 2009). Actually, the rate of dopaminergic neurons loss is 4.7% per decade for normal aging and 45% per decade for PD patients (Fearnley & Lees, 1991). Studies performed with neuroimaging techniques, such as positron emission tomography and single photon emission computed tomography, corroborate the results obtained using neuropathological examination, with a loss of 40-60% of dopaminergic markers at the time of the motor symptoms incidence. The annual rate decay for those markers is a 6-13% in PD patients and a 0-2.5% for healthy controls

(Gaig & Tolosa, 2009). Also, all the patients with PD reveal the presence of α-synuclein-immunoreactive inclusion bodies in vulnerable neurons (Hawkes *et al.*, 2010). These studies support the idea of a premotor period of the disease on which non-motor symptoms prevail at least during 3-6 years, but some of them point to a prolonged phase that could be as long as 20-40 years (Gaig & Tolosa, 2009).

As one of the main hallmarks for PD, the neuroanatomical study of the protein inclusions results essential. The inclusions are described as eosinophilic spindle-shaped radiating fibrils with a less defined core, and, in part, with branching Lewy neuritis (LN) within dendrites and axons (Olanov & Brundin, 2013). Somatic inclusions may appear as punctuate aggregations close to the deposits of neuromelanine or lipofucsin granules. Also, globular inclusions with a more weakly immunoreactivity can be observed in the form of pale bodies, which probably go on to evolve into strongly labelled LBs. Ultrastructurally, LBs are composed of 10-14 amyloid-like fibrils and α-synuclein. The cellular role of α-synuclein is still not clear but some authors reported its involvement on the fibrillization process, the activation of proteolitic pathways, the link with TAU and its natural relation with membranes (Betarbet *et al.,* 2005). For these reasons, its abnormal proteolysis or the formation of α-synuclein reservoirs could promote the neurodegeneration in humans. In fact, the malfunction of complex I with the consistent rise in reactive oxygen

species levels promotes the aggregation and accumulation of α-synuclein (Dawson & Dawson, 2003b). Furthermore, patients with clinical symptoms of parkinsonism in the absence of LNs or LBs form an heterogeneous group of motor dysfunctions, including multiple system atrophy, progressive supranuclear palsy, neurodegeneration with brain iron accumulation type I, and some forms of familial PD. Elderly individuals trend to present LBs and/or LNs but without a symptomatic phase, suggesting the incidental LB pathology as normal concomitant with aging (Braak *et al.*, 2006).

The onset of the disease is still obscure but several studies suggested the existence of a certain relation between disorders affecting olfaction, autonomic system, and depression with the development of the disorder (Hawkes *et al.*, 2010; Doty, 2012; Zahodne *et al*., 2012). Specific regions of central and peripheral nervous system are involved during the development of the disease like as *medulla oblongata*, *pontine tegmentum*, anterior olfactory structures, mid- and forebrain, and in the last stages, associative and primary regions of neocortex (Braak *et al.*, 2006). The distribution of neurons affected by the syndrome is not hazardous, suggesting a special prone of some neurochemical systems. Indeed, this characteristic is reflected in the regional distribution pattern of the pathology, as we discuss further.

1.1.3 Parkinson's disease stages: Braak's stage

It is now accepted that PD onset appears several years before the incidence of motor symptoms in a phase denominated premotor. In view of that, some authors have developed tools, like the Braak stage (Hawkes *et al.*, 2010), to evaluate the premotor phase for an early diagnosis of the disease (Fig. 1.4). Braak stage (Braak *et al.*, 2006) is based in the changes founded in the neuroanatomy of patients and in the presence of α-synuclein deposits (i.e. Lewy pathology) on their brain and peripheral tissues as is described below.

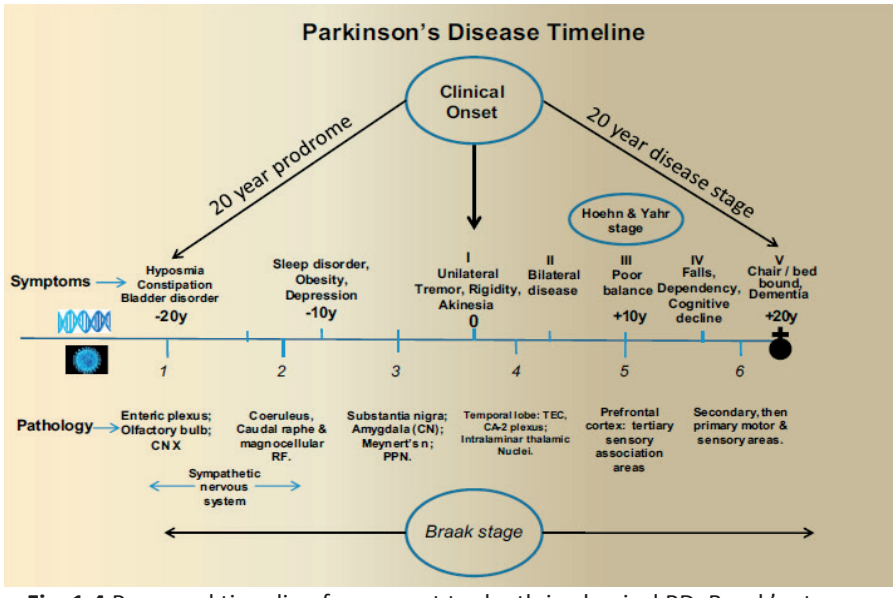

Fig. 1.4 Proposed time line from onset to death in classical PD. Braak's stage (Hawkes *et al.* 2010).

Initial stages (1-2)

The initial stage is characterized by peripheral hallmarks such as LNs related with the vagus nerve, olfactory bulb, anterior olfactory bulb and myenteric gastric plexus. As the initial step of the disease, it corresponds with the premotor phase and is asymptomatic. Once PD progresses, *locus coeruleus* shows more LNs and the lesions in dorsal motor nucleus and lower raphe nuclei gets worse. Commonly, the first alterations in peripheral nervous system are the α-synuclein deposits founded for both, gastric system and vagus nerve, suggesting its correlation with constipation. Regarding to the sympathetic cardiac nervous some patients showed a centripetal neurodegeneration. Also, during the first stage is characteristic the appearance of alterations in pelvic plexus related to erectile dysfunctions and bladder incontinence. In spite of the number of systems altered by the development of the disease, the pathology in non-olfactory sites is confined to the *medulla oblongata* and *pontine tegmentum*.

Threshold stage (3)

Third stage is considered the threshold of the symptomatic phase and is the first that involves the *substantia nigra.* During its development, lesions are observed above the *pontine tegmentum* and in the basal mid- and forebrain, including amygdala and *substantia nigra.* Microscopically, LNs are described in the SN*pc*

promoting the appearance of LBs in the melanized projections from this nucleus. At forebrain, central subnucleus of amygdala, tegmental pedunculopontine nucleus or magnocellular nuclei are altered too. This stage is usually the first reported in the early diagnosis of the disease and rarely concur with the typical symptoms of the disease except on the familial form of PD.

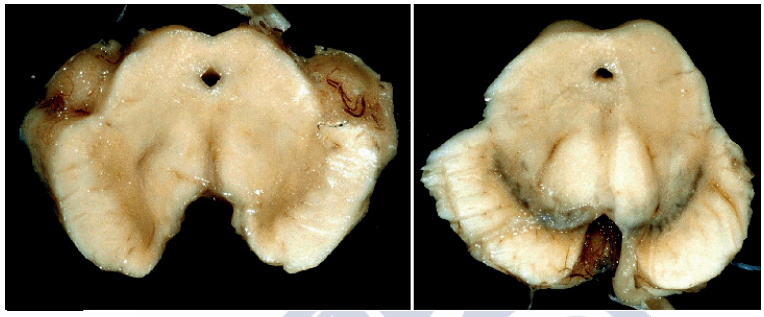

Fig. 1.5 Section of the brainstem at the *substantia nigra* level. Left, PD patient. Right, Healthy patient (Agamanolis, 2011).

Symptomatic stages (4-6)

Once the threshold has been exceeded, the amygdala is heavily affected and portions of the cerebral cortex are involved in the pathology. The superficial layers of the cortex show LNs and the deeper parts LBs, presenting the same pattern that Alzheimer's disease patients show on the incidence of amyloid inclusions. In final stages, the *substantia nigra* appears macroscopically damaged (Fig. 1.5) and the inclusion body pathology is extended into the cortex. The pyramidal cells of high-order association areas of neocortex have

LBs, initially settled in the first order association areas and, finally, even in primary and secondary sensitive cortex. On that stage, the symptoms of the PD are observed in full range.

1.1.4 Aetiology

Neurodegenerative disorders as PD present a high prevalence in the aged population; however its aetiology remains unknown. In order to prevent its incidence or to initiate an early treatment, the understanding of the molecular basis that dictates the syndrome onset is a major goal in biomedical research. Some studies (Zack & Langston, 1995; Malkus *et al.*, 2009) suggested the involvement of oxidative alterations, mitochondrial dysfunction, and impairment of the ubiquitin-proteasome system (UPS) as the main aetiological causes. However, which is the link between these factors? The oxidative stress caused by reactive oxygen species (ROS) and reactive nitrogen species (RNS) raises as the most plausible reason (Dawson & Dawson, 2003b; Jenner, 2003). The analysis of post-mortem brain tissue reveals high levels of lipid peroxidation, oxidize proteins and damage into the DNA (Schapira, 2008a). The redox reactions play a central role in some cellular processes and that is why an antioxidant system is always present to avoid oxidative damage. One of the main postulates for the PD aetiology suggests that alterations in some molecular processes are responsible to push oxidative levels towards the threshold of the antioxidant defences (Aon *et al.*, 2010).

Consequently, the oxidative imbalance triggers some signalling pathways that promote the apoptosis and the cellular death. However, many other factors could be implicated as: tissue inflammation, glutamatergic neurotoxicity, xenobiotics or DNA mutations. For this reason, the efforts in the study of PD should be focused in determine a common starting point to all the cellular unbalances or at least, with common points between the different approaches (Fig. 1.6).

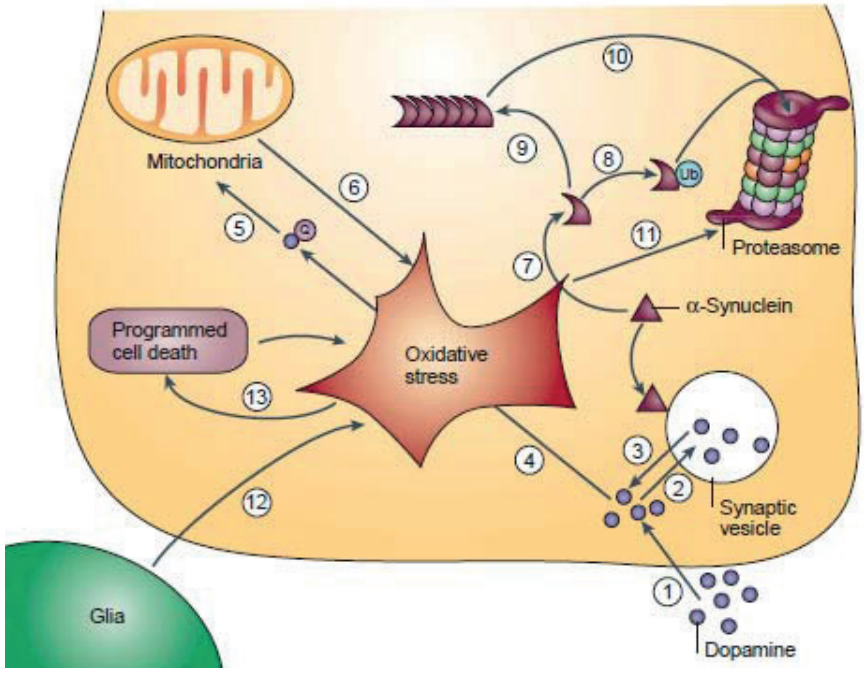

Fig. 1.6 Oxidative stress pathways in a dopaminergic neuron (Andersen, 2004).

The idiopathic PD represents almost 90% of the cases carrying out with the usual prognosis and an average incidence of 60 years old (Dauer & Przedborski, 2003). As previously described, PD is only diagnosed when the loss of neurons in SN*pc* is concomitant with proteinacious cytoplasmic inclusions (i.e. LBs). Clinically, any disease that includes striatal dopaminergic deficiency or direct striatal damage may lead to parkinsonism, a syndrome characterized by tremor at rest, rigidity, slowness, absence of voluntary movement, postural instability, and freezing. Indeed, PD is considered epidemiologically the most common cause of parkinsonism, comprising for ~80% of cases (Dauer & Przedborski, 2003). The main difference between both remains in the ineffective of dopamine replacement therapy for parkinsonism and the concomitance of symptoms not related with PD. Parkinsonism can result from exposure to xenobiotics as environmental toxins (e.g. rotenone, paraquat, maneb, MPTP, carbon monoxide, cyanide, methanol, etc.), infections (e.g. encephalitis letargica), use of medications (e.g. lithium, neuroleptics, reserpine, etc.), and intoxication with metals (e.g. manganese). All of the above xenobiotics appear in common with sporadic PD but the prognosis for parkinsonism could be not the expected. The neurochemical pathways concerning with the development of parkinsonism might be mainly involved in the onset of PD but not necessarily.

On the other side, the remaining 10% of the cases corresponds to familial PD. This PD typology is usually characterized by a worst progression and an early age of incidence. Genetic studies revealed that 10 *loci* are involved in some of the Mendelian and rare genetic forms of PD (Dawson & Dawson, 2003a). Some of the genes discovered have relation with the deficit in complex I of the mitochondria, the aggregation of α-synuclein, and the malfunction of the UPS. The heritability of maternal genes for this organelle, make possible a higher incidence of PD in families with malfunction in complex I, high levels of ROS and, as consequence, high activity of enzymatic excavengers. For example, a single-nucleotide polymorphism leading to a non-conservative amino acid change from threonine to alanine within the NADH dehydrogenase 3 of complex I, drive to a reduced risk of developing PD in Caucasians. This fact, highlight the importance of complex I for the development of the syndrome (Van der Walt *et al*., 2003). Post-mortem studies in humans reported the presence of ROS and a deficiency in complex I, suggesting them as important factors in the development of the disease (Hattori *et al*., 1991; Schapira, 2008a). In general, all the *loci* studied (Table 1.1) are able by themselves to trigger the disease. For example, the *locus* related with α-synuclein (PARK-1) has been linked with familial PD and as one of the main causes for the onset and development of the syndrome (Dawson & Dawson, 2003b). Also, alterations in *locus* PARK-4, like the transition of a nucleotide in the

α-synuclein or the triplication of the gene, results in the higher incidence of PD for few Italian-American Greek, German and Iowan families (Krüger *et al.*, 1998; Singleton *et al*., 2003).

Table 1.1 *Loci and genes linked to familial PD or implicated as genetic causes for PD. NA, not assigned (Dawson & Dawson, 2003b).*

Gene	Mode of inheritance	Locus	Chromosal location
α-synuclein	Autosomal dominant	PARK1	4q21-q23
Parkin	Autosomal recessive	PARK2	6q25.2-27
Unknown	Autosomal dominant	PARK3	2p13
α-synuclein	Autosomal dominant	PARK4	4q
UchL1	Autosomal dominant	PARK5	4p14
Unknown	Autosomal recessive	PARK6	1p35-p36
DJ-1	Autosomal recessive	PARK7	1p36
Unknown	Autosomal dominant	PARK8	12p11q13.1
Unknown	Autosomal dominant	PARK8	12p11q13.1
Unknown	Autosomal recessive	PARK9	1p36
Unknown	Late-onset susceptibility gene	PARK10	1p32
NR4A2	Susceptibility gene	NA	2q22-23
Synphilin-1	Susceptibility gene	NA	5q23.1-23.3
Tau	Susceptibility gene	NA	17q21

Finally, protein misfolding, aggregations and deposition lead to perturbed cellular function and eventually to cell death. Thus, cells present pathways for protein control and removal to maintain intracellular protein homeostasis. The successive impairment of the UPS in PD has been highlighted as the third factor relate with genes and directly involved in the onset and development of PD. For example, the mutation in DJ-1 (PARK-7), a protein related with chaperones, cause autosomal recessive PD (Valente *et al.*, 2001). Also, other mutations can promote a monogenetic form of PD like alterations in parkin (PARK2; an E3 ligase that can also modulate 26s proteasomal activity) or UCH-L1 (PARK5; an ubiquitin hydrolase) (Kitada *et al.*, 1998; Leroy *et al.*, 1998). Other homeostatic pathways of cellular clearance could be involved in the development of the disease, being responsible of autosomal PD. For example, the quinase 1 p-ten-induced (PINK-1) protect cells from stress induced by mitochondrial dysfunction promoting the bind of parkin to induce autophagia of depolarized mitochondria in a process denominated mitophagy (Youle & Narenda, 2011). Also, LRRK2 is binded to the mitochondria and interact with parkin. Its main function is not clear, but is related with the formation of autophagosomes (Friedman *et al.*, 2012).

1.1.5 Parkinson's disease models in research

6-Hydroxidopamine

6-Hydroxydopamine (6-OHDA) is one of the most extended models in PD due to its applicability for preclinical assays with new drugs and its link with oxidative stress (Sauer & Oertel, 1994; for a review see Betarbet *et al.*, 2002). Historically, 6-OHDA was described in 1959 as a chemical agent with specific neurotoxin effects on the catecholaminergic system. Its chemical structure does not allow the systemic injection due to its inability to cross the blood brain barrier. For this reason, 6-OHDA must be injected stereotactically in the brain, usually in the *substantia nigra*, nigrostraiatal burden or into the *striatum.* The injection of this neurotoxin in the brain results in an active transport mediated by the catecholaminergic transport system (DAT), as dopamine and norepinephrine do in neurons. These properties, which could be considered as a problem, makes 6-OHDA selective for the region on which is injected and to the catecholaminergic system present on it.

After 6-OHDA injection, the normal decay of the oxidative damage in dopaminergic neurons occurs during the first 24 hours and is completely depleted in 2-3 days (Sánchez-Iglesias *et al.*, 2007a). The neurodegeneration degree depends on the amount of the agent injected, the site of injection and the sensibility of the animal species. When 80-90% of neurodegeneration is achieved, specific behavioural changes are observed in the animal. The most used technique to

determinate the degree of the lesion and the hemisphere affected is rotation test with apomorphine. The main mechanism described for 6-OHDA neurotoxicity involves a direct interaction with complex I of the mitochondria (Glinka *et al.* 1996) and the increase in oxidative stress production (Glinka *et al.*, 1998; Kulich *et al.*, 2007). Some studies revealed that hydrogen peroxide (H_2O_2) and hydroxyl radical ($^{\bullet}OH$) radicals, in presence or absence of iron, are the responsible of the oxidative stress (Méndez-Álvarez *et al.*, 2001). Also, it has been reported the ability of 6-OHDA to decrease the activity of glutathione peroxidase (Gpx) and superoxide dismutase (SOD), promoting lipid peroxidation in *striatum* (Smith & Cass, 2007). Indeed, the presence of antioxidant agents results in a neuroprotective effect depending on the alteration of autoxidation kinetic of the 6-OHDA (Blum *et al.*, 2000; Soto-Otero *et al.*, 2000). The interaction with complex I and its corresponding inhibition increases the production of superoxide anion radical ($O_2^{\bullet-}$), an effect that can be prevented by chelating agents (Glinka *et al.*, 1996). However, despite of all 6-OHDA properties this neurotoxin cannot mimic all the features of PD, because the neurodegeneration is not progressive and apoptosis is not present, as they are in the syndrome (Ebert *et al.*, 2008).

1-Methyl-4-phenyl-1,2,3,6-tetrahydropyridine (MPTP)

MPTP was discovered due to the intoxication of Barry Kidston in 1976 after the injection of a synthetic opioid drug with MPTP as minor contaminant. Langston *et al.* discovered in 1984 that the injection of the chemical agent in monkeys resulted in a parkinsonism syndrome that is virtually impossible to difference from idiopatic PD. This effect could be prevented with pargyline, a monoamine oxidase inhibitor. Also, its lipophilicity allows MPTP to cross freely the blood brain barrier and the cellular membrane, facilitating its administration. For this reason, MPTP is one of the most extended models in the study of the motor symptoms and the side effects of L-DOPA treatment. The toxicity of the compound is due to MPP^+, a metabolite produced by the degradation of MPTP via MAO-B on glial cells. Once MPP^+ is into the neuron, is able to interact with the mitochondrion and inhibit the complex I. Also, Perier *et al.* described in 2005 the mechanism that relates MPTP toxicity with apoptosis, involving the transcription and post-translational activation of Bax. However, despite of its properties, MPTP lacks to promote the neurodegeneration in rats, probably due to the presence of MAO-B in the brain capillaries (Langston, 2002).

Rotenone

Rotenone is an hydrophobic compound and as consequence crosses the biological membranes very easily. For this reason is widely used as insecticide in vegetable gardens and to kill invasive fishes in lakes. Its toxicological mechanism involves the inhibition of complex I of the mitochondria, a characteristic that simulates one of the mitochondrial defects found in the brain of PD patients (Schapira, 2008a). Also, due to its hydrophobic properties is capable to inhibit mitochondria in a systemic way and is not limited to one neurochemical system (Betarbet *et al.*, 2000). When is used as PD model has been demonstrated its ability to inhibit complex I thought the whole brain, reproducing the behavioural, anatomical and neuropathological features of the syndrome. Indeed, nigro-striatal dopaminergic system shows a higher neurodegeneration, suggesting a special sensivity to the complex I inhibition. As conse-quence of the partial inhibition of the electron transport system of the mitochondria the production of anion superoxide and the oxidative damage is increase. Also, if the rotenone dose is maintained in time at low concentrations a progressive release of cytochrome c is observed (Sherer *et al.*, 2000). This mechanism could promote the α-synuclein aggregation and the formation of proteinaceous inclusions. However, despite of all the rotenone properties the neurotoxin is not specific for dopaminergic systems and its oral or i.p. administration could result with a high mortality of the rodents.

1.2 Mitochondria and bioenergetics

The cycle of life and death converges in the mitochondrion. This organelle is considered as the powerhouse of the cell due to its main role synthesizing ATP. Also, it is involved in other processes such as the regulation of the cellular cycle, apoptosis, cell growth, and intracellular signalling (Cadenas, 2004). The cellular cycle allows the tissues to replace the cells lost by wearing out, deterioration or programmed cell death. However, neurons maintain a post-mitotic status and cannot be replaced during aging or after an insult. For this reason, any factor that accelerates or promotes an early neuronal death results in a heavy deterioration of the individual that arduousness could be reversed.

The redox environment of the cell is composed by an imbalance between the free radical species (i.e. ROS and RNS) and the antioxidant systems. The aging oxidative stress hypothesis postulates that age-associated reductions in physiologic functions are caused by a slow steady accumulation of oxidative damage to macromolecules, which is associated with life span of the organisms (Lin & Beal, 2003; Muller *et al.*, 2007). Indeed, the genetic manipulation of oxidative damage scavengers can increase life expectancy in animals. For example, overexpression of Cu/Zn-SOD or Mn-SOD appears to extend life span. Also, the methionine sulfoxide *knock-out* result in a 30% reduction in life span for mice and its overexpression a 70% increase in the survivability of the Drosophila

(Lin & Beal, 2003). Nevertheless, tissues present different metabolic rates and the exposition to the oxidative stress is variable. For example, brain represents about 2% of the total body weight and consumes around 20% of the oxygen, representing an elevate metabolism if we compare with peripheral organs. This unusual balance supposes an enhance pressure on the antioxidant systems of the nervous tissue and one of the principal targets for oxidative stress. Specific markers for oxidative stress like 4-hydroxynonenal and malondialdheyde for lipid peroxidation and protein nitration has been found in brain from Alzheimer's disease, PD and Amyotrophic lateral sclerosis. Indeed, has been observed some of them surprisingly specific like nitrosilation in α-synuclein in PD (Giasson, 2000a; Giasson, 2000b). However, the pathological process exceeds the common development of aging itself and triggers mechanisms that alter the patient quality of life.

Mitochondrial bioenergetics is the study of the metabolic pathways, the mitochondrial respiration and the mechanisms that promotes the formation of free radicals species. Nowadays, some neurodegenerative disorders such as PD, Alzheimer's disease, and amyotrophic lateral sclerosis have been related with an alteration on mitochondria and oxidative stress (Andersen, 2004). Indeed, the study of bioenergetics results relevant to gain insight on these processes and in the aetiological mechanisms involved during the development of the neurodegenerative disorders. For this reason,

the role of mitochondria in oxidative stress and its implications in the aetiology of PD is one of our main objectives.

1.2.1 Structure and role of the mitochondria

The structure of mitochondrion is well bounded by a double-membrane highly specialized. This fact defines the outer and the inner membranes which contains different biochemical environments on it (i.e. intermembrane space and matrix). The outer mitochondrial membrane is considered almost permeable to ions and solutes due to the presence of porins, which act as non-specific pores for solutes of molecular masses less than 5-10 kDa. Its permeability is still not well understood, but recent studies suggested that could be strongly regulated (Duchen, 2004). This supposes that the biochemical environment of the intermembrane space is very similar to the cytosol. However, the outer membrane contains some distinctive characteristics that are involved in some of the processes described for the organelle function. For example, on its surface is formed the mitochondrial permeability pore concurring the voltage dependent anion channel, Bcl_2, Ras and other proteins. The mitochondrial permeability pore is responsible of the cytochrome c release under special conditions as a raised oxidative stress. Indeed, the formation of the pore is one of the main mechanisms that trigger the apoptosis, a process that can be prevented with the presence of ADP and a correct function of the mitochondrial bioenergetics, but not in all

circumstances (Andreyev & Fiskum, 1999). This grants to the mitochondria a central role in the control of cell survivability.

The space between the membranes is referred to as the intermembrane space. We still understand little about its biochemistry, but recently it has been revealed as an interesting microenvironment, housing some proteins which play major roles in cell physiology, mitochondrial bioenergetics and in cell death (i.e. cytochrome c and creatine kinase). The inner membrane usually presents multiple infoldings, forming the cristae, which delimit the matrix and house a variety of membrane-bounded enzyme systems. The membrane is highly enriched in cardiolipin and integral proteins (over 50% of the total content), containing the electron transport system and the ATP synthase. Those are a group of enzymes responsible of the redox reactions, protons pumping, oxygen oxidation and synthesis of ATP that occur during oxidative phosphorylation. Inner membrane is considered as impermeable and forms the major barrier between the cytosol and the mitochondrial matrix. This characteristic is determinant to generate the electro-chemical potential required to drive the oxidative phosphorylation. The structure of the cristae varies enormously between different tissues, and the functional significance of these differences remains largely a mysterious. Recently, several groups study these cristae structures and try to reproduce the bioenergetic consequences of changing shapes of the cristae (Manella *et al.*, 1998; Frey & Manella,

2000; Frank *et al.*, 2002; Hsieh *et al.*, 2002). However, we are still far enough to understand its implications.

Finally, the matrix contains the genome and most of the enzymes involved in cellular metabolism such as it is the case of those involved in the tricarboxylic acids cycle. The mitochondrial DNA ($_{mt}$DNA) is organized as several copies of a single circular chromosome, suggesting its phylogenetical origin from bacteria (Leblanc *et al.*, 1997). Its role is to encode a fraction of the proteins that are fundamental for the organelle functions, while the majority of the proteins required to build mammalian mitochondria are encoded in the nucleus and transported to the organelle. For example, human $_{mt}$DNA is double stranded with only 16.6k of pair bases encoding 13 proteins of the electron transport system (ETS). In addition, other 24 are present, encoding two rRNAs and 22 tRNAs. The mitochondrion is composed by a total of about 850 proteins, so the majority of the organelle is encoded in the nuclear DNA.

1.2.2 Tricarboxylic acid cycle

Krebs cycle is the central metabolic pathway in all aerobic organisms and its function comprise the generation of reducing equivalents for the subsequent oxidative phosphorylation. The cycle is a series of reactions in the matrix, taking a two carbon molecule

(i.e. acetate) and completely oxidizing it to carbon dioxide as is summarized in the following chemical equation:

$$\text{Acetyl-CoA} + 3\text{NAD}^+ + \text{FAD}^+ + \text{ADP} + \text{P}_i \longrightarrow 2\text{CO}_2 + \text{CoA} + 3\text{NADH} + \text{FADH}_2 + \text{ATP}$$

The regulation of the tricarboxylic acid cycle (TCA) is mainly determined by substrate availability, concentration, and feed-back inhibition by product (Fig. 1.7; e.g. the malate inhibits the fumarase if succinate is not added into the respirometry chamber). However, most of the enzymes involved are also allosteric (e.g. dehydrogenases), being modulated by Ca^{2+} and other molecules. For example, the first step of the cycle is a condensation reaction between acetyl-CoA and 2-oxoloacetate to form citrate. The acetyl-CoA serves as a link between different metabolic pathways and TCA, being formed on the catabolism of carbohydrates (by glycolysis), fatty acids (by β-oxidation), and proteins. For this reason, the amount of acetyl-CoA and the metabolic pathway that conclude with its formation is closely modulated.

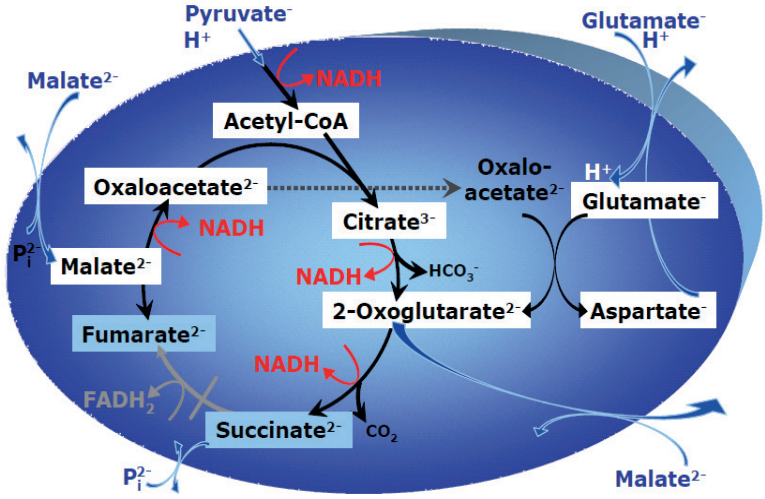

Fig. 1.7 Tricarboxylic acid cycle fuelled with substrates linked to complex I**.** White box: Active reactions. Blue box: Inactive reactions (Gnaiger, 2007).

Additionally, the cataplerosis of biomolecules to feed substrates into the TCA is tightly regulated by different carriers in the inner membrane. For bioenergetical studies, we should consider its metabolic control due to the capacity to modify the availability of some compounds. As previously reported, TCA enzymes are regulated by compound availability and product inhibition. One of the most relevant cases is the inhibition of complex II (i.e. succinate dehydrogenase) by 2-oxaloacetate and in higher concentrations by malate. However, the mitochondrion presents three different carriers that transport these compounds across the membrane. For example, malate can be antiported inside the matrix by the tricarboxylate, the dicarboxylate and, the 2-oxoglutarate carrier in exchange for citrate, phosphate and 2-oxoglutare respectively. Also, the discarboxylate

carrier can exchange succinate for phosphate. Indeed, malate and fumarate are in a stoichiometric balance with a 4.1 ratio. If the bioenergetical study uses only a high concentration of malate to feed the TCA, the concentration of fumarate rises up and inhibits the complex II by product concentration. These transports across the membrane can be used in bioenergetical studies to select the activation of particular sectors on the TCA. For example, we could select specifically the activation of complex I (Fig. 1.7; Glutamate + malate + pyruvate), complex II (Fig. 1.8; Rotenone + succinate) or complex I+II (Fig. 1.9; Glutamate + malate + pyruvate + succinate).

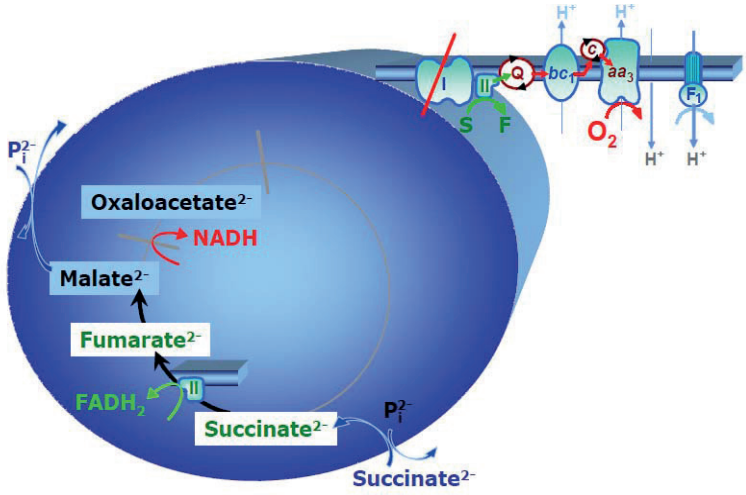

Fig. 1.8 Tricarboxylic acid cycle fuelled with substrates linked to complex II. White box: Active reactions. Blue box: Inactive reactions (Gnaiger, 2007).

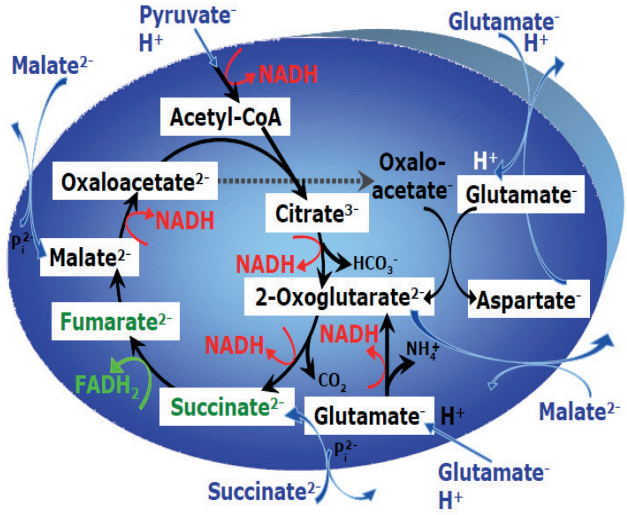

Fig 1.9 Tricarboxylic acid cycle fuelled with the substrates routinely used in respirometry. White box: Active reactions. (Gnaiger, 2007).

1.2.3 Electron transport system and oxidative phosphorylation

The electron transport system is responsible of the oxidative phosphorylation and is constituted by five enzymatic complexes (i.e. Complexes I-IV and ATP synthase or Complex V) bounded into the inner membrane. Complexes I-IV transfer the electrons from the reducing equivalents (i.e. NADH and $FADH_2$) provided by the TCA to the oxygen. The oxidation of NADH and $FADH_2$ are exergonic reactions that release Gibbs free energy to the system. The amount of energy provided depends to the difference between the redox potentials of the couple donor (i.e. $NADH/NAD^+$ and $FADH_2/FAD^+$) and the couple acceptor (i.e. O_2/H_2O and intermediary clusters) (Fig. 1.10).

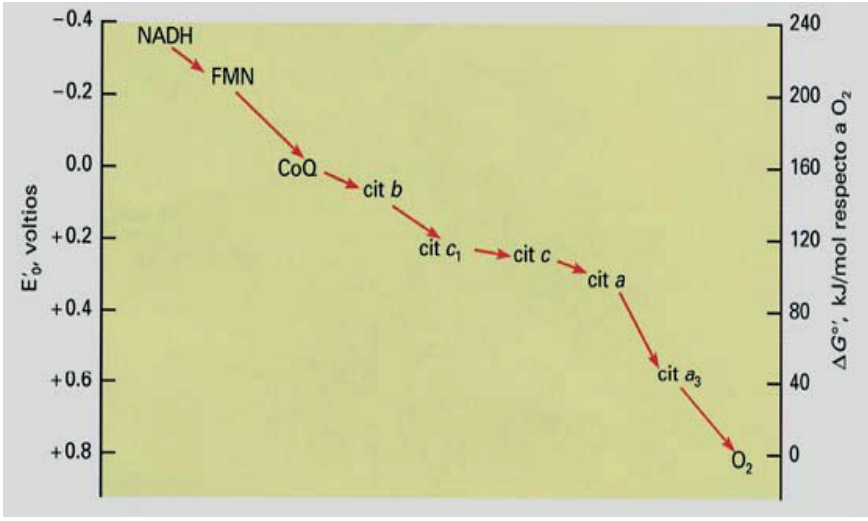

Fig 1.10 Redox potential on the electron transport system (Mathews & Van Holde, 1999).

Complexes I, III and IV use the free energy to pump protons into the intermembrane space, generating an electrochemical gradient of protons ($\Delta\mu_H^+$) through the membrane. The complete cycle yields ten protons ejected from the mitochondrial matrix per two electrons transferred from NADH to oxygen, or six protons for each electron pair passing from other quinone-linked dehydrogenases to oxygen. Once $\Delta\mu_{H+}$ is formed, it supposes a reservoir of the redox potential and; when the energy demand rises up in the cell, the influx of protons throughout the ATP synthase returns the free energy to the system, synthesizing ATP. The redox span across the entire ETS is approximately 1100mV, and the maximal $\Delta\mu_{H+}$ across the inner membrane is 180-220 mV. This process is known as oxidative phosphorylation and one of the most

remarkable things on that biochemical cycle is the coupling and proportionality between the oxygen consumed during the proton pumping and the amount of ATP synthesized.

On the classical conception of bioenergetics, the electrons are transferred in an arranged linear chain of reactions that go over each complex. However, nowadays the bioenergetics conception about how complexes are organized involves more dynamism. The Q-junction represents effectively the new perspective, on which the electron transport system is a non-linear convergent pathway. On that model, the electrons converge from complex I, complex II, the glycrophosphate dehydrogenase and the electron transferring flavoprotein into coenzyme Q (Q_{10}) (Fig. 1.11). Indeed, the fluidity of the membrane supports the idea of a Q_{10} pool that is constantly flowing to accept the electrons and to transfer them into complex IV to support the energy demand.

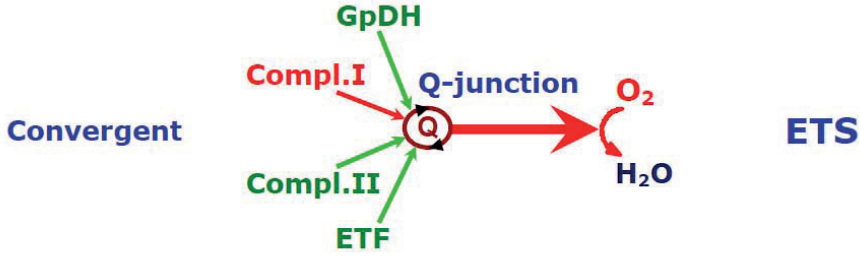

Fig. 1.11 Q-junction on ETS (Gnaiger, 2007).

Complex I

Complex I (CI; i.e. NADH:ubiquinone oxidoreductase) is the main entry point of the electrons to ETS. Its role is to oxidize NADH to NAD^+ and carry the resulting electrons to the Q_{10}. The Gibbs free energy released in the redox reaction is used to pump protons from the matrix to the intermembrane space, contributing to the proton-motive force. The exact mechanism that promotes the pump of protons is still not clear, but the stoichiometry of the reaction yields $4H^+/2e^-$ when Q_{10} is present. For this reason, the Q_{10} availability controls the reaction kinetic and acts as the final acceptor of the electrons. The cited availability depends on the quinone ability to transfer electrons, a reaction limited by the chemistry of the quinone itself. As consequence, the complex I is usually found in a reduced form.

The CI is an L-shaped multi-subunit enzyme organized in a modular-architecture with differential function and structure (Dieteren *et al.*, 2008). The phylogenetical study of the modules revealed a different origin for each of them (Friederich & Wiess, 1997; Finel, 1998). The complex is formed by 45 subunits encoded between the $_{mt}$DNA and the nuclear DNA. Indeed, only 14 of the evolutionary conserved CI subunits are required to carry out the catalytic function, seven encoded in the $_{mt}$DNA and seven by the $_{n}$DNA. The other 31 subunits are supposed to be involved in the

biogenesis and regulation of the metabolism (Roestenberg *et al.*, 2012).

Complex I is the biggest structure in the electron transport system and its synthesis and assembly in the mitochondria is highly regulated due to the amount of peptides that must be recruit. The structural analysis revealed three modules as the main components of the complex. Firstly, the N-module is responsible of the NADH oxidation and is relate with NAD^+-reducing hydrogenases of *Alcaligenes eutrophus*. Secondly, the Q-module is for quinone pool reduction and is similar to the NiFe-hydrogenases of *Methanosarcina barkeri*. Finally, the P-module promotes the H^+ pumping and presents homologous regions to Mrp-type Na^+/H^+ antiporters as in *Bacillus subtilis* (Mathiesen & Hägerhall, 2003). The cited modules contains 8 Fe-S clusters (i.e. $2Fe_2S_2$ and $6Fe_4S_4$) organized in a chain between the FMN on the size of NADH oxidation and with the N-module. The last cluster is the N_2, and presents special characteristics like a midpoint potential of -150mV and a high dependence of the pH (other clusters present a midpoint potential of -250mV). The P-module contains a hydrophobic region formed by 7 subunits. These subunits are highly preserved in the evolution, with an optimal functionality as proton pumps and encoded in the $_{mt}$DNA. The study of the mechanism revealed that the P-module pumps 3 protons for each NADH molecule. The mechanism responsible for the fourth proton is not clear.

Brandt purposes in 2011 a model of two-state stabilization change mechanism to explain the pump cycle (Fig. 1.11). The mechanism requires only two pump sites in the P-module to achieve the expected pumping stoichiometry of $4H^+/2e^-$. The basis is the ability of the redox intermediates of ubiquinone to drive conformational changes in the two pump modules of the membrane arm. The anion intermediates Q and QH switch the pump sites from the input mode of the E-State into output mode of the P-state. The conformation of the pump sites is linked to the movement of the transmission element, which suffer a rotation when the redox state of ubiquinone changes.

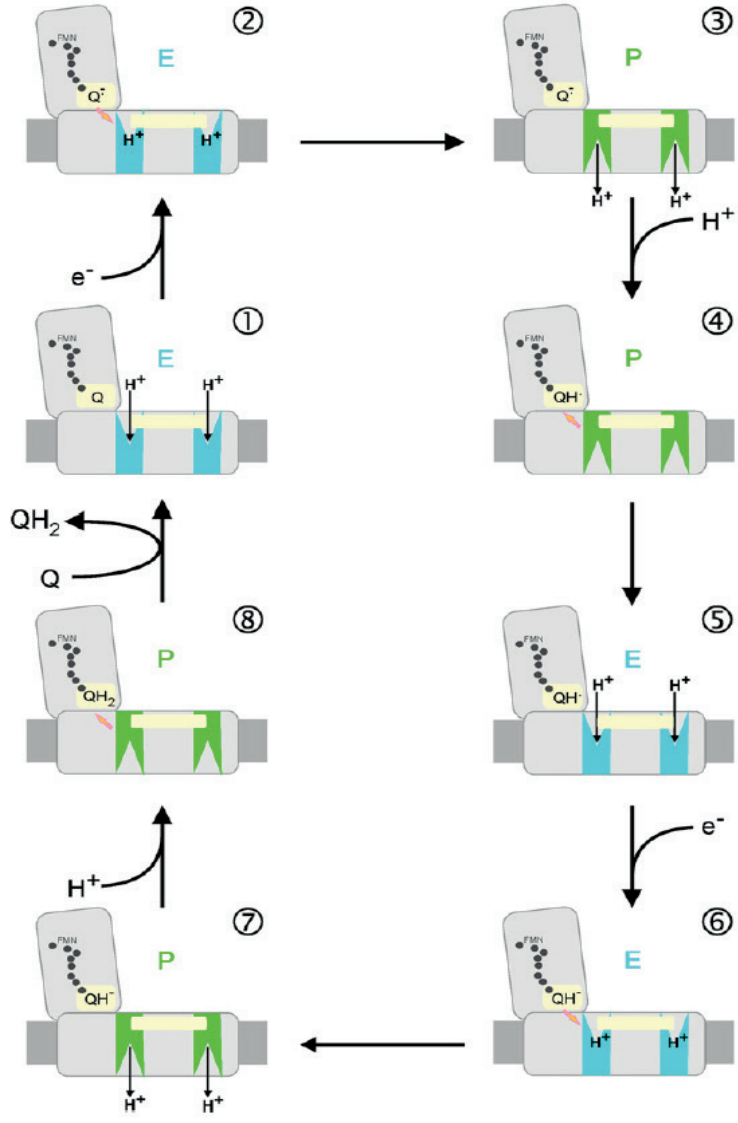

Fig 1.11 Pump cycle of the two-state stabilization change mechanism. The complex conformation change between the input mode of the E-State into output mode of the P-State (Brandt, 2011).

Complex II, electron-transferrin flavoprotein and α-glycerophosphate dehydrogenase

The ETS feed electrons into Q-junction through different pathways like complex II, which transfers electrons from succinate; electron-transferrin flavoprotein, feeding electrons from the flavoprotein-linked step of fatty acid β-oxidation; and α-glycerophosphate dehydrogenase. These enzymatic complexes are located into the inner membrane and present midpoint potentials close to 0 mV. As consequence, the electrons transference does not generate enough free energy to translocate protons from the matrix. However, their functions seem to be major on the maintenance of the oxidation cycle of Q_{10} and the subsequent oxygen flux consumption.

Complex II consist in several polypeptides that bounds FAD and two Fe/S centres. Results of special interest the presence of a cytochrome b of unknown function associate with the smaller polypeptide, being equimolar with FAD and with a different structure if its compare with cytochrome b of complex III.

Complex III and Coenzyme Q_{10}

Complex III (i.e. Cytochrome Bc_1) mediates the transference of electrons between Q_{10} and cytochrome c. The enzymatic complex is formed by 11 subunits which redox properties work in a linked sequence; these subunits include the Rieske protein and the cytochromes *b* and c_1. The redox clusters contain hemo groups that facilitate two points for Q_{10} union in a process that reduces Q_{10} and feed electrons into the cytochrome c.

The sequential process of Q_{10} reduction begins in the region Q_0 of the protein (i.e. low potential hemo *b*) catalyzing the oxidation of ubiquinol. The electron obtained is transferred to the Fe-S cluster of the Rieske protein that is quickly oxidated by cytochrome c_1 (Fig. 1.12, up). The ubisemiquinone formed reduces the hemo group of the low potential cytochrome and transfers the electron to the high potential region (Q_1). After that, Q_1 is oxidized due to the transference of the electron to ubiquinone to promote the formation of a stable semiquinone. In addition, the second phase of the sequence starts with the addition of a new ubiquinol molecule in Q_0, repeating all the process (Fig. 1.12, down). The described cycle presents a final yield of two electrons transferred into cytochrome c, four protons pumped and the reduction of a Q_{10} molecule, ready to accept new electrons from the complexes of the ETS.

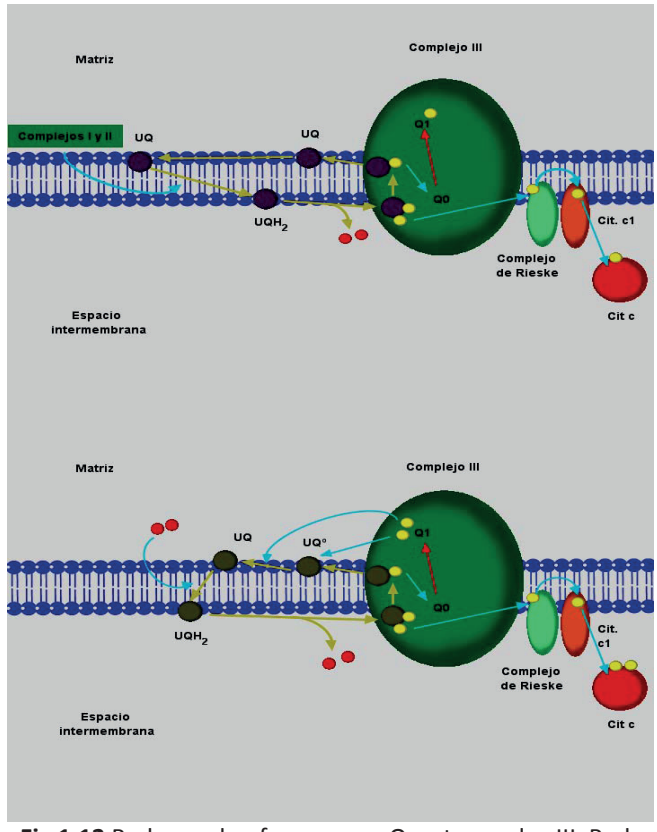

Fig 1.12 Redox cycle of coenzyme Q_{10} at complex III. Red: Protons. Yellow: Electrons.

Cytochrome c and Complex IV

Complex IV (i.e. Cytochrome c oxidase) is the last complex in the ETS feeding the electrons into the oxygen, the final redox acceptor on the oxidative phosphorylation. The enzyme is a multimeric complex formed by two hemo cytochromes (i.e. cytochrome *hemo a* and *hemo* a_3) and two clusters with copper that facilitates the electronic transport. Depending on the animal species, is formed by 6-13 subunits that catalyzes the reduction of the four O_2

yielding H_2O. First three regions are codified in $_{mt}$DNA and result essential for the complex function, however, the remaining subunits are synthesized from nuclear DNA, and its function is suppose to be as regulator (Devlin, 2004).

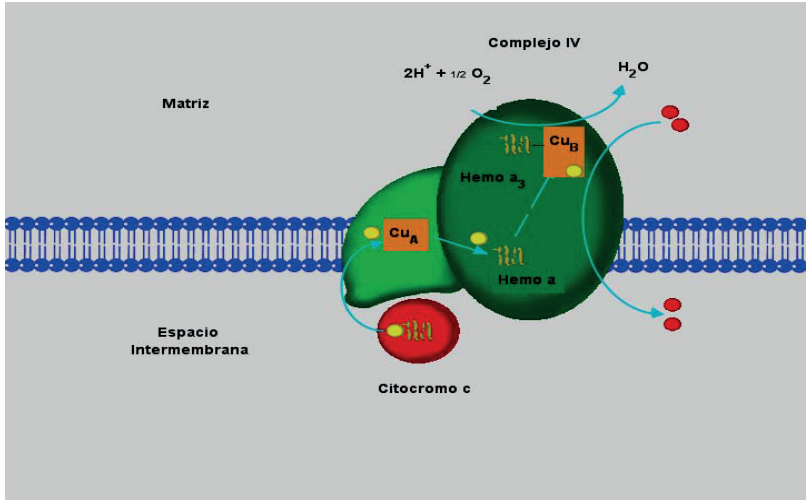

Fig. 1.13 Electron transfer to oxygen in complex IV. Red: Protons. Yellow: electrons.

The electronic transport through complex IV is initiated by the oxidation cytochrome c on the Cu_A cluster. The resultant electrons are carried to the *hemo a* of the subunit 1. The free energy released and the gap between the hemo and copper cluster is around 1.5 Å, allowing the proton pumping. Finally, electrons are directed to a complex formed by the Cu_B cluster and *hemo* a_3, which released them in the oxygen (Fig. 1.13). The reaction is performed in four different steps that bring different species derivate from the oxygen, all of them with harmful properties like peroxide ion (O_2^{2-}). For this

reason, the intermediate species are heavily bound to the cluster *hemo* a_3-Cu_B, avoiding the release of the ROS in the mitochondrial environment. Also, the free energy released on this reaction allows the proton pumping by an aminoacidic region related with the subunit 1. The final stoichiometry of the complex IV yield two protons pumped into the intermembrane space and two molecules of water for each molecular oxygen consumed

1.2.4 Steady-states, respiratory fluxes and flux control ratios

The mitochondrial respiration is a dynamic system that is in constantly shift depending on the energetic demand. In order to facilitate its study, Chance & Williams defined in 1955 a series of steady-states corresponding to the most characteristic respiratory rates obtained in oxygraph experiments with isolated mitochondria. Nowadays, we apply the same definition of the experimental terms with slight modifications (Nicholls & Ferguson, 2002).

The different steady-states studied represent the oxidative phosphorylation (OXPHOS; State3), the resting state (LEAK; $State4_o$) and the maximum capacity of the ETS (ETS_{max}; $State3_u$). Each of the steady states is limited by the different sections of the mitochondria involved on its function (Table 1.2). To achieve these states, different substrates and inhibitors are used in the bioenergetics study, allowing a wide range of possibilities for the study design. Once the

steady-states are registered we can study the respiration coupling control and the control exerted by the different complexes of the ETS.

Table 1.2 *Metabolic states of mitochondria* (Chance & Williams, 1955; Nicholls & Ferguson, 1992)

State	$[O_2]$	ADP level	Substrate level	Respiration rate	Rate-limiting substance	Coupling state
1	>0	Low	Low	Slow	ADP	-
2	>0	High	~0	Slow	Substrate	ROX
3	>0	High	High	Fast	Phosphorylation system	OXPHOS
4	>0	Low	High	Slow	ADP	LEAK
5	<0	High	High	0	Oxygen	-

Oxidative phosphorylation (OXPHOS; state3)

The oxidative phosphorylation capacity is the respiratory rate on which mitochondria produces ATP at the maximum rate. OXPHOS state could be resembled to the classic State 3 on which the respiration is only limited by the phosphorylative system (i.e. ATP synthase, ANT and phosphate carrier). There are some factors involved for the correct achievement of this rate, summarized as: Firstly, a saturating concentration of the substrates that feed the ETS complexes. In order to achieve the maximum OXPHOS capacity we must guarantee a flux of electrons into the Q-junction. The

respirometry studies mainly use substrates for complexes I+II (e.g. glutamate, malate and succinate) for this objective. Indeed, when both complexes are feeding electrons into the ETS, the mitochondrial respiration presents additive properties which origin remains unknown. Secondly, mitochondria requires a proton motive force for the properly formation of the redox reservoir into the intermembrane space. The outer membrane integrity results essential for this purpose and is a main factor to evaluate the mitochondrial integrity in our preparations. Finally, a saturating concentration of ADP assures a maximum rate of protons sink by the ATP synthase and as consequence the maximum coupled respiratory rate.

Resting state (LEAK; state 4_o)

The resting state is the common respiration rate that the mitochondria presents when the cell do not require the production of ATP. Physiologically, corresponds to the flux that compensates the proton leak and slip. To study this state, experimentally can be determined in three different ways: with the presence of substrates and absence of adenylates; after the addition of a non saturating amount of ADP and when is totally transformed in ATP; and adding an ATP synthase inhibitor after the register of OXPHOS respiration. The selection of one of those protocols depends on the purity of mitochondrial respiration and in the coupling rates that are expected

to be calculated with the same preparation. The objective is to obtain a LEAK state that allow assay properly LEAK respiration (i.e. proton leak, electron slip and cationic cycle) in a nonphosphorylating respiration of the mitochondria in a partially coupled state. Classically, LEAK flux corresponds to State4$_o$ on which the respiration is limited by the amount of ADP. The LEAK flux is due to the electron transport system rate and the proton motive force. However, ATP synthase is not involved on LEAK respiration and defects on the complex could be elucidated by comparison with OXPHOS respiration.

ETS maximum capacity (ETS$_{max}$; state 3$_u$)

The ETS$_{max}$ corresponds with a non-coupled state with maximum oxygen consumption. This state is not physiological and is achieved applying uncouplers as FCCP and CCP. These compounds present the ability to collapse the proton gradient due to the formation of pores on the surface of the outer membrane. Under these conditions, the respiratory control is completely release from the phosphorylative system, relying only in the enzymatic capacity of ETS itself (i.e. complexes I-IV) (Gnaiger, 2009). ETS$_{max}$ is a respiratory rate usually applied to normalize respiration and to study the magnitude of the physiological uncoupling or toxicological dyscoupling.

1.2.5 Membrane potential

The membrane potential of the mitochondria works as an energetically reservoir to synthesize ATP under demand. The chemiosmotic theory precludes that to obtain a membrane potential the transducer membrane must presents differential characteristics as impermeability and a double enzymatic system that pumps protons. The primary pump generates a gradient that force the secondary pump to work always in the synthesis way. As previously described, in the mitochondria the primary pump corresponds to the ETS complexes and the secondary pump to the ATP synthase. In energetically terms, mitochondrial respiration is an exergonic input tightly but not entirely coupled to the endergonic output that represents oxidative phosphorylation.

The electrochemical gradient of protons is thermodynamically quantified trough $\Delta\mu_H^+$ expressed as $Kj \cdot mol^{-1}$, measuring the distance between the ions gradient respect of its equilibrium, and in consequence, of its capacity to generate a work. $\Delta\mu_H^+$ presents two components: ΔpH, the chemical component corresponding to the transmembrane difference in the protons concentration across inner membrane; and $\Delta\Psi_{mb}$, the electrical component that corresponds with the difference in electrical potential between the cytoplasm and the matrix. The measurement of $\Delta\mu_H^+$ is considered a form of an electric potential (mV), referee to it as Δp (i.e. proton motive force). In the organelle, the main component that influences the Δp is $\Delta\Psi_{mb}$,

with ΔpH corresponding only with 0.5 units. This characteristic promotes an environment in the organelle close to a neutral pH, a feature in harmony with the cytosol.

$$\Delta\mu_{H^+} = \Delta\Psi_{mb} - 61.5 \log_{10} \Delta pH$$

1.3 Aluminium in neurodegeneration

1.3.1 Toxicokinetic and distribution of Al^{3+}

Aluminium (Al^{3+}) is extensively used in daily life and on industrial processes causing a possible human wide exposition trough tap water, air, food and some medications (Exley, 2013). In the nature, Al^{3+} is ubiquitous and the third abundance metal in the earth crush, representing 8.3% of total components (Becaria *et al.*, 2002) and being found in combination with other elements such as oxygen, silicon, sulphur, and other species (Brusewitz, 1984). As its main chemical property, Al^{3+} acts with a fix valence of three and consequently it does not show any redox activity, determining both characteristics its toxicological behaviour. However, its easy reaction with superoxide anion is able to generate the aluminium superoxide anion, a compound with stronger redox properties than anion superoxide itself. Although, Al^{3+} is widely distributed in the environment is usually not readily bioavailable and has not been relate with any biological function (Yokel 2002).

$$Al^{3+} + O_2^{\cdot -} \rightleftharpoons AlO_2^{\cdot 2+}$$

The main source of Al^{3+} intake is food due to the high concentration detected on additives, tea, vegetables, spices and soy-based milk products. Also, the leaching from daily used cookwares could contribute to dietary exposure (Lione, 1984; Kandiah & Kies, 1994; Lin *et al.* 1997). Indeed, an epidemiological study about total consumption of Al^{3+} in diet estimated a range from 1-20mg/day (Lione, 1983). Also, this metal is usually found as part of atmospheric particles of aluminium-silicates with concentrations in a range from 5 to 180µg/m^3 (Sorenson *et al.*, 1974) whereas in industrial areas the concentration is often in 1mg/m^3 range. Regarding to that, the occupational exposure to Al^{3+} dusts and fumes has been related with cognitive changes and possible brain impairments (Bast-Pattersen *et al.*, 1994; McLachlan, 1995). Finally, another important source of Al^{3+} intake is through drinking water. Natural concentrations in water are normally small but in urban areas may vary (Constantini & Giordiano, 1991) depending on the use of aluminium flocculents for purification purposes and to clarify the turbidity of drinking water (Lévesque *et al.*, 2000). Finally, the use of some medications has been also referred as an Al^{3+} source. For example, some epidemiological studies reported concentrations up to 5g/day in individuals that consume high doses of non-prescription aluminium-containing drugs, such as antiacids, buffered analgesics, antidiarroheal products, and hemorroidal medications (Lione, 1985; Nieober *et al.*, 1995).

However, the toxicokinetic studies of this metal highlighted the differential absorption and effects depending on the exposure route. The principal pathways for the absorption are oral, intranasal, transdermal, and parenteral (Roberts 1986; Exley, 2004). The oral intake presents a very low range from 0.06-1.5% (Moore *et al.,* 2000; Flaten*,* 2001; Yokel & McNamara*,* 2001) due to the dependence of several factors as pH, aluminium speciation and dietary agents (Deng *et al.*, 1998). The acidification environment of Al^{3+} increases the transport of the metal into the bloodstream and for these reason is common the use of citric acid in experimental models for oral treatment (Greger & Sutherland, 1997). The mechanisms that could explain this increase in Al^{3+} absorption are: enhanced aluminium solubility in the gastrointestinal tract, transport of aluminium citrate into mucosal cells, and opening of epithelial tight junctions that are present between mucosal cells (Taylor *et al*., 1998). Moreover, the intestinal absorption of Al^{3+} was shown to increase in various pathological conditions, such as Alzheimer's disease (Moore *et al.,* 2000).

The transport of aluminium in the bloodstream is performed bounded to various plasma proteins: 93% to transferrin, 6% to citrate and the remaining to hydroxide and phosphate (Harris *et al.,* 2003). The distribution of the metal in the body is not homogeneous in all the tissues and the highest levels are found in the bones and lungs

with approximately 50% and 25% of the 30 to 50 mg of aluminium body burden in the healthy human subject (Ganrot, 1986). Moreover, Al^{3+} is also accumulated in human brain, skin, lower gastrointestinal tract, lymph nodes, adrenals, and parathyroid glands (Tipton & Cook 1963; Hamilton *et al.*, 1973; Cann *et al.*, 1979; Alfrey, 1980). The metal percentage contained on each tissue fluctuates, but organs such as the brain, which present a blood brain barrier, usually contains low concentrations (Walker *et al.,* 1994; Andrási *et al.*, 2005; Yokel & McNamara, 2001).

1.3.2 Neurotoxicity

A recent neurotoxicological study in humans demonstrated that aged brains accumulate enough Al^{3+} to constitute a pathological risk (House *et al.*, 2012), and consequently is a factor able to promote the formation of reactive oxygen species in tissues. Also, Al^{3+} has been related with behavioural alterations (Miu *et al.*, 2003), memory and learning deterioration (Julka *et al.*, 1995), osteomalacia (Robertson *et al.*, 1983), dialysis encephalopathy (Bolla *et al.*, 1992), amyotrophic lateral sclerosis (Perl *et al.*, 1982), and parkinsonism (Garruto *et al.*, 1984). Its role in Alzheimer's disease is not clear, but it has been implicated in the development of neurofibrillar tangles (Zatta *et al.*, 2003; Walton, 2006). Our previous work demonstrated the ability of Al^{3+} to cross the blood brain barrier and accumulate into the rat brain (Sánchez-Iglesias *et al.*, 2007b), to reduce the activity of

some antioxidant enzymes (i.e. catalase, superoxide dismutase, glutathione peroxidise), and to enhance the dopaminergic degeneration induced by 6-hydroxidopamine in an experimental model of Parkinson's disease (Sánchez-Iglesias e*t al.*, 2009).

In spite of the broad bibliography there is not an agreement about the main mechanism for neurotoxicity, but the most important hypothesis is the aggravation of oxidative stress after metal exposition. However, some authors report differential properties attributed to aluminium as pro-oxidant (Zatta *et al.*, 2002; Exley, 2004) or antioxidant (Oteiza *et al.*, 1993; Abudakar *et al.*, 2004). The pro-oxidative properties have been shown *in vivo* and *in vitro* models, usually involving the stimulation of lipid peroxidation (Gutteridge *et al.*, 1985). The Al^{3+} ability to work as strong Lewis acid and the consequent reactivity with anion superoxide to form aluminium superoxide anion is probably the main mechanism involved on its toxicity (Exley, 2004). Also, has been related with a decrease in the antioxidant enzymes in different parts of the brain and promoting oxidative stress (Sánchez-Iglesias *et al.*, 2009). Numerous studies performed both *in vitro* and *in vivo* considered that the principal consequences of aluminium on the cerebral functions are mediated through cell membranes damage. Metals without redox capacity as aluminium were suggested to make fatty acids more available to the action of free radicals and therefore spreading lipid peroxidation (Oteiza *et al.*, 1993). The membrane alteration supposes a lack on

fluidity, variations in membrane potential, disruption of permeability and modifications on the bounded proteins (Palmeira & Oliveira, 1992).

Finally, Al^{3+} presents an important link with PD due to its capacity to interfere with dopaminergic metabolism. Studies performed in rat brain striatum showed a decrease concentration of the neurotransmitter (Ravi *et al*., 2000) and an alteration on the metabolite levels at hypothalamus (Tsunoda & Sharma, 1999). Indeed, the expression of the dopaminergic receptors D_1 and D_2 were also decreased (Kim *et al.*, 2007). These features generate a perfect frame for the onset of dopaminergic neurodegeneration and, in long term, of PD. For these reasons, some author purposes metal chelators like a potential treatment of neurodegenerative diseases since metals are considered as a pharmacological target (Gaeta & Hider, 2005).

1.3.3 Aluminium and mitochondria

Mitochondrial impairment and the foreseeable imbalance in the oxidative status of the cell are considered as two factors involved in the development of neurological disorders such as Parkinson's disease, as it has been previously remarked by Schapira (2008b). Previous studies also have revealed the interaction of Al^{3+} with cells to promote the mentioned effect, but the mechanism underlying the

neurotoxicity remains unclear (Kumar *et al.*, 2008; Sánchez-Iglesias *et al.*, 2009).

The ability of Al^{3+} to alter the function of this organelle depends on the dose and the exposition pathway (Swegert *et al.*, 1999; Dua & Gill, 2004; Niu *et al.*, 2005; Kumar *et al.*, 2008). The double-membrane structure of the mitochondria is a well-established goal of the metal toxicity by oxidative stress and affecting the bounded proteins activity. On one hand, Niu *et al.* reported in 2005 alterations in mitochondrial structure like local cavitation and cristae degradation. Also, other mechanisms like cellular depolarization and calcium influx were involved. Regarding to that, Tonitello *et al.* described in 2000 the binding of Al^{3+} to the mitochondrial inner membrane and the correlation with membrane permeability transition. The presence of thiol groups on the pore-forming structures emerges as a critical target to induce transition permeability (De Marchi *et al.*, 2004). Using both higher concentrations of Al^{3+} and *in vivo* exposition (i.e. >5mg/kg per day and i.p.), the metal causes swelling and destruction of mitochondrial cristae in nerve cells (Tang *et al.,* 2002) showing a widespread neurodegeneration in animals brain. On the other hand, the presence of the metal has been correlated with a decrease activity of enzymes, especially those related with divalent cations such as Mg^{2+} and Ca^{2+} (Trapp, 1980). The regulation of TCA remains in a higher degree in the influx of calcium in the matrix by promoting an increase in

dehydrogenases activity. For this reason, the presence of Al^{3+} alters its activity, particularly acting on aconitase (Zatta *et al.*, 2000; Mailloux *et al.*, 2006). Furthermore, the properties of the mitochondrial cytochromes cyt *a*, cyt *b*, cyt c_1, and cyt *c* and succinate dehydrogenase activity at the electron transport system are also altered (Kumar *et al.*, 2008).

USC
UNIVERSIDADE
DE SANTIAGO
DE COMPOSTELA

Chapter 2

Justification and aims

USC
UNIVERSIDADE
DE SANTIAGO
DE COMPOSTELA

Justification and aims of the thesis

The aetiology of Parkinson's disease is multifactorial and has been related with several biochemical alterations such as mitochondrial dysfunction, free-radical-mediated damage, excitotoxicity, and inflammatory changes (Schapira, 2008a). Most of these features present mitochondria playing a central role or at least triggering mechanisms that eventually promote cellular death. The energy flow is essential to keep the cellular function and homeostasis, particularly in human dopaminergic neurons that present a complex axonal arborization, a massive number of synapses (~1.0-2.4 million million synapses/SN*pc* neuron), and unmyelinated axons (Bolam & Pissadaki, 2012). Any factor disrupting the metabolism and consequently increasing oxidative stress and reducing ATP availability may promote apoptosis. For this reason, the underlying objective of this Thesis was to perform a bioenergetic study using isolated rat brain mitochondria in order to shed some light on the aetiology of Parkinson's disease. Taking into account the methodological difficulties due to the absence of an animal model including all the clinical manifestation of this disorder, this Thesis was focused on the analysis of a widely used neurotoxin model of Parkinson's disease through oxidative stress such is 6-hydroxydopamine and the study of a xenobiotic (i.e. aluminium) that could be related with the onset and development of

this syndrome. Within this framework, the following hypotheses are formulated:

- Bioenergetic studies by high-resolution respirometry rely on the optimal conservation of both mitochondria structure and function during the isolation procedure. However, free Ca^{2+} is released during tissue disruption and must be controlled by chelants to avoid mitochondrial impairment. Our first hypothesis is that metal chelants routinely used in the organelle isolation could modify mitochondrial function.

- 6-Hydroxydopamine model for Parkinson's disease through oxidative stress is mediated by an interaction with the mitochondrial function. Our second hypothesis is that, the molecular mechanism of 6-hydroxydopamine toxicity is due to specific chemical species made up of free radicals that disrupt bioenergetics. This effect may be prevented by the presence of antioxidant enzymes such as catalase and superoxide dismutase.

- Aluminium is accumulated into the brain of elder patients, thus representing a potential factor for the onset of Parkinson's disease. However, the mechanism of its neurotoxicity has been often associated with oxidative stress but still remains unclear. Our third hypothesis is that, Al^{3+} toxicity may

involve mitochondrial disruption and bioenergetics impairment.

Specific objectives

- To analyze a wide range of concentrations of the most used chelants (i.e. EDTA and EGTA) in order to establish a rat brain mitochondrial isolation protocol reporting the optimal conditions for our subsequent bioenergetics studies. This specific objective included a structural and a functional study of the isolated organelle.

- To assess mitochondrial bioenergetics in presence of 6-hydroxydopamine in order to determine its ability to modify bioenergetics parameters and to insight on the corresponding molecular mechanisms.

- To study the capacity of some antioxidant systems to mitochondrial impairment caused by the neurotoxicity of 6-hydroxydopamine in both rat brain mitochondria and human neuroblastoma cells (i.e. SH-SY5Y).

- To describe the underlying mechanism of 6-hydroxydopamine and gain insight on the nature of the free radicals species involved in its neurotoxicity.

- To analyze the *in* vivo and *in* vitro ability of Al^{3+} to affect the electron transport system and in this way modify the mitochondrial bioenergetics in the different respiratory steady-states.

- To determine the molecular mechanisms underlying Al^{3+} exposition on both coupling control ratios and enzymatic activities of each electron transport system complexes.

Thesis outline

In order to test the hypothesis and to achieve the specific objectives previously stated, three lines of work were carried out. Firstly, to obtain both structurally and physiologically well preserved mitochondria in order to perform the subsequent bioenergetic studies. This specific objective included an investigation on the effects caused by the required chelators, leading to the development of a mitochondrial isolation protocol covering the above mentioned requirements. The results of this first line of work are reported in **Chapter 4** of the present Thesis and have been recently published by

Iglesias-Gonzalez *et al.* (2013). Secondly, the study of 6-hydroxydopamine was developed to validate our respiratory assays and to analyse the bioenergetics alterations promoted by oxidative stress in different models (i.e. rat brain mitochondria and SH-SY5Y cells). The details and results of this approach are shown in **Chapter 5** of the present Thesis and have been published by Iglesias-González *et al.* (2012). Also, the aluminium ability to interfere on mitochondrial bioenergetics and eventually to promote oxidative stress was studied in both an acute *in vitro* model and in a short-term *in vivo* model. The results of this study are presented in **Chapter 6** and have been submitted for publication (Iglesias-González *et al.,* in review). Finally, **Chapter 7** presents a summary of the main results of this Thesis.

USC
UNIVERSIDADE
DE SANTIAGO
DE COMPOSTELA

Chapter 3

Material and Methods

USC
UNIVERSIDADE
DE SANTIAGO
DE COMPOSTELA

3.1 Reagents

All the reagents used to perform the experiments were purchased with the maximum purity available from Sigma-Aldrich (St. Louis, MO, USA) unless otherwise stated. The reagents used, dispose in alphabetical order, were: adenosine 5'-diphosphate sodium salt; albumin bovine serum essential fatty acid free; antimycin A; ascorbic acid; Bradford reagent; carbonyl cyanide p-(trifluoruromethoxy) phenylhydrazone (FCCP); catalase; cytochrome c; LDH assay kit (CytoTox-ONE^{TM}, Promega, Southampton, UK); Eagle's minimal essential medium (E-MEM); ethylenediamine-tetraacetic acid dipotassium salt, dehydrate (EDTA-2K); ethylene glycol-bis-(β-aminoethylether)-N,N,N',N',-tetraacetic acid (EGTA); foetal bovine serum; glutaraldehyde; L-glutamic acid monosodium salt; L-glutamine; 4-(2-Hydroxyethyl-)-piperazine-1-ethane-sulfonic acid (HEPES); 6-hydroxydopamine; lead citrate; magnesium chloride hexahydrate; L-malic acid; D-mannitol; malonic acid; non-essential aminoacids; oligomycin; osmium tetraoxide; penicillin; potassium chloride; protease inhibitor cocktail; potassium phosphate dibasic; pyruvic acid sodium salt; rapid ELISA kits for rodents (MitoSciences, Eugene, OR, USA); rotenone; sodium azyde; sodium cacodylate; sodium phosphate dibasic dodecahydrate; Spurr's epoxy resin; streptomycin; succinate disodium salt, hexahydrate; D(+)-sucrose; superoxide dismutase; sodium bicarbonate; sodium pyruvate; tetraphenylphosphonium chloride; and uranyl acetate.

3.2 Animals

Male Sprague-Dawley rats (*Rattus norvegicus*; 200–250g), provided by the breeder of the University of Santiago de Compostela, were used as animal model to develop this study. To facilitate their acclimatization, animals were housed by pairs in separate cages with *ad libitum* access to tap water and standard laboratory chow. The animal room was under controlled temperature (22 ± 1^{o}C) and 12h light-dark cycle (light on from 8:00h to 20:00h). All experimental protocols used were approved by the Ethical Committee of the University of Santiago de Compostela and conformed to the *European Community Council Directive of 24th November 1986 (86/609/EEC)*. Animals were housed over four days before the starting of experiments. After the acclimatization period, animals were treated as corresponding for each experimental group. To ensure a good yield in mitochondrial recovery, animals were deprived of food during the sixteen hours previous to the mitochondrial isolation (Fleischer *et al.*, 1979).

3.3 Animal treatments

Experimental design and animal treatment were evaluated by the Ethical Commission of the University of Santiago de Compostela. Furthermore, both the treatment and care of rats were done by personnel with the European accreditation for animal care

and handling. Animal treatments were designed for each objective as follows:

- *Effects of chelatants on mitochondrial isolation:*

Thirty six male Sprague-Dawley rats were used to analyze the effect of chelants in mitochondria bioenergetics. Animals were randomly divided in six experimental groups: the first three groups containing six rats for every group were used to isolate rat brain mitochondria with 1-3mM EDTA in the isolation medium; the second three groups containing six rats for every group were used to isolate rat brain mitochondria with 1-3mM EGTA in the isolation medium.

- *Protective role of antioxidant enzymes on a 6-hydroxydopamine model of Parkinson's disease by oxidative stress:*

Sixty six rats were used to perform the different experiments designed to evaluate the neurotoxicity of 6-OHDA and the role of antioxidant enzymes. Animals were randomly divided in three experimental groups: eighteen rats were used for the determination of the IC_{50} for 6-OHDA; thirty rats were used to study the effects of 6-OHDA on the activity of antioxidant enzymes; eighteen rats were used to evaluate the effects of 6-OHDA on the activity of the different complexes of mitochondrial respiratory system.

- *Effects caused by aluminium on rat brain mitochondria:*

Twenty four Sprague-Dawley rats were used to analyze the effect of aluminium on mitochondria bioenergetics. Animals were randomly divided in four experimental groups: for *in vitro* experiments, two groups with six rats for every group were used as control or treated mitochondria; for in vivo experiments, the control group received a daily i.p. saline solution for ten days, and the treated group received a daily i.p. dose of aluminium (10mg of Al^{3+}/Kg/day) for ten days.

3.4 Mitochondrial Isolation

The protocol used to isolate rat brain mitochondria was based in the method originally described by Berman & Hastings (1999) and Rosenthal *et al.* (1987). To maximize both mitochondria recovery and the purity of mitochondrial preparations to be used in the planned experiments on bioenergetics and oxidative stress, a series of modifications were introduced that will be discussed in detail afterwards.

Animals were stunned with carbon dioxide prior to decapitation in order to minimize suffering. To assure that anoxia did not alter bioenergetic parameters, a preliminary study was performed, showing that our mitochondrial population is not sensitive to the carbon dioxide treatment (data not shown). After

animal sacrifice, the brain was quickly removed and immersed in an ice-cold isolation buffer (IB) containing 225mM mannitol, 75mM sucrose, 5mM HEPES, 3mM EDTA-2K, 1mg/mL fatty acid free BSA (pH 7.4) and supplemented with a proteases inhibitor cocktail.

Forebrains were dissected with a rostral transection at the level of the two colliculli and meninges were carefully pulled out with a curve forceps. The removal of meninges and residual blood from brain tissue is essential to avoid further disturbances caused by a contamination with erythrocytes. The resulting tissue was weighed and cut in small pieces for subsequent manual homogenization in a Dounce-type glass homogenizer (15mL maximum volume and pestle clearance: 0.089-0.165mm and 0.025-0.076mm) using IB (1/10, w/v). The homogenate resulting from 3 g of nervous tissue were combined, distributed in polycarbonate tubes, and then centrifuged at 600×*g* for 10min. The centrifuge used for the isolation was a Beckman Avanti™ J-25 (Beckman Instruments, Palo Alto, CA, USA) provided with a JA-20 fixed angle rotor and set at maximum acceleration and low deceleration for speed ramps. The supernatant obtained was reserved in a chilled recipient and the pellet resuspended in 10mL of IB, followed by centrifugation in the conditions above described to recover the fast-sedimented mitochondria. Then, the resulting supernatants were pooled together and centrifuged in four tubes at 12,000×*g* for 8min. The pellets were reconstituted in IB, distributed into two tubes containing each a final volume of 10mL, and

centrifuged at 12,000×*g* for 10min. The new pellet shows some layers that differ in consistency and color, with a white fluffy layer on the top that contains myelin, synaptosomes, and lipids. The brown mitochondria obtained, after a carefully discarding of the synaptosomal layer with a Pasteur pipette, were resuspended in 10mL of IB and recentrifuged at 12,000×*g* for 10min. The resulting mitochondria pellet was reconstituted in enough volume of IB without chelators to obtain a final concentration of ~20-25mg/mL. Then, the mitochondrial pellet was homogenized using a Dounce-type homogenizer (7mL maximum volume and pestle clearance: 0.071-0.119mm and 0.02-0.056mm), stocked in chilled Eppendorf tubes and, maintained into an ice-bath until the assays were carried out. This procedure yields 8-10mg of protein per rat brain, and the mitochondria population remains metabolically active for 4–5h. All procedures were performed at 4ºC in order to maintain the temperature under control throughout all the isolation process.

3.5 Mitochondrial respiration

Steady-states and rates of oxygen uptake were determined using an Oxygraph-2K high-resolution respirometer (Oroboros® Instruments, Innsbruck, Austria). The respiration was measured with 0.2-0.6mg/mL of mitochondrial protein in chambers filled with 2mL of a standard respiration medium (RM) containing 110mM sucrose, 60mM KCl, 10mM KH_2PO_4, 3mM $MgCl_2$, 0.5mM EGTA and 1mg/mL

fatty acid free BSA (pH 7.4). The respiratory fluxes were fuelled for complex-linked substrates as corresponds: Complex I (10mM glutamate, 2mM malate and 5mM pyruvate); Complex II (0.5µM rotenone and 10mM succinate) and; whole electron transport system activity (10mM glutamate, 2mM malate and 5mM pyruvate, 10mM succinate). For each group a substrate-uncoupler-inhibitor titration (SUIT) protocol was applied for respiratory measurements. Then, experiments started with mitochondria in our RM and with the chemical under study in the incubation if it corresponds. Afterward, the corresponding substrate was added and the oxygen consumption flux rate registered during 5min or until the achievement of a steady-state. To obtain the active state (i.e. State3, OXPHOS), ADP (2.5mM) at saturating concentration was used and the oxygen uptake measured for 5min. To avoid the bias in our measurement of the resting state due to ATP*ase* activity, oligomycin (2µg/mL) was added to obtain State 4_0 (i.e. LEAK). Then, maximal ETS capacity (i.e. ETS_{max}), with electron convergent electron flow from Complexes I or/and II was reached after the titration with FCCP as uncoupler in successive steps. If the experiment is Complex I-linked, rotenone (0.5µM) was added to the chamber, and if it is complex II-linked, malonate (5mM) was used as inhibitor. Finally, to evaluate residual respiration, the Complex III inhibitor antimycin A (2.5µM) was used. The oxygen flux obtained from the last step is subtracted to the other fluxes in order to eliminate the oxygen-noise generated in side-reactions. All the

experiments were performed in the double-chamber system of the respirometer at 37°C and using a constant stirring of 500rpm.

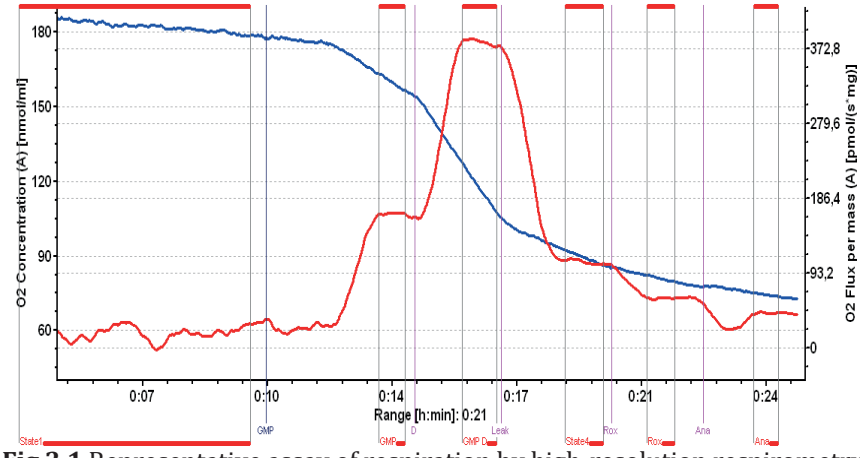

Fig 3.1 Representative assay of respiration by high-resolution respirometry. Blue: O_2 Concentration. Red: O_2 Flux per mass.

3.6 Mitochondrial membrane potential

The membrane potential was measured with 0.3mg/mL of mitochondrial protein in chambers filled with 2.6mL of a standard RM containing 110mM sucrose, 60mM KCl, 10mM KH_2PO_4, 3mM $MgCl_2$, 0.5mM EGTA, and 1mg/mL fatty acid free BSA (pH 7.4). RM was supplied with 1µM of TPP^+ to assess the ion flux between the medium and the mitochondrial matrix during the experiment, according to the procedure described by Fasching & Gnaiger (2009). In order to obtain the membrane potential on each respiratory steady-state, we applied the SUIT protocol described for mitochondrial respiration. All the experiments were carried out after evaluation of the optimal concentration TPP^+ to avoid the respiratory

inhibition observed when using high concentrations of TPP^+. Finally, the results were transformed to percentage in order to make easier the comparison with the corresponding control.

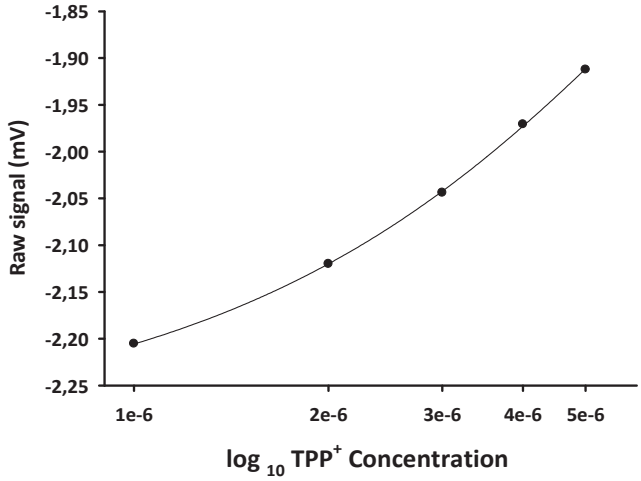

Fig. 3.2 Calibration curve obtained for the membrane potential (r^2 = 0.9997; y = -4.05 E^9 x^2 + 9.78 E^4 X – 6.8985).

3.7 Activity of Respiratory Chain Complexes

The enzymatic activity for each complex of the ETS was evaluated performing an ELISA (monoclonal antibody pre-bounded ELISA kits, MitoSciences®, Eugene, OR, USA) or by the spectrophotometric assay described below. ETS complexes are multi-subunit enzymes that to be evaluated by ELISA must be extracted in a non-denatured state, in order to keep their enzymatic activity and to facilitate their recognition by antibodies. For these reasons,

mitochondrial samples were pre-treated with lauryl maltoside, a non-ionic detergent used for both stabilization and activation of enzymes.

Mitochondria samples were distributed in Eppendorf tubes and centrifuged at 20,000*xg* for 20min at 4^{o}C in an Eppendorf centrifuge, model 5417R (Eppendorf AG, Hamburg, Germany). Then, the resulting pellet was reconstituted to 5-10mg/mL in extraction buffer (1.5% lauryl maltoside) with protease inhibitors added. The resulting suspension was well-mixed and incubated on ice-bath with continuous agitation for 30min. Then, samples were centrifuged at 12,000*xg* (Complex I) or 20,000*xg* (Complex II-V) for 20min at 4^{o}C. The resultant supernatants were collected and the protein concentration measured by the method of Bradford, following by adjustement to 5mg/mL with phosphate-buffered saline (PBS; 1.4mM KH_2PO_4, 8mM Na_2HPO_4, 140mM NaCl and 2.7mM KCl, pH 7.3). The only exception to this extraction method is to evaluate ATP synthase, which requires a previous freeze/thaw cycle and wash the pellet to remove any soluble, non-membrane associate proteins.

3.7.1 Complex I

The evaluation of NADH dehydrogenase activity was determined following the oxidation of NADH to NAD^+ and the simultaneous reduction of a dye (λ_{max}= 450nm). This assay measures the diaphorase-type activity of Complex I, which is not dependent on

the presence of ubiquinone and, as consequence, is rotenone-insensitive. However, any post-translational phosphorylation or assembly deficiency occurring during the different treatments used in the experiments were detected by the assay.

Previous extracted supernatants were diluted in the incubation solution provided by the kit (1:1, v/v) and 200µL of the resultant suspension added to each well of the microplate. One well containing only buffer was used as a negative control. The microplate containing the sample was incubated for 3h at room temperature with a continuous light agitation. Then, wells were emptied by turning the plate over and shaking out any remaining liquid. To ensure a good developing of the ELISA, 300µL of PBS were added for rinsing, wells were emptied again, and this operation was repeated at least once more again. Finally, 200µL of the assay solution (a mixture of reagents 1 and 2 provided by the kit) were added to each empty well, bubbles were popped, and the microplate placed into the microplate reader. An ASYS UVM340 microplate reader (ASYS Hitech GmbH, Eugendorf, Austria) was used and the kinetics followed at 450nm for 45min with a lecture interval of 1min.

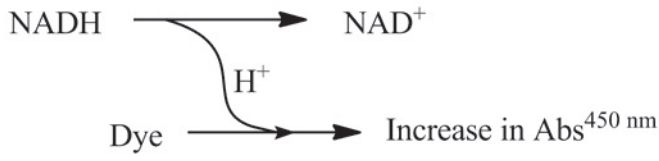

Complex I activity is proportional to the increase in absorbance at 450nm and is obtained as the linear rate of increase over time. The activity is expressed as the change in absorbance per minute per amount of sample loaded into the well or as a percentage of the control.

3.7.2 Complex II

The enzymatic activity of Complex II was determined as a decrease in absorbance at 600nm. This enzymatic complex catalyzes an electron transfer from succinate to the electron-carrier ubiquinone (Q) to give fumarate and ubiquinol (QH_2). The formation of ubiquinol is used as reductant agent of DCPIP, decreasing its absorbance at 600nm and recycling the substrate ubiquinone as shown below.

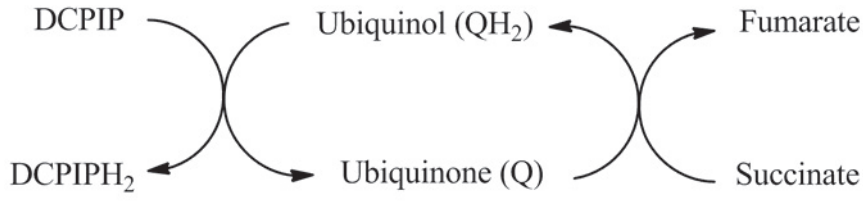

The succinate-coenzyme Q reductase was extracted as it has been previously described, followed by dilution with the incubation solution provided by the kit (1:1 and 1:2, v/v). 50µL of the resultant suspension were added to each well of the microplate. One well with buffer alone was included as a negative control. The filled microplate was incubated for 2h at room temperature with a continuous light agitation. Afterwards, wells were emptied by turning the plate over and shaking out any remaining liquid. To ensure a good developing of the ELISA, 300µL of PBS were added to each well for rinsing, the wells were emptied again, and the operation repeated at least once more again. Then, 40µL of lipid solution was added and the microplate incubated for 30 min at room temperature with continuous agitation. Finally, 200µL of assay solution (a mixture of ubiquinone 2, succinate, DCPIP and, activity buffer provided with the kit) were added to each empty well, the bubbles popped, and the microplate submitted to the microplate reader. The kinetics was followed microplate at 600nm for 60min, using a lecture interval of I min. Shaking is not allowed before or between readings.

Complex II activity is determined from the decrease in absorbance at 600nm minus the background, and is obtained as the linear rate over the time. The activity is expressed as the change in absorbance per minute or as a percentage of the control.

3.7.3 Complex III

Complex III activity was estimated by monitoring the reduction of cytochrome c in the presence of coenzyme Q_{10}, according to a slight modification introduced to a previously reported procedure (Zhang *et al.*, 2004). Briefly, cytochrome c (15µM) and coenzyme Q_{10} (100 µM) were added to an assay medium containing 25mM KH_2PO_4, 2mM KCN, 5mM $MgCl_2$, and 2mg/mL rotenone at pH 7.2. The previously extracted sample (0.25mg/mL) was added to the mixture and the increased in the absorbance recorded at 550nm for 5min. Data were expressed as percentage of activity compared to control.

3.7.4 Complex IV

The evaluation of cytochrome c oxidase activity was determined following the oxidation of cytochrome c at 550nm. Previous extracted samples were diluted with the solution 1 provided with the kit (1:1, 1:2, and 1:4; v/v). Two hundred µL of the resulting suspension were pipetted into each well and the microplate incubated for 3h with continuous agitation. Once the monoclonal antibody has immobilized the enzyme, wells were emptied by turning the plate over and shaking out any remaining liquid. To ensure a good developing of the ELISA, 300µL of PBS were added to each well for rinsing, the wells were emptied again, and the operation repeated

at least once more again. Then, 200µL of assay solution (a mixture of reagent C and solution 1 provided with the kit) were added to each empty well, bubbles popped, and the microplate placed into the microplate reader. The kinetics was followed at 550nm for 2h, using a lecture interval of 1min.

Complex IV activity was calculated from the increase in absorbance at 550nm in the linear region and comparing it with control and null samples. The activity is expressed as the change in absorbance per minute or as a percentage of the control.

3.7.5 Complex V

The enzymatic activity of ATP synthase was determined from the decrease in absorbance at 340nm, resulting from the coupled consumption of NADH. The enzymatic complex that forms the F_1F_0ATP*ase* catalyzes the hydrolysis of ATP to ADP and this reaction is coupled to the oxidation of NADH to NAD^+ as shown below.

The extracted sample as previously described was diluted in the incubation solution 1 provided with the kit to 1:1 and 1:2, and 50µL of the resultant suspension added to each well of the microplate. To include a negative control, one well with buffer was added to the experiment. The microplate with the sample was incubated for 3h at room temperature with continuous agitation.

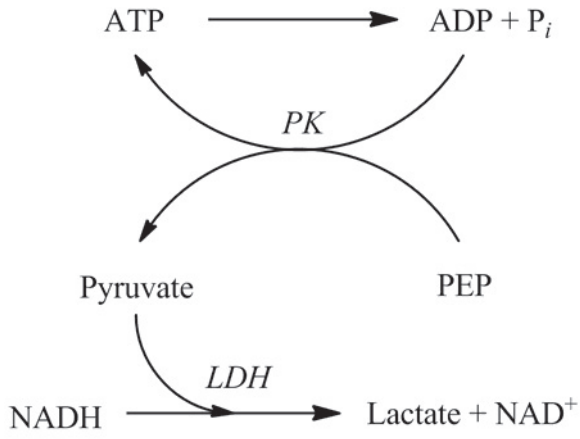

Then, wells were empty by turning the plate over and shaking out any remaining liquid.To ensure a good developing of the ELISA, 300µL of solution 1 was added to rinse, wells were emptied again, and the operation repeated at least once more. Then, 40µL of lipid mix solution were added and the sample incubated at room temperature for 45min with agitation. Finally, 200µL of the reagent mixture were added to each empty well and bubbles popped. To read the kinetics, the microplate spectrophotometer was programmed for a lecture interval of 1 min during 2h at 340nm.

The Complex V activity is proportional to the decrease in absorbance at 340nm and is obtained as the linear rate of decrease over time. The activity is expressed as the change in absorbance per minute per amount of sample loaded into the well or as a percentage of the control.

3.8 Enzymatic markers

The activity of the enzymatic markers lactate dehydrogenase (LDH), cytochrome oxidase c (CytcOx), and citrate synthase (CS) were determined by spectrophotometric techniques and these data used to evaluate the purity and integrity of the mitochondrial population.

3.8.1 Lactate dehydrogenase

The LDH enzyme is located in the cytosol of the cell and, for this reason, was used as a marker for the cytosolic and nuclear fractions during the isolation. The method used was previously published by Bergmeyer *et al.* in 1965. Sample was sonicated (10% amp. for 2s) in an ice-bath to assure the release of the enzyme from the mitochondrial suspension. Further, 2.8mL of PBS containing 0.23mM β-NADH and 0.33% Triton X-100 were combined with 100µL of sample and incubated until 37ºC were reached. Then, 100µL of 1.4mM pyruvate were added and the decrease in absorbance at 340nm monitored for 5min using a PerkinElmer Lambda 35 spectrophotometer. To obtain LDH activity (U/mL) a molar extinction coefficient for β-NADH of ε= 6,300$mM^{-1}s^{-1}$ was used.

3.8.2 Cytochrome c oxidase

The cytochrome c oxidase activity was used as a mitochondrial marker for the inner membrane space. Therefore, CytcOX is very useful to evaluate the integrity of the external membrane. The spectrophotometric method applied is based in the previous publication of Sampson & Allen in 2001. A micro-cuvette was filled with 400µL of PBS 80mM and 100µL of our sample, followed by thermostatization at 25ºC. Two minutes later, 40µM of reduced cytochrome c were added and the kinetics monitored at 550nm for 30s. A molar extinction coefficient of ε= 28,500$mM^{-1}s^{-1}$ was applied to obtain the final activity of the enzyme. A fresh solution of the reduced form of cytochrome c had been always prepared prior to the assay.

3.8.3 Citrate synthase

The release delay of citrate synthase, or latency, was used as a mitochondrial marker for internal membrane integrity. The method applied was previously described by Clark *et al.* in 1997. The mitochondrial sample was processed in two different manners to obtain the latency: a first group was centrifuge at 12,000*xg* for 2min; a second group was incubated with 0.33% triton X-100 during 10 min in an ice-bath and then processed as in the previous group. In an spectrophotometry cuvette, 100µL of our sample were added to the

assay medium (DTNB 0.01mM, oxaloacetate 0.52mM, acetil-CoA 0.1mM in TRIS 0.2M buffer, pH 8.0), following by monitoring of the change in absorbance at 412nm during 3min at 30ºC. To calculate the final activity of the enzyme, a molar extinction coefficient for DTNB of ε= 13,600$mM^{-1}s^{-1}$ was used. All the reagents, with the exception of the TRIS buffer, were freshly prepared.

3.9 SH-SY5Y cells line culture

Human neuroblastoma SH-SY5Y cells were grown at 37ºC in Dulbecco's Modified Eagle Medium (DMEM), containing 10% of foetal bovine serum, 100U/mL of penicillin and 100µg/mL of streptomycin. For culture preparation, cells were removed from liquid nitrogen and warmed in a water bath at 37ºC during 1-2min for acclimatization. Carefully, SH-SY5Y cells were placed in a falcon tube containing 10mL of DMEM and centrifuged at 2000rpm for 5min. The resultant pellet was reconstituted in 1mL of fresh DMEM and gently mixed with a pipette. Then, the cellular suspension was transferred to a 25 cm^2 flask containing 9mL of pre-warmed DMEM. The plate was introduced in an incubator at 37ºC, 5% CO_2 and 95% of air until the cellular confluence was around 60-70% (4-7 days of grow). The DMEM was renewed each 2-3 days to maintain a constant input of nutrients.

Once the confluence was achieved cells must be trypsinized and transferred to a 12-wells plate, with Poli-D-Lysine coverslips, to facilitate the adherence of the culture. The SH-SY5Y cells grow as a mixture of floating and adherent cells. For this reason, the medium was removed and centrifuged at 2,000rpm for 5min to recover the floating cells. Next, the flask was briefly rinsed with 2mL of 0.25% trypsine-0.53mM EDTA solution to remove all traces of serum and, 2mL of trypsine-EDTA solution was added to the flask and cells were observed under an inverted microscope until cell layer is dispersed (~15min). To avoid clumping, agitation is not recommended and, if the cells were difficult to detach, flask was placed at 37ºC to facilitate dispersal. The plate was introduced in an incubator at 37ºC, 5% CO_2 and 95% of air until the cellular confluence was around 80-90% (4-7 days of grow). The DMEM was renewed each 2-3 days to maintain a constant input of nutrients.

3.10 LDH cytotoxicity assay

Cellular death was fluorimetrically quantified by monitoring the activity of the cytoplasmic enzyme LDH released by cells with damaged plasma membranes and comparing this data with that obtained after a complete lysis of cells. SH-SY5Y cells grown onto 96-well plates were treated as described above. LDH activity was determined using the CytoTox-ONETM assay kit (Promega, Southampton, UK), according to manufacturer's instructions. Briefly,

CytoTox-ON reagent was added to the culture medium (1:1, v/v) up to 100 µl on each well, following by plate shaken for 30s. After 20min of plate incubation at 37ºC, stop solution supplied with the kit was added and fluorescence recorded with a microplate spectrofluorometer (Spectra Max Gemini XS, Molecular Devices, Sunnyvale, CA, USA), using an excitation wavelength of 560nm and an emission wavelength of 590nm. LDH release was quantified by comparison with 100% LDH release and was obtained using the lysis solution supplied with the kit.

3.11 Electron microscopy

Mitochondria samples were centrifuged at 13,000rpm for 30s, fixed by immersion for 45min in 2.5% glutaraldehyde in 0.15M sodium cacodylate buffer (pH 7.3), postfixed with 2% OsO_4 in the same buffer, dehydrated, embedded in Spurr's epoxy resin, and sectioned. Sections were stained with uranyl acetate and lead citrate and examined in a Zeiss 902 electron microscope (Carl Zeiss, Oberkochen, Germany) at 80kV accelerating voltage and film magnification of 20,000× or 12,000×.

3.12 *p*-Quinone formation during 6-hydroxydopamine autoxidation

The formation of *p*-quinone during 6-hydroxydopamine autoxidation was monitored spectrophotometrically at 490nm. The incubation medium was a buffer solution (Na_2PO_4/ KH_2PO_4 isotonized

with KCl, pH 7.4) and p-quinone formation was followed after the addition of 20µl of a fresh stock of 6-OHDA (20µM) dissolved in 1mM KCl (pH 2.0) to prevent its autoxidation. Final volume of the incubation was 400µl and all concentrations are final concentrations in the incubation.

3.13 Total protein concentration

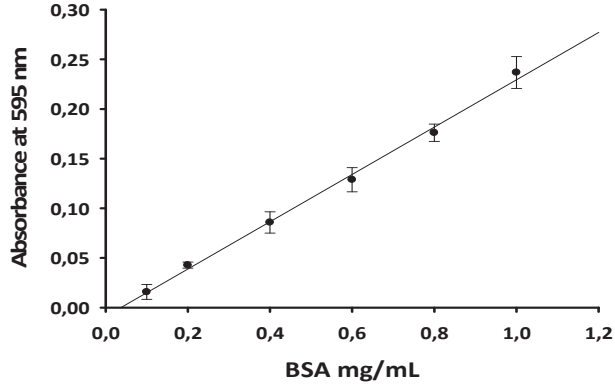

Fig. 3.3 Calibration curve obtained for the Bradford assay (r^2 = 0.9962; y = 0.2383 x – 0.0088). BSA was used as pattern diluted in isolation buffer. Each data represents mean ± S.d. for three replicas. The regression was performed with the programme SigmaPlot 11.0.

The method of Bradford was used to determine total protein concentration in mitochondrial samples from rat brain. The Bradford assay is based in the formation of a complex between the Brilliant blue G and proteins in solution. The resultant complex protein-dye, shift the absorption dye from 465 to 595nm in a proportional amount

to the protein content of the solution. To obtain the resultant concentration of protein a standard curve performed with BSA in a range of 0.1-1.4mg/mL were used.

A microplate was filled with 250µL of Bradford reagent at room temperature and 10µL of the mitochondrial suspension added. To assure a correct measurement of protein concentration, samples were used at 1:1, 1:10 and 1:100 dilutions. Furthermore, a standard curve with BSA in IB or PBS was performed. The microplate was incubated at room temperature for 20min with continuous agitation prior to the measurement of the absorbance in a microplate spectrophotometer ASYS UVM340 at 595nm. The net absorbance was plotted versus the protein concentration of each standard to obtain the total concentration.

3.14 Statistics

The Sigmaplot statistical software package version 11.0 (Dundas Software LTD., Germany) and Statgraphics version Centurion 16.1.5 (Statpoint Technologies, Inc., Warrenton, V, USA) was used to analyze the data from this study. Routinely, descriptive statistics and Analysis of variance (ANOVA) was performed to compare the effect of the different treatments. For comparison of average between two independent groups t-student was used. The distribution of the data was always checked and if is not normal was transformed with

common logarithms or square root. Post-hoc study was done with Holm-Sidak or Bonferroni. Results were considered significant when $p<0.05$.

Chapter 4

A Simple method for isolating rat brain mitochondria with high metabolic activity: Effects of EDTA and EGTA

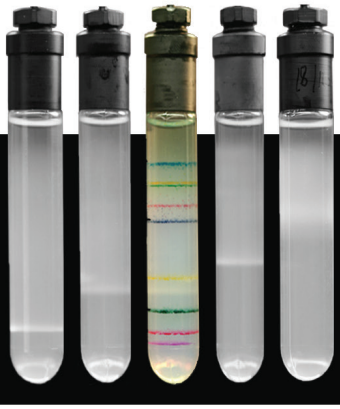

This chapter has been recently published as article in Journal of Neuroscience Methods, 213, 39-42. 2013.

Abstract

Isolated mitochondria are widely used in metabolic and oxidative stress studies for neurodegenerative diseases. In the present work, the influence of EGTA and EDTA has been tested on a sucrose-based differential centrifugation protocol in order to establish the optimal concentrations to be used in this process. Our results showed alterations in both active and resting respiration, which were dependent on both the addition of EDTA or EGTA to the isolation buffer and the chelator concentration used. However, the addition of chelator to the isolation medium does not modify the mitochondria structure as assessed by both distribution of biological markers and electron micrography in the final pellet. Our results endorse this protocol as the method of choice for metabolic and oxidative stress experiments with fresh isolated rat brain mitochondria.

USC
UNIVERSIDADE
DE SANTIAGO
DE COMPOSTELA

4.1 Introduction

Mitochondria isolation has recently been revealed as one of the main tools for the study of the bioenergetics of neuronal disorders. Post-mortem studies (Schapira, 2008b) have shown that neuronal cells affected in certain disorders such as Parkinson's disease, Friedrich's ataxia, and amyotrophic lateral sclerosis present alterations in the electron transport system, markers of oxidative stress, and fluctuation in metabolic parameters. To evaluate these parameters, the study of neurodegenerative disorders requires a precise isolation of mitochondria, preserving metabolic activity and an intact membranous system, both related to the activity of the ETS and maintenance of the membrane potential. Nowadays, we know that the released of free Ca^{2+} ions during the isolation process are one of the most influential factors on the quality of the mitochondria preparation. For this reason, EGTA and EDTA are commonly added to the isolation media used.

Isolation methods to obtain mitochondria from neuronal tissue have been widely described in the literature (Whittaker, 1968; Booth & Clark, 1978; Berman & Hastings, 1999; Lesnefsky & Hoppel, 2006; Frezza *et al.*, 2007; Fernández-Vizarra *et al.*, 2010; Sims & Anderson, 2008). The main difference to previously reported protocols resides in the composition of the isolation buffer and in the application of isopycnic or differential centrifugation. Indeed, these parameters strongly influence the bioenergetic parameters and consequently

make it difficult to compare different studies. Classical procedures for organelle isolation are commonly based on the formation of a density gradient with polymeric compounds such as Ficoll or Percoll (Clark & Nicklas, 1970; Cohen *et al.*, 1997). These compounds are essentially non-osmotic, with relatively low densities and high viscosities, but they require a high-speed centrifugation and long isolation times to achieve an efficient gradient. Furthermore, sucrose gradients exhibit high osmotic activity and consequently remove water from membrane-bound particles, thus causing damage to membranous organelles, even though its gradients are formed at a relative low speed of centrifugation. On the contrary, sucrose-based differential centrifugation maintains the osmotic pressure highly controlled, but fails in isolating particles with similar sedimentation coefficients. This present study addresses the ability of chelators to modify structural and functional parameters of our mitochondrial population. In order to test mitochondria functionality we performed a respiratory assay to determine the respiratory oxygen consumption rates and the respiratory control ratio (RCR).

4.2 Experimental design and methods

Thirty six male Sprague-Dawley rats (200-250g) were used to perform the here reported study. Animals were randomly divided in six experimental groups: the first three groups were used to isolate rat brain mitochondria with 1-3mM EDTA in the isolation medium; the second three groups were used to isolate rat brain mitochondria with 1-3mM EGTA in the isolation medium. All the procedures used are detailed in Chapter 3. To carry out this study we used the following methodological procedures: mitochondrial isolation, mitochondrial respiration, enzymatic markers (LDH, CytCOx, and CS), electron microscopy, and total protein concentration.

4.3 Results

The study of mitochondrial morphology is an essential step when the main objective is to optimize the isolation protocol or when toxicological actions on organelle are been analyzed. The purity of the isolated mitochondrial fraction and its morphology were analyzed using molecular markers (Table 4.1) and electron microscopy (Fig. 4.1 A-B), respectively. Electron micrographs of crude mitochondrial fractions obtained from rat forebrain homogenates showed a mitochondria population with minor contamination by traces of myelin and other membranous components (Fig. 4.1A). It has also been observed that some of the isolated synaptosomes contain

internalized mitochondria (Fig. 4.1B), which exhibited a high preservation state of both cristae and external membrane.

Table 4.1 *Biochemical markers used with homogenates and mitochondrial fractions*

	Specific activity		Relative activity
	Homogenate	Mitochondria fraction	
LDH	30 ± 0.60	12 ± 0.30	0.4
CytcOx	33 ± 8.30	86 ± 13.00	2.6
CS	0.33 ± 0.02	2.6 ± 0.01	7.9

Table 4.1 shows the specific and relative activities of the mitochondria markers used for assessing the purity and integrity of the isolated rat brain mitochondria. In particular, LDH was used as a marker for cytosolic contamination and its activity was measured in both brain homogenates and final mitochondria pellets. The specific activity of LDH in forebrain homogenates (30nmol/min/mg protein) was 40% higher than that found in mitochondrial fractions (12nmol/min/mg protein) (Table 1). Otherwise, CytCOx was used as a marker for mitochondria population and also to assess the integrity

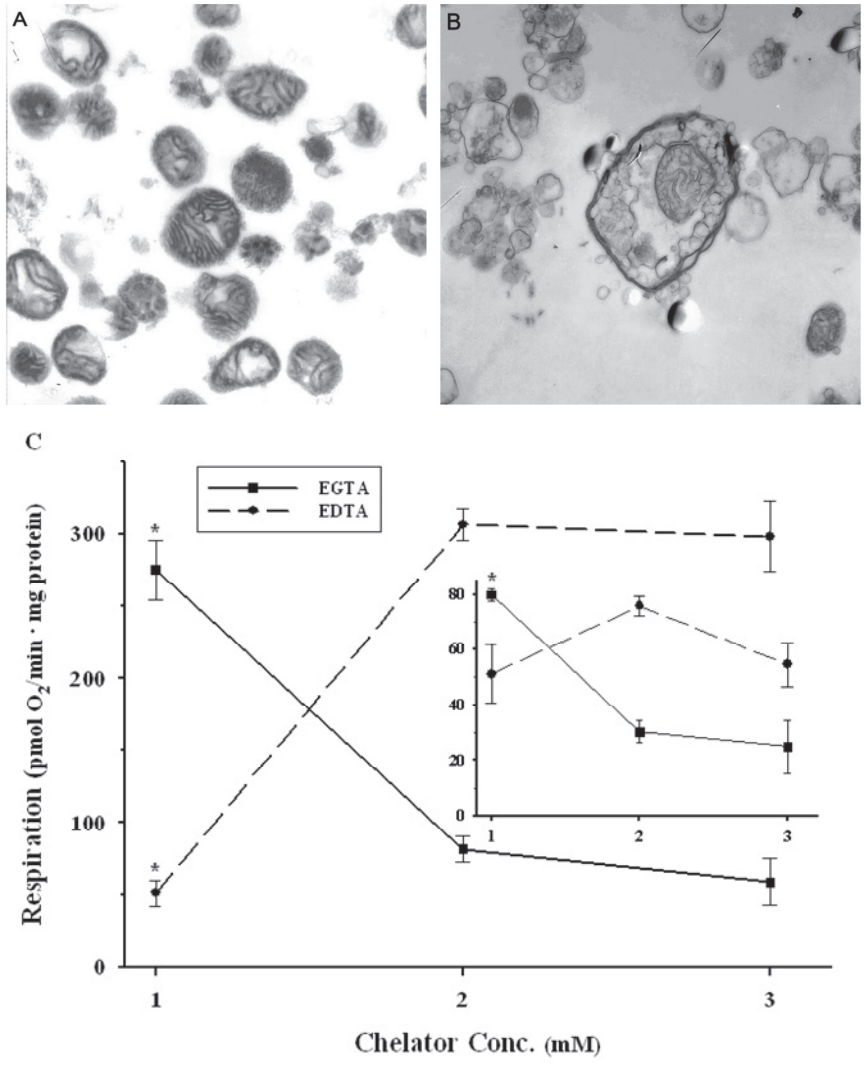

Fig. 4.1 Study of the morphology and structural function of mitochondrial fractions. (A and B) Electron microscope images showing a representative mitochondrial pellet and a detail of a synaptosomal inclusion. The magnification was fixed at 20,000× and 12,000×, respectively. (C) Mitochondrial respiratory measurements performed with high-resolution respirometry. Active respiratory state in presence of progressive concentrations of chelator added to isolation buffer. Resting state is showed in small graph. *Significant difference within groups at $p < 0.05$.

of the outer membrane. Mitochondrial fractions showed an enriched pellet in mitochondria (86nmol/min/mg protein) when compared with the value obtained in brain homogenates (33nmol/min/mg protein), representing a relative activity of 2.6. CS was used as both a marker for the integrity of the inner mitochondrial membrane and as the principal hallmark for the matrix of this organelle. The mitochondrial-enriched fraction (2.6mol/min/mg protein) exhibited an increase in CS relative activity of 7.9 when compared with the values found in the initial forebrain homogenate (0.33mol/min/mg protein). All mitochondrial fractions showed latencies over 10, which confirmed the integrity of the inner membrane. Thus, our results confirmed that the mitochondrial population obtained by the here reported procedure was formed of well-preserved mitochondria.

The viability of performing metabolic experiments with the isolated organelles was assessed by measuring the electron transport system activity linked to complex I, using high-resolution respirometry. As shown in Fig. 4.1C, the presence of EDTA in isolation buffer improved the active (state 3) respiratory rate but did not significantly alter the resting state (State 4_0). On the contrary, EGTA dramatically decreased both respiratory states due to an increase concentration added to the isolation buffer. According to Fernández-Vizarra *et al.* (2010), a coupling value with NADH-linked substrates higher than 4 is indicative of well-coupled mitochondria. The RCR values obtained

were over six for 3mM of EDTA, which corroborates the presence of both enriched and well-preserved mitochondria in our preparations.

4.4 Discussion

The assessment of mitochondrial function is a widely used tool in the aetiological study of models for neurodegenerative disorders such as Alzheimer's disease, Parkinson's disease, and amyotrophic lateral sclerosis (Duchen, 2004). Nowadays, the development of oxygen-selective electrode systems are more precise than Clarke-type electrodes, such those used in high-resolution respirometry, and provide a new insights into the bioenergetics of these disorders. High-resolution respirometry requires mitochondria to be structurally and physiologically well preserved in order to detect very low variations in the oxygen consumption rate. Due to these requirements, the choice of an appropriate protocol to isolate the organelles is a key point in bioenergetics studies. In this study we compare the function and structure of a mitochondrial population obtained by differential centrifugation in the presence of progressive concentrations of the most used chelators. Both our electron micrographs (Fig. 4.1A and B) and biochemical markers (Table 4.1) showed a highly enriched mitochondrial fraction with a preserved phenotype, characterized by both spherical shapes and little swollen cristae, and a low presence of myelin. Furthermore, electron micrographs also showed the presence of intact outer and inner

mitochondrial membranes with cristae homogenously distributed throughout the entire mitochondria matrix, which agrees with the conservative status described by Whittaker (1968). The presence of chelators did not alter both structural and functional properties of isolated organelles, suggesting that our media prevents from both the swelling and opening of mitochondrial permeability pore. Also, the results obtained in analyzing the purity of mitochondrial fractions demonstrated a higher decrease in LDH activity and an increase in both CytCOx and CS activities (Table 4.1). These results corroborate the achievement of fractions highly enriched in mitochondria and with a high degree of integrity (Schnaitman and Greenawalt, 1968). Also, biological markers showed no alterations caused by the presence of different amounts of chelators.

Cytosolic calcium (Ca^{2+}) represents one of the main secondary messengers in cells and, consequently, its free concentration is highly regulated. The ability of mitochondria to buffer Ca^{2+} shows a three phase behaviour related to the extramitochondrial and matrix concentration of free Ca^{2+} (for a review see Szabadkai & Duchen, 2008). The kinetic aspect of this behaviour depends on the activity of different transporters and channels, such as the voltage-dependent anion channel, mitochondrial calcium uniporter, Na^{+}/Ca^{2+} antiport, and Na^{+}/H^{+} antiport, which are directly linked to both ETS activity and membrane potential gradient. Indeed, mitochondria couple the metabolic activity to the ion transport process across their double

membrane barrier, thus promoting the link between calcium-transduction cascades and the production of ATP. Stressful situations for the cell, including oxidative-, metabolic- and endoplasmic reticulum-stress, as well as over-activation of Ca^{2+}-mediated signaling pathways during pathologies, lead to cellular Ca^{2+} overload. Under mitochondrial Ca^{2+} overload, increasing Ca^{2+} concentration in the matrix promotes the opening of the mitochondrial transition pore, thus providing a diffusion route for ions and metabolites into the mitochondria, together with the release of cytochrome c (Gunter *et al.*, 2000; for a review see Szabadkai & Duchen, 2008). Furthermore, during the disruption of nervous tissue with Dounce glass-type homogenizers, a high amount of calcium is released into the media (Gunter *et al.*, 2000; for a review see Szabadkai & Duchen, 2008). To prevent the above-mentioned alterations during Ca^{2+} overload, the maintenance of a low and constant Ca^{2+} concentration during the isolation was one of the main goals in the set up of a protocol for mitochondria isolation. For these reason, chelators are generally used in protocols for mitochondria isolation, as previously emphasized by (Berman & Hastings, 1999; Puka-Sundvall *et al.*, 2000; Lesnefsky & Hoppel, 2006; Frezza *et al.*, 2007; Sims & Anderson, 2008; Fernández-Vizarra *et al.*, 2010; Kamboj & Sandhir, 2011).

Likewise, ATP synthase activity, and consequently respiratory rates, seems to be very dependent on the concentration of magnesium for the correct stabilization of the electrochemical gradient in the membranous system of mitochondria (Panov & Scarpa, 1996). However, the ability of chelators to coordinate metal ions depends on the chemical species used and its concentration. These differences provide buffers with a broad range to control the presence of both free calcium and magnesium ions in the media. In fact, EGTA is accepted as having a lower capacity to buffer calcium than EDTA, but it does not alter the availability of magnesium. Our functional study showed a decrease in active respiration when the concentration of EGTA was increased, which means an opposite effect to that observed with EDTA (Fig. 4.1C). Free Ca^{2+} inflow into the mitochondria might be uncontrolled when chelator concentration is low, consequently causing the uncoupling of respiration and/or altering ETS activity. In addition, oxygen rate consumption in resting state supports a lack in proton motive force caused by the used of low concentrations of EGTA. Therefore, the modification of proton motive force by free calcium due to cytochrome c release, the alterations in the phosphorylation system and substrate oxidation could explain this effect. Indeed, in the group treated with the higher concentration of EDTA, the respiratory control ratio did not greatly exceed the value of six. This led us to suggest that the buffering ability of mitochondria is replaced by EDTA, which maintains the

respiratory characteristics and protects these organelles from the alterations caused by the isolation process. On the strength of these here reported results we may conclude that this protocol constitutes a simple and reliable method, which is particularly suitable for performing bioenergetic and oxidative stress experiments with fresh isolated mitochondria from rat brain.

USC
UNIVERSIDADE
DE SANTIAGO
DE COMPOSTELA

Chapter 5

Differential toxicity of 6-hydroxydopamine in SH-SY5Y human neuroblastoma cells and rat brain isolated mitochondria: Protective role of catalase and superoxide dismutase

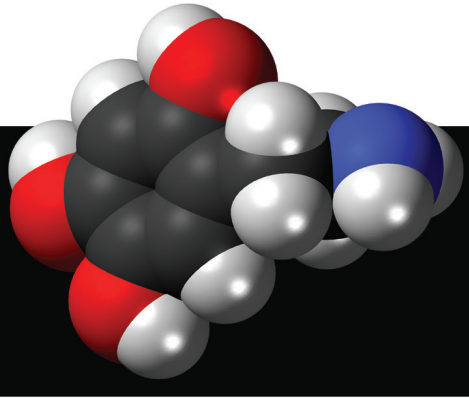

Abstract

Oxidative stress and mitochondrial dysfunction are two patho-physiological factors often associated with the neurodegenerative process involved in Parkinson's disease. Although, 6-hydroxy-dopamine is able to cause dopaminergic neurodegeneration in experimental models of PD by an oxidative stress-mediated process, the underlying molecular mechanism remains unclear. It has been established that some antioxidant enzymes such as catalase (CAT) and superoxide dismutase (SOD) are often altered in PD, which suggests a potential role of these enzymes in the onset and/or development of this multifactorial syndrome. In this study we have used high-resolution respirometry to evaluate the effect of 6-OHDA on mitochondrial respiration of isolated rat brain mitochondria and the lactate dehydrogenase cytotoxicity assay to assess the percent-tage of cell death induced by 6-OHDA in human neuroblastoma cell line SH-SY5Y. Our results show that 6-OHDA affects mitochondrial respiration by causing a reduction in both respiratory control ratio (IC50 = 200 ± 15nM) and state 3 respiration (IC50 = 192 ± 17nM), with no significant effects on state 4_0. An inhibition in the activity of both complex I and V was also observed. 6-OHDA also caused cellular death in human neuroblastoma SH-SY5Y cells (IC50 = 100 ± 9µM). Both SOD and CAT have been shown to protect against the toxic effects caused by 6-OHDA on mitochondrial respiration. However, whereas SOD protects against 6-OHDA-induced cellular death, CAT enhances its cytotoxicity. The here reported data suggest that both superoxide anion and hydroperoxyl radical could account for 6-OHDA toxicity. Furthermore, factors reducing the rate of 6-OHDA autoxidation to its p-quinone appear to enhance its cytotoxicity.

USC
UNIVERSIDADE
DE SANTIAGO
DE COMPOSTELA

5.1 Introduction

Parkinson's disease is a neurodegenerative disorder characterized by a progressive motor dysfunction as a result of the loss of nigrostriatal dopaminergic neurons. Although its aetiology is still not fully understood, there is no doubt that animal models of PD provide useful mechanistic data for the understanding of this disorder and for the ongoing development of neuroprotective strategies for its treatment. Thus, 6-hydroxydopamine is a catecholaminergic neurotoxin widely used to generate experimental models of PD (Blum *et al.*, 2000; Bové *et al.*, 2005). The administration of 6-OHDA into certain areas of the rat brain (striatum, substantia nigra, and third ventricle) in combination with desipramine, to prevent noradrenergic neuron destruction, is able to cause a selective loss of dopaminergic neurons (Sauer & Oertel, 1994; Rodríguez *et al.*, 2001; Soto-Otero *et al.*, 2002). It has been reported that in these models 6-OHDA promotes an apoptotic process in dopaminergic neurons (Biswas *et al.*, 2005; Kulich *et al.*, 2007; Gomez-Lazarro *et al.*, 2008) mediated by oxidative stress, which leads to cell death (Marti *et al.*, 1997; Jenner, 2003). In view of the well-known ability of 6-OHDA to react rapidly and non-enzymatically with molecular oxygen and form a series of reactive oxygen species (Graham *et al.*, 1978; Gee & Davidson, 1989), the molecular mechanism proposed to explain its neurotoxicity includes the action of these ROS on different cellular structures and metabolic systems (Halliwell *et al.*, 1992; Soto-Otero *et al.*, 2000;

Méndez-Álvarez *et al.*, 2001). However, the precise molecular mechanism involved in 6-OHDA-induced neurotoxicity remains to be clearly established (Blum *et al.,* 2001; Simola *et al.*, 2007).

It is recognized that the mitochondrial electron transfer system in association with mitochondrial oxidative phosphorylation set up the primary source of high energy compounds for cells, and that a dysfunction of mitochondrial energy metabolism leads to both a reduction in ATP production and an increase in ROS formation (Vercesi *et al.*, 1997; Lenaz *et al.*, 2002). Under normal conditions a small amount of molecular oxygen is continuously reduced by a single electron transfer to superoxide radical ($O_2^{\cdot-}$) by complexes I and III (Boveris *et al*., 1976; Cadenas *et al.*, 1977; Turrens & Boveris, 1980), but an impairment in mitochondrial respiration may dramatically increase the production of $O_2^{\cdot-}$. This has been demonstrated in dopaminergic neurons where the inhibition of complex I activity causes an increase in the production of ROS and subsequent oxidative damage to proteins, lipids and DNA (Dauer & Przedborski, 2003; Liss *et al.*, 2005). Evidently, this supports the opinion that the specific deficiency in the activity of complex I found in the substantia nigra of some PD patients is the etiological factor involved in the pathogenesis of these particular cases of PD (Parker & Swerdlow, 1998; Schapira *et al.*, 1990). With regard to 6-OHDA, although some authors found no significant evidence of its effect on

complex I activity (Mazzio *et al.*, 2004), others have reported a clear inhibitory effect (Glinka *et al.*, 1996; Glinka *et al.*, 1998).

However, to understand mitochondria behaviour it should be borne in mind that cells in a homeostatic state present an antioxidant defence, mainly composed of enzymatic systems, which help to protect mitochondria against oxidative stress. Evidently, the status of the cellular defence determines the viability of cells. Superoxide dismutase (SOD), catalase (CAT), and glutathione peroxidase (GPx) are the major enzyme systems in charge of modulating the mitochondrial redox environment, developing its activity mainly inside the mitochondria (Mn-SOD), in the cytosol (Cu, Zn-SOD and GPx), and inside the peroxisome (CAT). For this reason, the use of cell cultures can provide valuable and additional information on the mitochondrial response to a particular insult and vice versa. SH-SY5Y is a human neuroblastoma cell line which expresses the dopamine uptake system and is sensitive to the toxicity of 6-OHDA (Tiffany-Castiglioni *et al*., 1982; Simantov *et al.*, 1996). Furthermore, it has been reported that both CAT and SOD protect against 6-OHDA-induced cytotoxicity (Kullich *et al*., 2007; Asanuma *et al.*, 1998; Kabuto *et al*., 1999*;* Barkats *et al.*, 2002). Nevertheless, several studies have failed to find a protective role for both SOD (Blum *et al.*, 2000; Hanrott *et al.*, 2006) and CAT (Choi *et al.*, 1999; Saito *et al.*, 2007; Izumi *et al.*, 2005) against 6-OHDA-induced cytotoxicity.

In order to obtain fresh data on the molecular mechanisms involved in the toxicity of 6-OHDA we used two models: rat forebrain mitochondria and human neuroblastoma SH-SY5Y cells. To evaluate the effects of 6-OHDA on mitochondrial function we investigated its action on mitochondrial respiration and on the activity of each of the complexes of the electron transport system. The effects caused by the presence of CAT and SOD on this process were also investigated, together with the ability of 6-OHDA to induce cell death and the capacity of CAT and SOD to affect this process.

5.2 Experimental design and methods

Sixty Sprague-Dawley rats (200-250g) were used to perform the here reported study. Animals were randomly divided in three experimental groups: eighteen rats were used for the determination of the IC_{50} for 6-OHDA; twenty four rats were used to study the effects of 6-OHDA on the activity of antioxidant enzymes; eighteen rats were used to evaluate the effects of 6-OHDA on the individual activity of the different complexes of mitochondrial respiratory system. All the procedures used are detailed in Chapter 3. To carry out this study we applied the following methodological procedures: mitochondrial isolation, mitochondrial respiration, enzyme activity of respiratory chain complexes (CI-V), SH-SY5Y cells line culture, LDH citotoxicity assay, *p*-quinone formation during 6-hydroxydopamine autoxidation, and total protein concentration.

5.3 Results

5.3.1 Effect of 6-OHDA on both cellular viability and mitochondrial functionality

6-OHDA was described as a dopaminergic neurotoxin whose effects are mediated by oxidative stress. Human SH-SY5Y dopaminergic neuroblastoma cells were exposed for 24h (peak-time for LDH release (Ossola *et al.*, 2008)) to different concentrations of the neurotoxin (1µM-1mM). To evaluate the toxicity of 6-OHDA, the percentage of cellular death was estimated by using the LDH assay. The IC_{50} value was calculated by non-linear regression analysis of the toxicity-concentration curve, obtaining a value of 100 ± 9µM after 24h of exposition (Fig. 5.1A).

Under control conditions, the mean active respiration rate (state 3) was 468 ± 60pmol O2/min mg protein and the mean resting respiration rate (state 4_o) was 86 ± 19pmol O2/min mg protein, which results in a mean RCR of 5.45 ± 0.02. As illustrated in Fig. 5.1B-C, the treatment of forebrain mitochondria with different concentrations of 6-OHDA caused a significant reduction in both RCR and rate of oxygen consumption at state 3, with no significant change in the rate of oxygen consumption at state 4_o. The non-linear regression of the inhibition-concentration graph obtained for RCR inhibition revealed

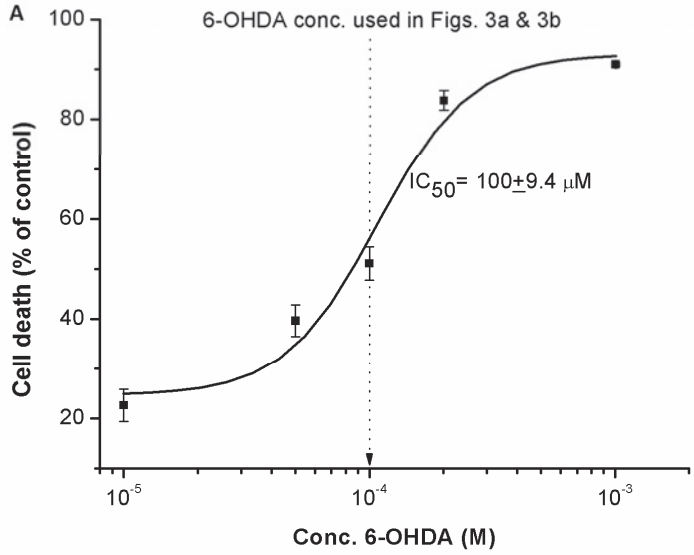
A
6-OHDA conc. used in Figs. 3a & 3b
Cell death (% of control)
100
80
60
40
20
IC50= 100±9.4 μM
10-5
10-4
10-3
Conc. 6-OHDA (M)

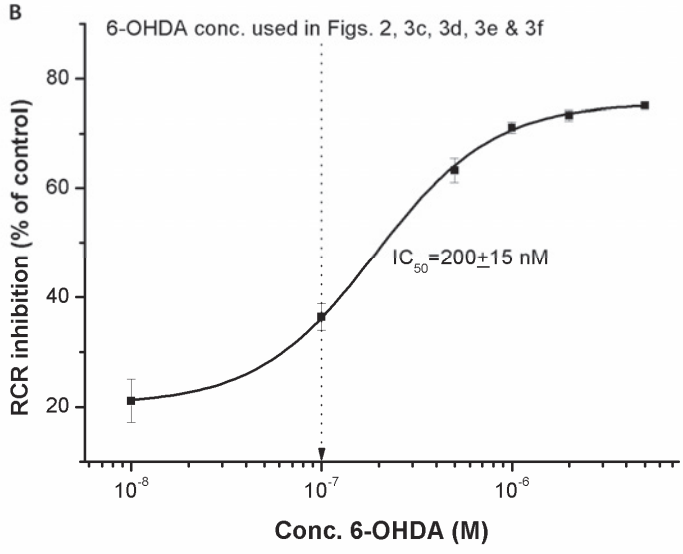
B
6-OHDA conc. used in Figs. 2, 3c, 3d, 3e & 3f
RCR inhibition (% of control)
80
60
40
20
IC50=200±15 nM
10-8
10-7
10-6
Conc. 6-OHDA (M)

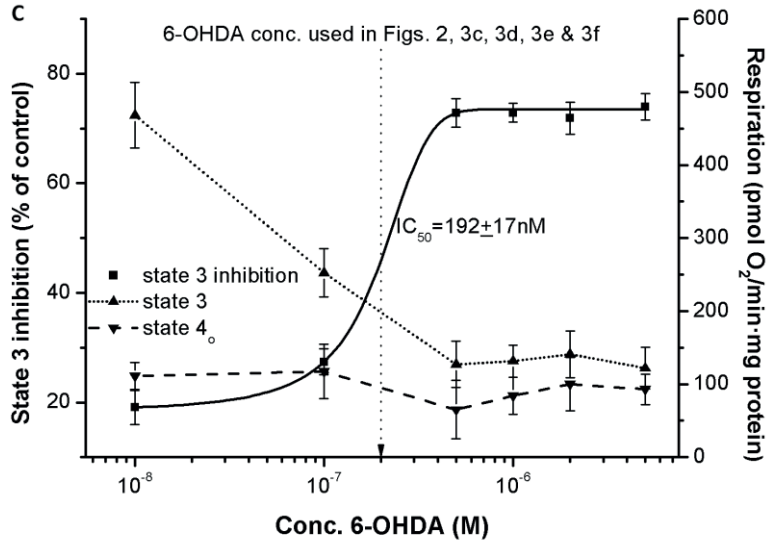

Fig. 5.1 (A) Cellular death induced by 6-OHDA in human neuroblastoma SH-SY5Y cells after 24h of incubation. Cell death was assayed by LDH assay and represented as the percentage of untreated control (in the absence of 6-OHDA). (B) Reduction of mitochondrial respiratory control ratio (RCR) caused by 6-OHDA after incubation of rat brain mitochondria in the presence of L-glutamate (2.5mM) plus L-malate (1.25mM). RCR was obtained as the quotient of active respiratory rate (state 3; 200 μM ADP) and resting rate (state 4_o; 4μg/ml oligomycin), and represented as the percentage of inhibition in relation to untreated control. (C) Effects of 6-OHDA on the rate of oxygen consumption in state 3 and state 4_o. Data are expressed as mean±SD from three different experiments with three replicas per experiment (*n*=3). IC_{50} values were obtained by non-linear regression analysis (Sigmaplot v. 11.0).

the existence of a decrease in the degree of coupling that was dependent on 6-OHDA concentration and gave an IC50 of 200 ± 15nM. As shown in Fig. 5.1C, the inhibition of state 3 respiration by 6-OHDA gave an IC_{50} value (192 ± 17nM) very close to that obtained for RCR inhibition. In addition, our results also show that concentrations of 6-OHDA higher than 10μM shift the active oxygen consumption

rate (state 3) into the value obtained for resting respiration (state 4_o). To understand the point of electron transport system altered by the presence of 6-OHDA (200nM), the activity of complexes I–V was analyzed. As shown in Fig. 5.2, only complex I and V showed a significant reduction in their activity of 12 and 27 %, respectively, when compared with control, while complexes II–IV remained unaltered.

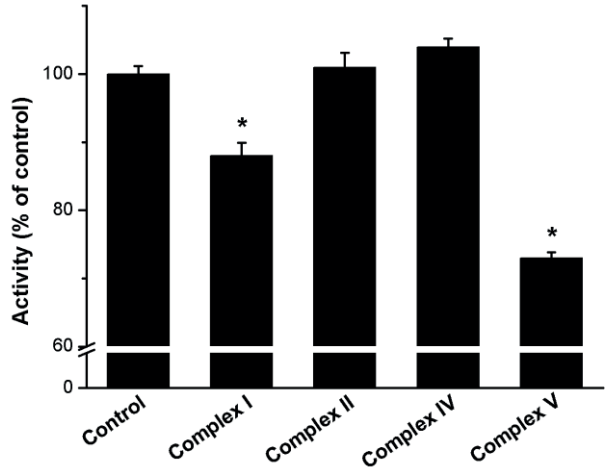

Fig. 5.2 Effects of 6-OHDA (200µM) on the activity of complexes from the mitochondrial electron transport system. Mitochondria were isolated from forebrains as detailed in the section Experimental Procedure, using an antibody for each complex (Complex I, II, IV and V) to perform an ELISA. Values are mean±SE (*n*=3) from independent experiments with three replicas and represent the percentage of activity compared with controls. *Statistical significance (one-way ANOVA followed by Duncan's test) was $p<0.05$.

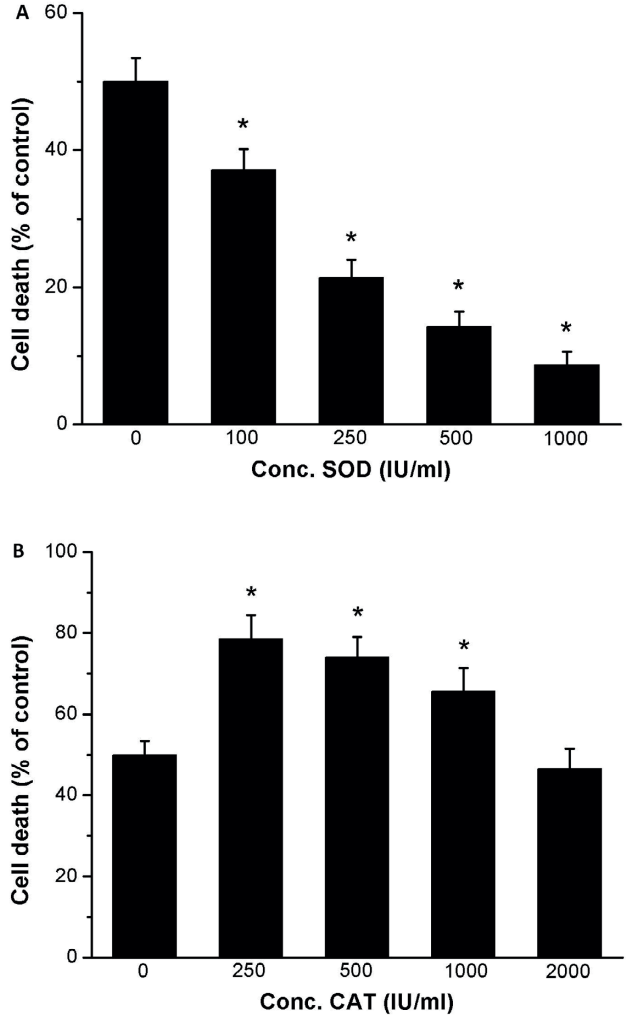

Fig. 5.3 Effect of SOD (A) and CAT (B) on SH-SY5Y cell death induced by 6-OHDA (100μM) after 24 hours of incubation. Cell death was assayed by LDH assay and represented as the percentage of untreated control (in the absence of 6-OHDA). Data are presented as the mean±SE from three different experiments with three replicas per experiment. *Significant difference (p<0.05) when compared with control exposed to 6-OHDA but in the absence of the antioxidant enzyme (one-way ANOVA followed by Duncan's test).

5.3.2. Neuroprotection of SH-SY5Y cells and isolated mitochondria by CAT and SOD

To assess the potential neuroprotective activity of the antioxidant enzymes SOD (100-1000 U/mL) and CAT (250-2000 U/mL) on the neurotoxicity induced by 6-OHDA, SH-SY5Y neuroblastoma cells were pre-treated with each of the antioxidant enzymes 24h prior to the addition of 6-OHDA. At this point, it is interesting to note that the hydrophilicity and molecular size of SOD and CAT restrict their action to the outside of cells. As shown in Fig. 5.3A, SOD protects significantly SH-SY5Y cells against the cellular death induced by 6-OHDA (100µM). Furthermore, this effect resulted dependent on enzyme concentration. Nevertheless, CAT failed to prevent the damage induced by 6-OHDA (100µM), even showing a high ability to enhance the cellular death caused by 6-OHDA (Fig. 5.3B). This enhancement decreased in a concentration-dependent manner for concentrations over 250 IU/ml.

Mitochondria were also pre-treated with increasing concentrations of both SOD and CAT prior to their exposition to 6-OHDA (200nM). In this study we observed that both antioxidant enzymes caused an increase in active respiration (state 3) with no significant effects on resting respiration (state 4_o). As illustrated in Fig. 5.3C-D, our results clearly show how the presence of both SOD and CAT cause a significant increase in the value of the RCR (state 3/ state 4_o) when compared with the value obtained in the absence of

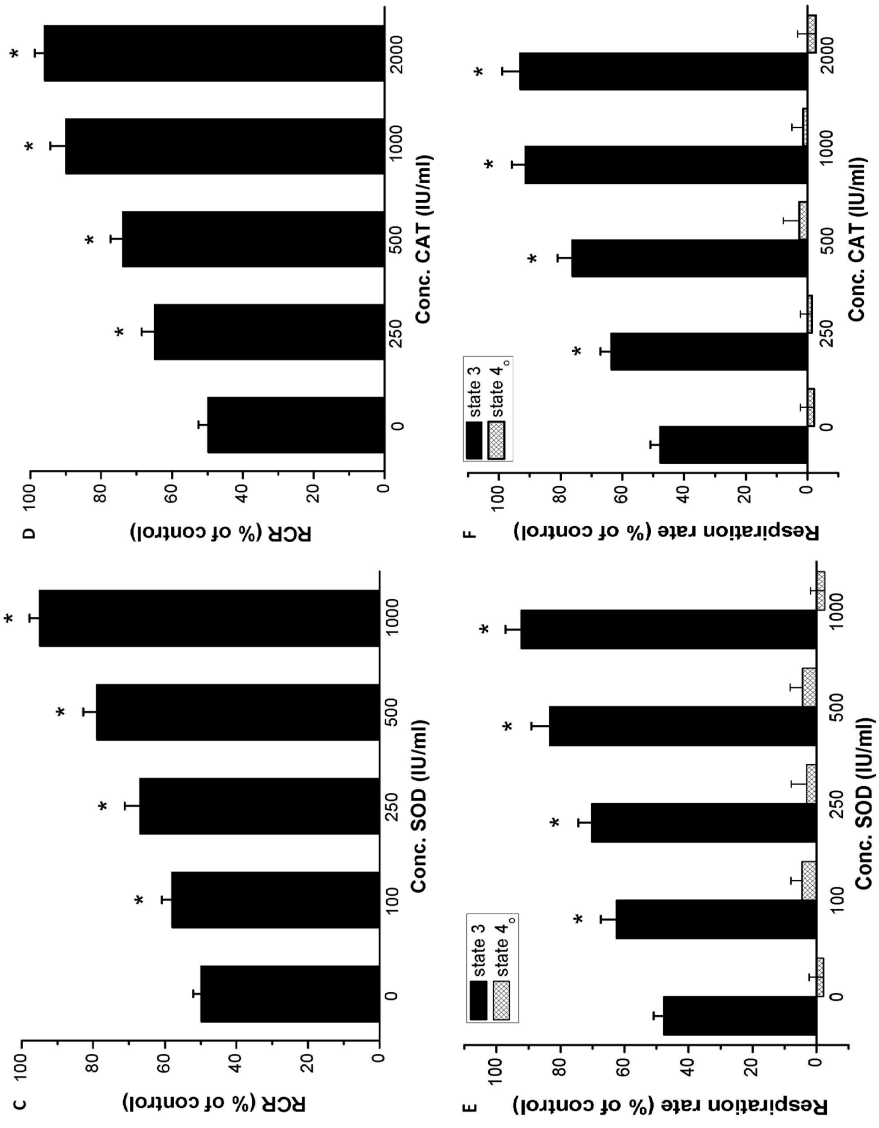

Fig. 5.3 Effect of SOD (C) and CAT (D) on the ability of 6-OHDA (200nM) to reduce coupled respiration of rat brain mitochondria in the presence of L-glutamate (2.5mM) plus L-malate (1.25mM). RCR was obtained as the quotient of active respiratory rate (state 3) and resting rate (state 4_o), as the percentage of untreated control (in the absence of 6-OHDA). Effects of SOD (E) and CAT (F) on the disruption caused by 6-OHDA (200nM) on the rates of oxygen consumption in state 3 and state 4_o. Data are presented as the mean±SE from fifteen different experiments with three replicas per experiment. *Significant difference (p<0.05) when compared with control exposed to 6-OHDA but in the absence of the antioxidant enzyme.

the assayed enzymes. In both cases, the protective action of both SOD and CAT against 6-OHDA toxicity was dependent on the enzyme concentration.

5.3.3 Effect of CAT and SOD on p-Quinone formation during 6-OHDA autoxidation

To determine whether the presence of both CAT and SOD affects the rate of 6-OHDA autoxidation, the formation of the corresponding p-quinone (pQ) was followed by direct recording of the increase in the absorbance at 490nm. As illustrated in Fig. 5.4, the presence of both CAT (1,000 IU/ml) and SOD (1,000 IU/ml) caused a visible reduction in the rate of pQ formation during the autoxidation of 20µM 6-OHDA under physiological conditions of pH. As can be seen, the slowing down observed in pQ formation was higher with CAT than with SOD.

5.4 Discussion

Oxidative stress has been cited as one of the main factors involved in the pathogenesis of PD (Jenner, 2003; Halliwell, 2006). The use of different neurotoxins (6-OHDA, MPTP, and rotenone) to develop experimental models of PD has become an essential tool to gain insight into the molecular mechanisms involved in the aetiology

of this disorder. Although there is consensus that 6-OHDA neurotoxicity is due to the oxidative stress triggered by the production of ROS (Bové & Perier, 2012), the precise mechanism of

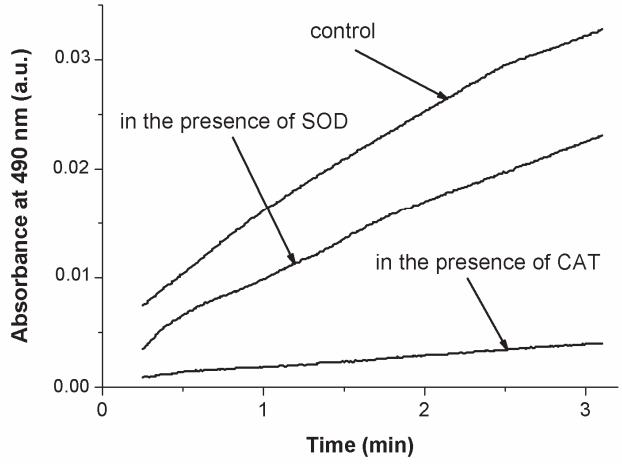

Fig. 5.4 Representative recording of the formation of *pQ* during 6-OHDA autoxidation in the absence (control) and presence of either CAT or SOD. The formation of *p*Q was followed spectrophotometrically after the addition of 6-OHDA (20µM) to a phosphate buffer (isotonic with KCl, pH 7.4) containing none of the antioxidant enzymes, CAT (1,000 IU/ml) or SOD (1,000 IU/ml). All concentrations are final concentrations in the incubation.

its cytotoxicity remains uncertain. In this study we report the results obtained from a combined study carried out on the toxicity of 6-OHDA using two models: rat forebrain mitochondria and human neuroblastoma SH-SY5Y cells. The aim of this study is to shed some new light on the molecular mechanisms involved in the toxicity of 6-OHDA from the effects caused by this toxin on mitochondrial function

and cell viability, and particularly from the response of both models to the addition of SOD and CAT.

It is well-known that under physiological conditions 6-OHDA is rapidly oxidized in the presence of molecular oxygen to form the corresponding pQ and a series of ROS, which include the corresponding semiquinone radical ($^{\cdot}$sQH), superoxide radical ($O_2^{\cdot-}$), hydrogen peroxide (H_2O_2), hydroxyl radical ($^{\cdot}$OH), and hydroperoxyl radical ($HO_2^{\cdot}$) [Graham *et al.*, 1978; Gee & Davidson, 1989; Soto-Otero *et al.*, 2000; Méndez-Álvarez *et al*., 2001). To illustrate our arguments, Fig. 5.5 shows the reactions involved in the formation of the above mentioned substances, together with the potential involvement of SOD and CAT in such reactions.

Assuming the reported involvement of mitochondria in the generation of ROS and the subsequent implication of these reactive compounds in neurodegeneration, our first goal was to quantify the effects caused by the presence of different concentrations of 6-OHDA on mitochondrial respiration. In our opinion, high-resolution respirometry appeared to be the most appropriate technique to perform this study because, as previously reported by Gnaiger (Gnaiger, 2008), it requires only small amounts of mitochondria, thus allowing the use of low respiratory fluxes without the problems derived from the low signal–noise ratio reported by using Clark type oxygen electrodes. Thus, the accuracy of this technique to measure oxygen concentration at the picomolar level gave us the opportunity

to investigate events occurring at very low concentrations of 6-OHDA and in the presence of antioxidants altering the concentration of oxygen into the chamber. However, high-resolution respirometry requires the use of metabolically well-preserved mitochondria with good degree of integrity in order to detect slight variations in the rate of oxygen consumption. The RCR obtained under our experimental conditions with untreated brain mitochondria confirms the usefulness of the here reported procedure to obtain mitochondria with an appropriate degree of integrity and functionality for high-resolution respirometry. Under our experimental conditions, 6-OHDA clearly showed a high capacity to reduce mitochondrial respiration in rat forebrain mitochondria and to cause cellular death in human neuroblastoma SH-SY5Y cells. Both effects were dependent on 6-OHDA concentration and gave IC_{50} values of 200nM for mitochondrial respiration (expressed in terms of RCR inhibition) and of 100µM for cellular death in human neuroblastoma SH-SY5Y cells. Our results also show that 6-OHDA causes a noteworthy decrease in NADH-linked state 3 respiration, with no significant effects on state 4_o. Curiously, similar behaviour was previously observed using dopamine at high concentrations (Berman & Hastings, 1999).

Fig. 5.5 Schematic representation of 6-OHDA autoxidation showing its ability to generate different reactive oxygen species (ROS) and the potential involvement of SOD and CAT in this process. As illustrated, ferrous iron (Fe^{2+}) can convert H_2O_2 to $^{\bullet}OH$ through what is called the Fenton reaction, but note that in the absence of Fe^{2+}, H_2O_2 can also generate $^{\bullet}OH$ by reacting with 6-OHDA (QH_2) or the semiquinone radical ($^{\bullet}$sQH) (Méndez-Álvarez *et al.*, 2001).

Taking into account that under our experimental conditions 6-OHDA reduces the activity of complex I, a fact which agrees with previously reported data (Glinka *et al.*, 1996; Glinka *et al.*, 1998), our findings may be interpreted as a consequence of a reduction in the flow of electrons through the mitochondrial electron transport system. At this point, it should be emphasized that under our experimental conditions state 4_o mitochondrial oxygen consumption is limited by the rate of protons influx across the inner membrane, and consequently the resulting absence of change in state 4_o respiration by 6-OHDA shows that the permeability of mitochondria membranes to protons is not affected by the presence and autoxidation of 6-OHDA. To assess the potential ability of 6-OHDA to affect proton leak through the inner mitochondrial membrane and taking into consideration the results reported by Masini *et al.* in 1983, we made some additions to the incubation medium. These were: EGTA (to prevent the cycling of Ca^{2+} across the inner membrane of mitochondria), fatty acid free BSA (to prevent the oxidation of fatty acids), and oligomycin (to prevent the action of broken mitochondria with uncoupled ATPase activity). The inhibition observed in the activity of ATP synthase by 6-OHDA may also contribute to the reduction found in active respiration. Evidently, the uncoupling found in respiration-phosphorylation may help to explain the neurotoxicity of 6-OHDA through the consequent reduction in neuronal ATP production. Assuming the known ability of 6-OHDA to

undergo autoxidation and generate ROS (Fig. 5.5), in both models (i.e. human neuroblastoma SH-SY5Y cells and rat forebrain mitochondria) it seems understandable to attribute the toxicity of 6-OHDA to the formation of ROS and their ability to cause both lipid peroxidation and protein oxidation (Tiffany-Castiglioni *et al.*, 1982). The particular toxicity here reported of 6-OHDA on mitochondrial function could also be linked to the presence of cytochromes and Fe-Cu clusters involved in mitochondrial respiration and the well-known ability of iron and copper to promote the reduction of H_2O_2 through the participation of the Fenton reaction to give $^{\cdot}OH$, which is considered the most damaging free radical for living cells (Pryor, 1986). With regard to dopaminergic neurons, this effect could be enhanced by: (a) the presence of neuromelanin in these cells and its ability to accumulate iron (Enochs *et al.*, 1994), and (b) the reported ability of 6-OHDA to release iron from strongly coordinating ligands (Linert *et al.*, 1996). Evidently, when cells are the model, the toxicity of 6-OHDA for mitochondrial function may be diminished by the antioxidant machinery within the cell which protects the mitochondrial function (Tatsuta & Langer, 2008).

Both SOD and CAT have been shown to protect against the toxic effects caused by 6-OHDA on mitochondrial respiration. Although, the neuroprotective role of CAT and SOD against the neurotoxicity induced by 6-OHDA has been previously reported under different experimental conditions (Kulich *et al.*, 2007; Tiffany-

Castiglioni *et al.*, 1982; Asanuma *et al.*, 1998; Kabuto *et al.*, 1999; Barkats *et al.*, 2002), some reports have failed to show the protective role of SOD (Blum *et al.*, 2000; Hanrott *et al.*, 2006) and CAT (Choi *et al.*, 1999; Saito *et al.*, 2007) against 6-OHDA-induced cytotoxicity. The protective effect here reported for both SOD and CAT on mitochondrial respiration appears to corroborate the involvement of ROS in early stages of 6-OHDA toxicity and the ability of these highly reactive substances to affect state 3 respiration and consequently to uncouple respiration to phosphorylation. As can be seen in Fig. 5.5, the activity of SOD may boost the formation of H_2O_2, and consequently the participation of the Fenton reaction in the formation of $^{\cdot}OH$. However, the dismutation of superoxide radical caused by the activity of SOD decreases the formation of $HO_2^{\cdot}$, with a slight alteration in the rate of pQ formation. Assuming the previously suggested role of $HO_2^{\cdot}$ in the initiation of both lipid peroxidation and in particular protein oxidation (Aikens & Dix, 1991; Gebicki & Gebicki, 1993; Fu *et al.*, 1995), our hypothesis explains the protective effects of SOD on mitochondrial respiration. The protective effect of CAT on the toxicity induced by 6-OHDA on mitochondrial respiration appears to be caused by an efficient elimination of H_2O_2, which must be associated to a significant decrease in the rate of 6-OHDA autoxidation, together with a reduction in the production of $^{\cdot}OH$ by the Fenton reaction. It is evident that CAT activity diverts the 6-OHDA autoxidation to the direct reaction between 6-OHDA and molecular

oxygen without the involvement of H_2O_2. The possibility that this effect could increase the production of $O_2^{\cdot-}$, and consequently the formation of $HO_2^{\cdot}$ (Fig. 5.5), is precluded by the notable decrease observed in the rate of 6-OHDA autoxidation. Furthermore, our results show that SOD is more efficient than CAT in reducing the 6-OHDA-induced toxicity, which underlines the particular contribution of $O_2^{\cdot-}$ to the toxicity of 6-OHDA. In this way, our findings appear to corroborate the view that the actual free radical acting on the components of electron transport system and uncoupling mitochondrial respiration is the $HO_2^{\cdot}$ generated from $O_2^{\cdot-}$. As we previously reported (Hermida-Ameijeiras *et al.*, 2004), it is reasonable to think that an uncharged free radical with a relatively non short half-life such as $HO_2^{\cdot}$ could be involved in this process because of the following features: (a) its ability to pass through biological membranes to reach the inner mitochondrial membrane, (b) its easy access to the internal hydrophobic environment of proteins, and (c) its reported ability to oxidize proteins (Gebicki & Gebicki, 1993; Fu *et al.*, 1995). Thus, we suggest $HO_2^{\cdot}$ as the main chemical species involved in mitochondrial impairment.

Finally, our results revealed a difference in behaviour concerning the effects of SOD and CAT on the cytotoxicity induced by 6-OHDA in human dopaminergic neuroblastoma cells. Thus, SOD showed a highly protective effect against 6-OHDA-induced toxicity, while CAT surprisingly enhanced the potential of 6-OHDA to cause

cellular death, at least, when relatively low concentrations of CAT were used. Once again, these observations suggest the involvement of ROS in 6-OHDA-induced cellular death. Nevertheless, this lethal effect diminished as CAT concentration increased, but without achieving a protective effect, even at the highest concentrations used in this study. A putative explanation for these data may be the reduction in the rate of 6-OHDA autoxidation caused by the elimination of hydrogen peroxide by CAT, which causes an increase in the half-life of 6-OHDA and its derivates in the environment of the dopaminergic SH-SY5Y cells. In this way, the toxic potential of 6-OHDA is increased, particularly by the increased accessibility of 6-OHDA to the inside of cells by active transport (Tiffany-Castiglioni *et al.*, 1982). It is probably that CAT at concentrations over 1,000 IU/ml displaces completely the reaction of $O_2^{\cdot-}$ dismutation to the formation of H_2O_2 and consequently, the instantaneous consumption of H_2O_2 by CAT prevents the formation of $HO_2^{\cdot}$ during 6-OHDA autoxidation, thus contributing to the protective effect observed under these circumstances.

In summary, this study demonstrated that low concentrations of 6-OHDA (at nanomolar levels) are able to affect mitochondrial function by causing both a reduction of active respiration (state 3) and an inhibition of complex I and V activities. At higher concentrations (at micromolar levels) this neurotoxin is also able to cause cellular death in human dopaminergic neuroblastoma SH-SY5Y

cells. Whereas both SOD and CAT have been shown to protect efficiently against the toxicity caused by 6-OHDA on mitochondrial respiration, only SOD has a protective effect on 6-OHDA-induced cellular death. Evidently, these data contribute to corroborate the involvement of oxidative stress in 6-OHDA toxicity. Furthermore, our data appear to suggest that a low rate of 6-OHDA autoxidation, the amount of superoxide anion formed and a high production of hydroperoxyl radical are the major causes of the toxic effects induced by 6-OHDA. This indicates that only specific ROS derived from 6-OHDA autoxidation are involved in its neurotoxicity and that more work is required to confirm the chemical nature of the species involved in mitochondrial and cellular injury.

Chapter 6

Effects caused by aluminium on rat brain mitochondria bioenergetics: an *in vitro* and *in vivo* study

USC
UNIVERSIDADE
DE SANTIAGO
DE COMPOSTELA

Abstract

Aluminium has been included in numerous neurotoxicological studies in humans highlighting its role as a toxicological risk. Our previous work showed that aluminium is able to cause oxidative stress, to reduce the activity of some antioxidant enzymes, and to enhance the dopaminergic neurodegeneration induced by 6-hydroxydopamine in an experimental model of Parkinson's disease in rats. In the present work we performed an in vitro and in vivo study on the effects caused by aluminium on mitochondrial bioenergetics, using high-resolution respirometry under conditions of coupling, uncoupling, and non-coupling. Our study showed a common alteration in leakiness, electron transport system maximum capacity complex II-linked respiratory pathway, a reduction in the respiration efficiency, and a decrease in complexes III and V activity for both *in vivo* and *in vitro* treatments. The observed effects also showed an alteration in mitochondrial transmembrane potential and a decrease in oxidative phosphorylation capacity when high concentrations of the metal are present *in vitro*. These findings contribute to explain both the previous reported ability of aluminium to generate oxidative stress and the suggested potential of aluminium to act as an etiological factor by promoting the progression of neurodegenerative disorders such as Parkinson's disease.

USC
UNIVERSIDADE
DE SANTIAGO
DE COMPOSTELA

6.1 Introduction

Aluminium (Al^{3+}) is extensively used in daily life and on industrial processes causing a possible wide human exposition to this metal through air, tap water, food, and some medications (Exley, 2013). In the nature, Al^{3+} is ubiquitous and the third metal in abundance in the Earth crush. However, Al^{3+} has not been related with any biological function. A recent neurotoxicological study in humans has demonstrated that aged brains accumulate enough Al^{3+} to constitute a pathological risk (House *et al.*, 2012). It has been previously reported the presence of relatively high levels of this metal in the brain of some persons affected of Parkinson's disease (Hirsch *et al.*, 1991; Yasui *et al.*, 1992). The neurotoxicity of Al^{3+} has been often associated to its ability to promote the formation of reactive oxygen species (ROS) (Bondy *et al.*, 1998; Kumar & Gill, 2009; Wu *et al.*, 2012), which is difficult to understand bearing in mind that Al^{3+} is a non-redox metal. Aluminium has been also related with behavioural alterations (Miu *et al.*, 2003), memory and learning deterioration (Julka *et al.*, 1995), osteomalacia (Robertson *et al.*, 1983), dialysis encephalopathy (Bolla *et al.*, 1992), amyotrophic lateral sclerosis (Perl *et al.*, 1982), and parkinsonism (Garruto *et al.*, 1984). Although, its role in Alzheimer's disease is not clear, it has been implicated in the development of neurofibrillar tangles (Zatta *et al.*, 2003; Walton, 2006). Our previous work demonstrated the ability of Al^{3+} to cross the blood brain barrier and accumulate into the rat

brain (Sánchez-Iglesias *et al.*, 2007), to cause brain oxidative stress, to reduce the activity of some antioxidant enzymes in the brain (catalase, superoxide dismutase, glutathione peroxidase), and to enhance the dopaminergic degeneration induced by 6-hydroxydopamine in an experimental model of Parkinson's disease in rats (Sánchez-Iglesias *et al.*, 2009). The complexity of the neurodegenerative process involved in the pathogenesis and progression of Parkinson's disease, together with the lack of a precise knowledge on the aetiological factors involved in this process, main due to its multifactorial character (Zhou *et al.*, 2008), greatly limits the development of new therapeutic approaches. Nowadays, the pharmacological treatments for Parkinson's disease are designed to alleviate the symptoms of the disease and not to stop its development. However, the design of drugs orientated to stop the progression of the disease or to reverse some of its pathological consequences results essential for the development of new therapeutic strategies. Metal chelators have been purposed for their potential in the treatment of neurodegenerative disorders in general (Gaeta & Hider, 2005; Ward *et al.*, 2012) and Parkinson's disease in particular (Levenson, 2003; Youdim *et al.*, 2004) since metals are considered as a pharmacological target.

Mitochondrial impairment and the foreseeable imbalance in the oxidative status of the cell are considered as two factors involved in the development of neurological disorders such as Parkinson's disease (Schapira, 2008). It is well-known that both a mitochondrial dysfunction caused by a complex I defect may be the aetiological factor involved in the pathogenesis of some cases of Parkinson's disease (Schapira *et al.*, 1989; Keeney *et al.*, 2006) and some mitochondrial toxins used to generate experimental models of parkinsonism act on the electron transport system (ETS) (Dauer & Przedborski, 2003; Cannon & Greenamyre, 2012). These facts are consistent with the central role that mitochondrion plays for the cell as a powerhouse (Cadenas, 2004) and the particular high energy requirement of nigrostriatal dopaminergic neurons mainly due to their unique cellular architecture (i.e. >400,000 synapses/neuronal cell body) on normal cell function (Bolam & Pissadaki, 2012). Furthermore, mitochondria are also involved in regulating the cell cycle and triggering the apoptosis. That is why the evaluation of mitochondria bioenergetics is a very valuable tool to understand the interaction between this organelle and a xenobiotic like Al^{3+} and also to clarify the reported consequences of this interaction. Previous studies revealed this interaction by describing an altered metabolism and an increase in ROS production when this metal is present (Kumar *et al.*, 2008; Sánchez-Iglesias *et al.*, 2009). In addition, Tonitello *et al.* described in 2000 the ability of Al^{3+} to binding the mitochondrial

inner membrane and its correlation with the opening of the membrane permeability transition pore. However, there are not studies analyzing the physiological respiration rates of the mitochondria in conditions of coupling, non-coupling and uncoupling in presence of different substrates. Consequently, the aim of the here reported study is to assess the effect of Al^{3+} on the bioenergetics of rat brain mitochondria under the described conditions. To understand possible differences depending on the organelle source or the way of Al^{3+} administration, we performed a complete analysis using *in vitro* and *in vivo* models.

6.2 Experimental design and methods

Twenty four Sprague-Dawley rats (200-250g) were used to perform the here reported study. Animals were randomly divided in four experimental groups: for *in vitro* experiments, two groups with six rats for every group were used as control or treated mitochondria; for in vivo experiments, the control group received a daily i.p. saline solution for ten days, and the treated group received a daily i.p. dose of aluminium (10mg of Al^{3+}/Kg/day) for ten days. All the procedures used are detailed in Chapter 3. To carry out this study we applied the following methodological procedures: mitochondrial isolation, mitochondrial respiration, mitochondrial membrane potential, enzyme activity of respiratory chain complexes (CI-V), electron microscopy, and total protein concentration.

6.3 Results

6.3.1 Animal response and mitochondrial structure

To analyze general effects of the metal, the weight and behavior of the animals were controlled during the whole treatment. The only remarkable effect of the intraperitoneal injection of Al^{3+} (10 mg/Kg/day) was a significantly decrease on the body weight gain (Fig. 6.1A). However, these animals did not show any change on behavior or in the whole-brain wet tissue weight in comparison with control rats (data not shown). Also, in order to evaluate structural modifications mitochondria were studied by electron microscopy as is shown in figure 6.1 (B-G). The micrographs did not reveal alterations in the morphology due to the presence of Al^{3+}. All the organelles showed round or elongate shape, continuous membranous structure and internal cristae forming a gather group.

6.3.2 Mitochondrial bioenergetics

Bioenergetic studies were carried out using high-resolution respirometry in both models studied (i.e. *in vivo* and *in vitro*) in order to analyze the Al^{3+} capacity to alter the mitochondrial respiration. To obtain the optimal concentration of Al^{3+} for *in vitro* assays, a preliminary study was performed exposing the organelles to a wide range of metal concentrations, revealing a dose-dependent decrease

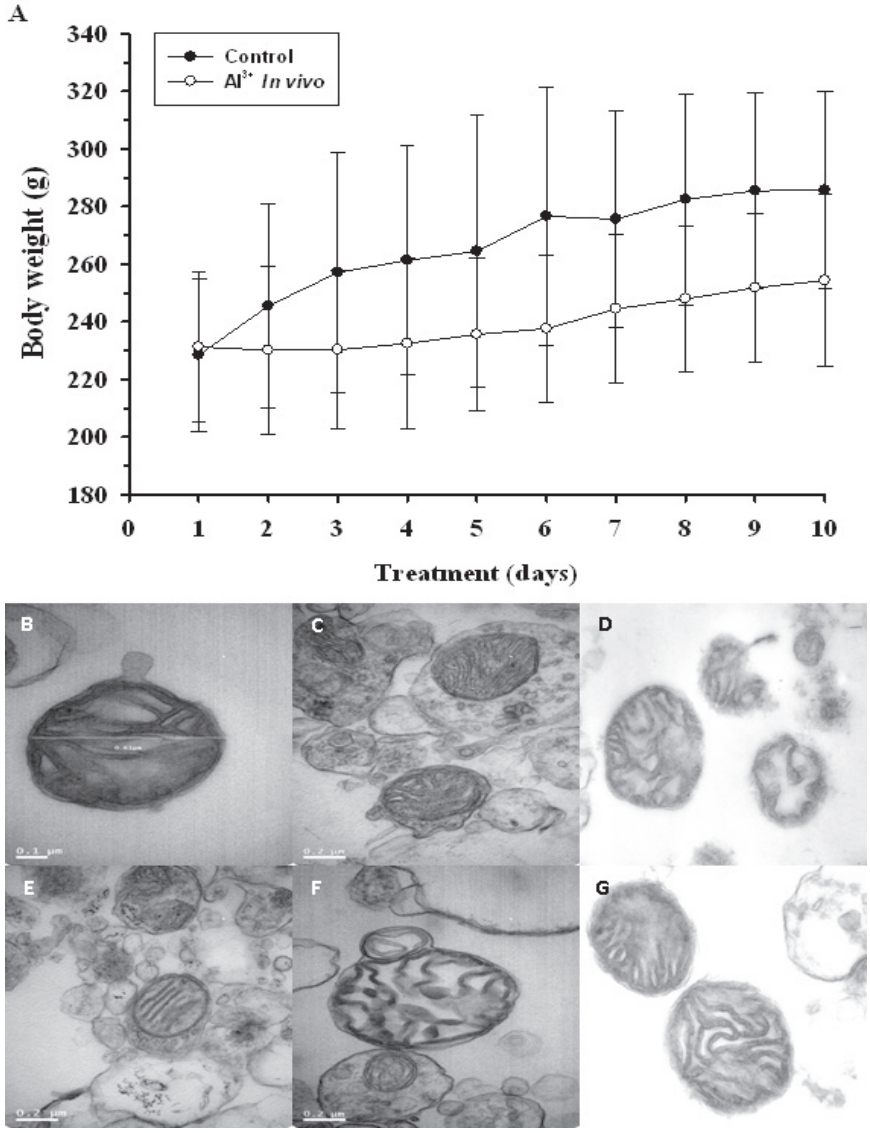

Fig 6.1 (A) Effect of aluminium exposure on body weight gain (control, filled circle; Al^{3+} treatment, open circle). (B-G) Electron micrographs of isolated mitochondria in presence or absence of Al^{3+}. B. Control CI OXPHOS; C. Al^{3+} CI OXPHOS *in vitro*; D. Al^{3+} CI OXPHOS *in vivo;* E. Control CI+II OXPHOS; F. Al^{3+} CI+II OXPHOS *in vitro*; G. Al^{3+} Complex I+II OXPHOS *in vivo*.

capacity in OXPHOS and ETS_{max} (Table 6.1). We found that 50nM is the optimum concentration of Al^{3+} to perform an acute treatment *in vitro*. Both experimental models were analyzed applying a SUIT protocol that guarantee the analysis of the control exerted by different metabolic pathways (CI-, CII- or CI+II-linked) in conditions of coupling, uncoupling and non-coupling. As shown in Fig. 6.2, *in vitro* OXPHOS respiration showed a significantly decrease for complex I (-81%) and complex I+II (-53%) respiratory capacities. Nevertheless, *in vivo* assays did not show significantly alterations in either complex I (-15%) or complex I+II (-18%) OXPHOS capacity (Fig. 6.2). Moreover, the assessment of the non-coupled state linked to complex II revealed a decrease activity (-42% and -44%) in presence of Al^{3+} for both, *in vitro* and *in vivo* respectively. On the other hand, a decrease capacity for complex I+II ETS_{max} was described *in vitro* but not *in vivo* (Fig. 6.2).

Flux control ratios were obtained as coupling control ratios in order to understand the metabolic control exerted by each respiratory pathway and the influence of Al^{3+} on it (Table 6.2). The limitation of OXPHOS capacity by the phosphorylation system (i.e. ANT, P_i translocator, ATP synthase), expressed as P/E index ($CI+II_P/CI+CII_E$), showed a decreased in both models studied (i.e. -49% *in vitro* and -14% *in vivo*; Table 6.2). In addition, the coupling control ratio L/E ($CI+II_L/CI+CII_E$) expresses the leakiness and the efficiency of the mitochondrial coupling, revealing a possible dyscoupling effect

due to a toxic action. Our data showed a differential effect depending on the model studied (Table 6.2), with an increase of the index for *in vitro* (143%) and a decrease for *in vivo* (-53%).

Table 6.1 *Respiratory parameters from SUIT protocol applied on isolated rat brain mitochondria in presence of aluminium chloride*

Group	OXPHOS (pmol $O_2 \cdot s^{-1} \cdot mg^{-1}$)	ETS_{max} (pmol $O_2 \cdot s^{-1} \cdot mg^{-1}$)
	CI: GM_P	CI: GM_E
Control	388.66 ± 19.27	717.45 ± 10.98
5nM	203.41 ± 19.36*	375.69 ± 2.30*
10nM	137.45 ± 10.45*	306.93 ± 16.88*
50nM	72.43 ± 7.34*	247.98 ± 17.28*
100nM	21.94 ± 1.48*	238.41 ± 29.13*
1µM	25.55 ± 2.93*	78.79 ± 13.55*
10µM	28.76 ± 3.05*	87.30 ± 12.65*
100µM	23.23 ± 0.97*	20.08 ± 2.64*

6.3.3 Aluminium alters complexes III and V, and proton motive force

The analysis of proton motive force was assessed as a change in membrane potential (Δψ) with a TPP^+ electrode. Our results showed a differential effect of the metal over Δψ, with a wide decrease for *in vitro* (-70%) and not either one *in vivo* (Fig. 6.3). Furthermore, the interaction of Al^{3+} with the enzymes that form the electron transport system is one of the main reasons that could explain the decrease on respiration capacities. To evaluate this possibility, we assessed individually the enzymatic activity of each complex with ELISA kits in both models studied. Figure 6.4A shows altered activities for complex III (-23%) and complex V (-24%) for *in vitro*. Moreover, when we supply Al^{3+} *in vivo,* complex III activity decreased a -17% and complex V activity a -13% (Fig. 6.4). Finally, we evaluated the Complex IV respiratory capacity to work out if the Al^{3+} interaction with the electron transport system is up- or downstream Q-junction. Our data do not reveal a significantly inhibitory effect of Al^{3+} on complex IV activity (Fig. 6.4).

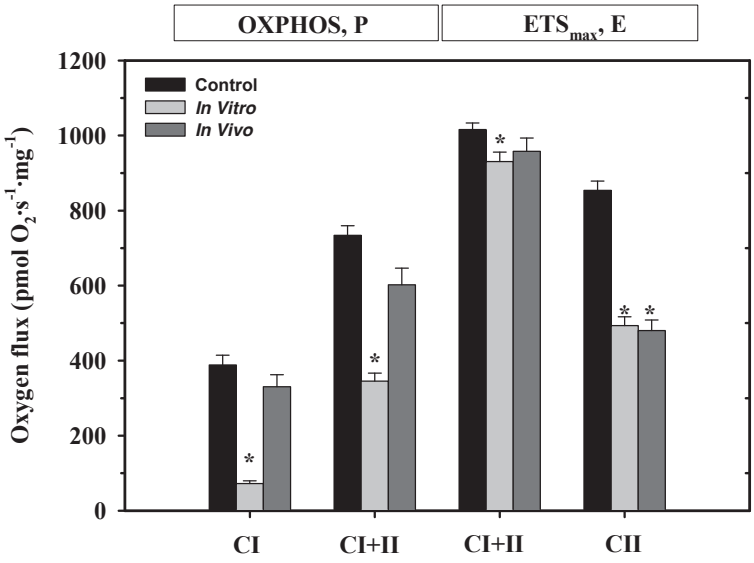

Fig. 6.2 Evaluation of mitochondrial respiratory capacities in isolated rat brain mitochondria from control, *in vitro* (50nM Al^{3+}) and *in vivo* (10mg of Al^{3+}/Kg/day i.p.). Mitochondrial coupling states are differentiated as OXPHOS (saturating ADP, 1.5mM) and ETS_{max} (non-coupled).

Table 6.2 *Flux control Ratio obtained for each model studied using $CI+II_E$ capacity to normalize*

Group	CCR	
	$CI+CII_P/CI+CII_E$ (P/E)	**$CI+CII_L/CI+CII_E$ (L/E)**
Control	0.722±0.005	0.061±0.005
In Vitro	0.372±0.002*	0.149±0.001*
In Vivo	0.628±0.004*	0.029±0.001*

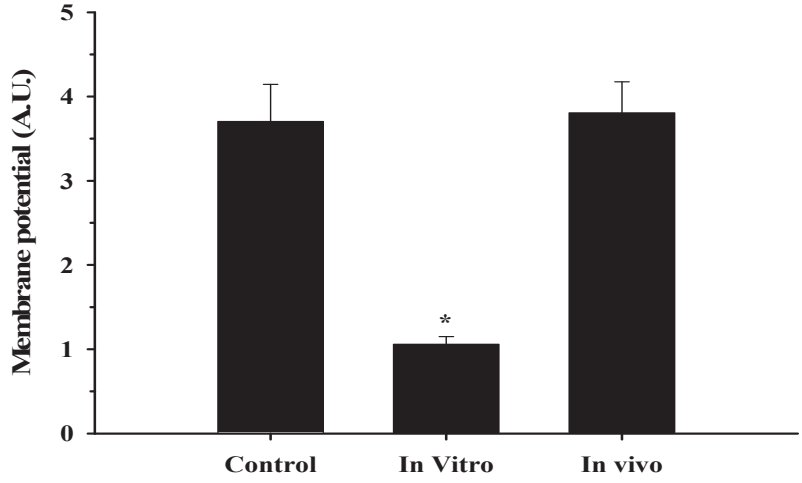

Fig. 6.3 Membrane potential in presence of the metal for each group: control, *in vitro* (50nM Al^{3+}) or *in vivo* (10mg of Al^{3+}/Kg/day i.p.).

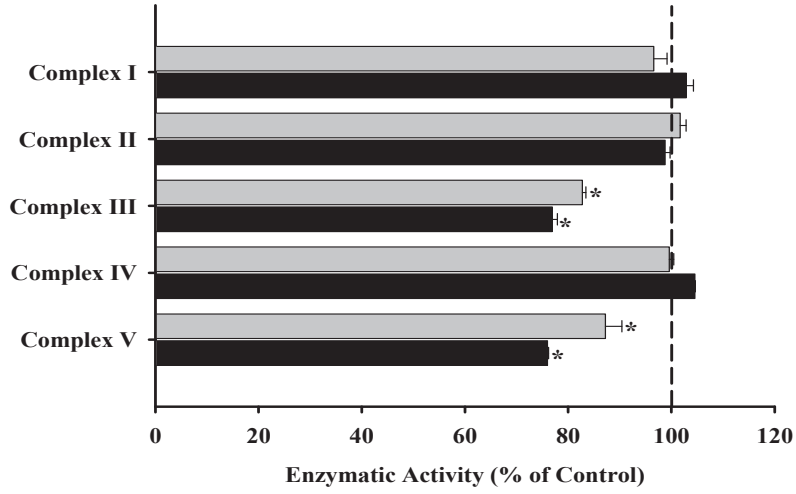

Fig. 6.4 Enzymatic activity of electron transport system complexes for *in vivo* (grey) and *in vitro* (black; 50nM Al^{3+}) in presence of Al^{3+}.

6.4 Discussion

In the present study we demonstrate that Al^{3+} alters brain mitochondrial respiration. The extent and nature of the alteration caused seems to be different depending on the model used for the study, being the *in vitro* model the most affected by the presence of this metal. The mitochondrion is not only the powerhouse of the cell, but it is also involved in the regulation of cellular cycle, apoptosis, and oxidative stress (Cadenas, 2004). In order to understand the mechanisms triggered by Al^{3+} to affect mitochondrial function, we analyzed the different bioenergetic capacities of this organelle (i.e. OXPHOS, LEAK, and ETS_{max}) using high-resolution respirometry. Redox signalling regulates mitochondrial function and the oxidative stress production (Daiber, 2010). Regarding to that, metals may play an important role on the redox environment due to their catalytic capacity to promote ROS and to their potential interaction with the clusters of the ETS. The imbalance between radical species production and the activity of antioxidant systems has been found in both neurodegenerative disorders and aging (Lin & Beal, 2003). For this reason, the study of the influence of Al^{3+} on mitochondrial respiration and its ability to modify the redox environment gains importance for the development of new therapeutic strategies.

In order to detect differential effects of Al^{3+} on the different components of the mitochondria we applied a SUIT protocol to evaluate the bioenergetics in a modular way. The disruption of the phosphorylation system by uncouplers enables us to obtain the maximum activity of the enzymes that constitute the electron transport system (ETS_{max}). From that point of view, our results showed that the presence of Al^{3+} in both models promotes a decrease on complex II-linked ETS_{max} capacity. The ETS_{max} respiratory rate, without the electrochemical backpressure on the proton pumps and with the membrane potential collapsed, remains only in both the activity of the TCA and the respiratory complexes. For this reason, we analyzed the effect of the presence of Al^{3+} on the isolated enzymatic activity of complex II itself, but this activity was not affected by the metal. Nevertheless, other previous studies reported an alteration in the activity of complex II in the presence of Al^{3+} together with an increase in ROS production (Mailloux *et al.*, 2006; Kumar *et al.*, 2008). Assuming that, Al^{3+} appears to cause inhibitory effects on biochemical reactions involving the binding to other metals such as Mg^{2+} and Ca^{2+} (Trapp, 1980). A possible explanation to the here reported reduction in the complex II-linked ETS_{max} capacity could be an upstream inhibition on aconitase or other TCA dehydrogenases, whose activity is closely related to the involvement of Ca^{2+} (Zatta *et al.*, 2000).

Membrane integrity results essential for energy transducer systems such as mitochondria, being the impermeability of the inner membrane determinant to generate the electrochemical potential required to drive oxidative phosphorylation. The present study showed a differential effect of Al^{3+} on membrane properties. On the one hand, the acute exposure to the metal in the *in vitro* experiments showed a significantly leakiness of the mitochondria as shown by the increase observed in L/E rate and the Δψ decay, thus suggesting a dyscoupling of the organelle. As it is known, a mitochondrial dysfunction caused by alterations in the membrane properties may lead to the opening of the mitochondrial permeability transition pore. The expected consequence of this effect is a dissipation of the membrane potential, followed by an uncoupling in the oxidative phosphorylation and therefore an impaired cellular ATP production, which ultimately could cause cell death (Le Masters *et al.*, 1998). It has been previously reported that Al^{3+} is able to promote the opening of the membrane pore, but being less effective than Ca^{2+} to induce the transition permeability (Tonitello *et al.*, 2000), with only some mitochondrial subpopulations affected. Moreover, this membrane transition permeability appears to occur without any Δψ decay (De Marchi *et al*., 2004). Concerning that, our electron micrographs support the dissipation of Δψ without the concomitant need of swelling. In spite of that, Niu *et al.* (2005) has previously reported an alteration in both mitochondrial membrane and cristae when using

Al^{3+} concentrations higher to those used in our study. On the other hand, the short-term *in vivo* exposition to Al^{3+} did not show any alteration in the $\Delta\psi$, but showed a decrease in mitochondrial leakiness. Van Rensburg *et al.* described in 1992 a similar effect in an Alzheimer's disease model in which the fluidity of the membrane was modified by the presence of small amounts of Al^{3+}, attributed to the binding of this metal to membrane phospholipids. The here reported absence of alterations in $\Delta\psi$ suggests that the short-term *in vivo* treatment with Al^{3+} is less capable to modify the bioenergetics of the organelle in relation to the effects found *in vitro*. This effect is probably due to the fewer amount of Al^{3+} present inside the cell and/or the existence of natural inducible chelants able to protect the cell from the action of free metals (e.g. ferritin, transferrin, etc.). However, we have previously reported that a similar *in vivo* short-term treatment with Al^{3+} causes brain oxidative stress and enhances the neurodegenerative damage induced by 6-hydroxydopamine in the rat nigrostriatal system (Sánchez-Iglesias *et al.*, 2009). De Marchi *et al.* (2004) attributed the induced membrane transition permeability to the ROS generated by Al^{3+} and to its ability to oxidize critical thiol groups in the pore-forming structures of the membrane. Consequently, the here reported differences between acute *in vitro* and short-term *in vivo* treatments on membrane properties suggest the existence of a first action in Al^{3+} toxicity, mainly derived from ROS

production that could induce both membrane transition permeability and Δψ decay, thus compromising cell bioenergetics.

As it is well-known, OXPHOS requires the involvement of all mitochondria components (i.e. phosphorylation system, TCA, ETS, and Δψ) to achieve a coupled respiration. The interaction of Al^{3+} downstream complex II is one of the main reasons that might explain the decrease of respiratory capacities in ETS. Our results showed a significant decrease on OXPHOS capacity for the acute *in vitro* model and only a decreasing trend for the short-term *in vivo* model. Regarding to that, as we have above highlighted, the amount of Al^{3+} inside the cell could explain this difference as a dose-dependent effect. In addition, the evaluation of isolated enzymatic activities in both models showed a decrease for complexes III and V, thus supporting the hypothesis of an altered ETS downstream complex II. A similar decrease on enzyme activity for *in vivo* experiments has been also reported by other authors, showing alterations in all the ETS complexes activities, together with a decrease in ATP turnover (Kumar *et al.*, 2008). Under our experimental conditions, the control coupling ratio P/E expresses the limitation of OXPHOS capacity for the phosphorylation system (i.e. ANT, P_i translocator and ATP synthase). When P/E <1 the difference between OXPHOS and ETS_{max} capacities represent a wide mitochondrial respiratory capacity to modulate its response to energetic demands. However, when P/E=0 state that the phosphorylation system does not exert any control on

the respiration, consequently, it can not be modulated in this way (Gnaiger, 2009). Indeed, both our *in vitro* and *in vivo* data support the idea of an alteration in the phosphorylation system (i.e. ANT, P_i translocator, ATP synthase). Evidently, as the control exerted by ATP synthase results essential to achieve a coupled respiration, the here reported decreased in the activity of this complex due to the presence of Al^{3+} disrupts the respiratory efficiency. For this reason, our *in vitro* data demonstrated that Al^{3+} causes a loss of mitochondrial capacity to control the respiration through the phosphorylation system, which jeopardise cell bioenergetics.

In conclusion, Al^{3+} disrupts mitochondrial bioenergetics and promotes the dyscoupling of the organelle in a dose-dependent manner. Our data suggest that both *in vivo* and *in vitro* treatments promote mitochondrial leakiness, ETS_{max} complex II-linked respiratory pathway, and a decrease in both complexes III and V activity. Moreover, our *in vitro* study also showed that the direct action of Al^{3+} include other additional toxic effects such as an alteration in $\Delta\psi$ and a decrease in OXPHOS capacity. The lack of respiratory efficiency together with both an enhance oxidative stress and a decrease in antioxidant enzymes activity (Sánchez-Iglesias *et al.*, 2009) may contribute to the progression of neurodegenerative disorders as Parkinson's disease.

USC
UNIVERSIDADE
DE SANTIAGO
DE COMPOSTELA

Chapter 7

Summary

USC
UNIVERSIDADE
DE SANTIAGO
DE COMPOSTELA

Summary

The study of mitochondria during the last years have revealed that this organelle plays an important role in the development and onset of neurodegenerative disorders such as Alzheimer's disease, Huntington's disease, Friedreich's ataxia, amyotrophic lateral sclerosis, and Parkinson's disease (Dauer & Pzerdborsky, 2003; Jenner, 2003; Duchen, 2004; Schapira, 2008b). Thus, post-mortem studies with Parkinson's disease patients showed that the impairment in mitochondrial respiratory, an increase in the brain free radicals levels, and an alteration in brain metabolic parameters are important factors in the onset and development of this disorder (Schapira, 2008a; Hattori *et al.*, 1991).

As above reported in Chapter 1, in response to cellular energetic demands, the mitochondrial metabolic function is regulated by and regulates the molecular redox states, ion gradients, mitochondrial membrane potential, and the phosphorylation condition of the ATP system. Furthermore, mitochondrion is the powerhouse of the cell through the aerobic pathway, regulates the cellular cycle, triggers the apoptosis, and modulates the oxidative stress (Cadenas, 2004). As consequence, any alteration in the mitochondrial function may jeopardise the cellular homeostasis.

However, which is the factor that makes neuronal populations involved in Parkinson's disease especially sensitive to bioenergetic alterations? The neurons affected by the onset of the disease are the dopaminergic population, particularly those belonging to *substantia nigra*. These neurons show some characteristics that made them different, such as a highly spread axonal arborization, unmyelinated fibres and a massive number of synapses. In fact, the number of synapses projected from SN*pc* to striatum per neuron (~200,000-350,000) is up to two orders of magnitude higher than found in other neuronal populations (Bolam & Pissadaki, 2012). These factors impose a very high energy demand that push the cell close to the bioenergetics edge, thus explaining the especial vulnerability of the dopaminergic neurons to metabolic imbalances. Evidently, under normal circumstances, there are not deleterious effects of this energy demands on the neuron viability. However, any situation that promotes the imbalance between energy production and demand, such as mitochondrial impairment or the rise in the oxidative stress status, can tips the balance towards the edge, causing an excess on the energy demand that cannot be fulfilled. A negative energy balance do place the neuron in risk due to an increase in oxidative stress, occurrence of mitochondrial dysfunctions, alterations in protein renewal and the impairment of autophagic pathways. Bolam & Pissadaki (2012) related all the above mentioned factors with the onset and development of Parkinson's disease. In addition, aging has

been also pointed out as a key factor in the onset of this disorder, mainly as a consequence of bioenergetics changes experienced by the brain with aging. For this reason, the bioenergetic assessment of mitochondrial metabolism is relevant to gain insight on the aetiology of Parkinson's disease.

Another factor involved in the pathogenesis of neurodegenerative disorders is the presence of metals at relatively high concentrations in the patient brain. Indeed, in a previous study our group demonstrated in an experimental model of PD that Al^{3+} promotes brain oxidative stress, decreases the antioxidant activity of some enzymes, and triggers neuronal death (Sánchez-Iglesias *et al.*, 2009). However, the mechanism underlying the cellular death and the metabolic alteration associated has not been determined yet. Our hypothesis is that energetic deficits related with the metabolic impairment due to the exposition to toxics might be favorable conditions for the onset of Parkinson's disease. Within this framework, and in order to gain insight in the aetiology of Parkinson's disease, this Thesis was developed as a bioenergetics study in Parkinson's disease models involving oxidative stress and metals.

7.1 Mitochondrial isolation and the effect of chelators on respiratory parameters

The development of more sensitive oxygen electrodes than those used in classical metabolic studies (e.g. Clarke-type), such as the high-resolution respirometry (Gnaiger, 2008), allows us to carry out more precise bioenergetic studies on neurodegenerative disorders. High-resolution respirometry presents a high sensitivity, being able to detect small changes in the oxygen consumption rate. However, a high conservation degree of both structure and physiological properties in isolated mitochondria is required. For this reason, the establishment of an appropriate isolation protocol emerges as a key point for our bioenergetical studies.

The presence of free Ca^{2+} during mitochondrial isolation has been related with alterations in mitochondrial properties (Gunter *et al.*, 2000; Szabadkai & Duchen, 2008). As it is known, mitochondria act as a Ca^{2+} buffer reservoir, but if its buffering capacity is exceed, the permeability transition pore is opened (Gunter *et al.*, 2000). Given that during the mechanical homogenization of the tissue, the release of Ca^{2+} from cellular reservoirs cannot be prevented, several published protocols for mitochondrial isolation reported the addition of chelants at some point of the isolation procedure (i.e. EDTA and EGTA). However, there is no agreement about the range of concentrations to be used, on which the moment of the procedure to

be added and on the general methodology to follow (Berman & Hastings, 1999; Puka-Sundavall *et al.*, 2000; Lesnefsky & Hoppel, 2006; Frezza *et al.*, 2007; Sims & Anderson, 2008; Fernández-Vizarra *et al.*, 2010; Kamboj & Sandhir, 2011).

Mg^{2+} results essential in the mitochondria for both to establish the electrochemical gradient and to perform the oxidative phosphorylation (Panov & Scarpa, 1996). In addition, EDTA and EGTA show different chemical properties to establish coordinate bonds with Ca^{2+} and Mg^{2+}. Indeed, EGTA has less bonding strength to Ca^{2+} than EDTA, but does not affect the availability Mg^{2+} for the organelle. Evidently, if a chelant capable to bonding Mg^{2+} is used in the respiration medium, mitochondria are not able to perform the oxidative phosphorylation. For those reasons, in the present Thesis a modification in the amount of the chelant is reported in the isolation medium, but not in the respiration medium.

In order to optimize a methodological protocol comprising the mentioned requirements for our research, in the first part of this Thesis (Chapter 4) we studied the effect of chelants on both mitochondrial function and structure. To achieve this aim, a wide range of EDTA or EGTA concentrations were added to the isolation medium, which was followed the corresponding and essential bioenergetics studies. Our results demonstrated that EGTA does not prevent the alterations on the bioenergetic capacities suffered by the mitochondria during the isolation procedure. However, EDTA maintains both the respiratory capacities and the coupling control

ratio. This might be due to the buffer capacity of EDTA in relation to the free Ca^{2+}, which prevents the opening of the permeability transition pore that could dramatically damage the bioenergetics capacities of the mitochondria.

The minimum requirements established for high resolution respirometry are achieved by our isolation protocol. The analysis of both the mitochondrial structure and integrity using electronic microscopy and molecular markers showed optimal parameters. In particular, the biochemical markers showed optimal parameters, which is essential to characterize the isolated mitochondrial sample. Indeed, this biochemical technique allowed us to certify the integrity of the outer membrane, the inner membrane integrity, the presence of mitosomes, and the purity of the isolated fraction. Finally, our results supported the functionality and preservation of our mitochondrial samples during 4-5 hours. Therefore, we developed a mitochondria isolation procedure by differential centrifugation using an isolation buffer containing 3mM of EDTA, that we found essential to perform the planned bioenergetic studies.

7.2 Bioenergetics study on the 6-hydrosydopamine-induced model of Parkinson's disease by oxidative stress

Oxidative stress has been highlighted as one of the main factors involved in the pathogenesis and development of Parkinson's disease (Jenner, 2003; Halliwell, 2006). For this reason, the experimental models for the study of this neurodegenerative disorder are focused to this factor through the case of neurotoxins (e.g. MPTP, 6-hydroxydopamine, paraquat, rotenone, etc.). In the rat, 6-hydroxydopamine is the most used model due to its capacity to promote dopaminergic death through apoptotic processes (Biswas *et al.*, 2005; Kulich *et al.*, 2007; Gomez-Lazarro *et al.*, 2008). Under physiological conditions and in the presence of molecular oxygen, 6-hydroxydopamine is quickly oxidized to its *p*-quinone (Soto-Otero *et al.*, 2000). The chemical reactions during the autoxidation release reactive oxygen species such as anion superoxide radical ($O_2^{\cdot-}$), hydrogen peroxide (H_2O_2), hydroxyl radical ($OH^{\cdot}$), and hydroperoxyl radical ($HO_2^{\cdot}$) (Fig. 5.5) (Graham *et al.*, 1978; Gee & Davidson, 1989; Soto-Otero *et al*., 2000; Méndez-Álvarez *et al.*, 2001).

The second part of this Thesis (Chapter 5) was focused to the toxic effect of 6-hydroxydopamine on both mitochondrial bioenergetics and human neuroblastoma cells (SH-SY5Y). In addition, it has been also studied the possible neuroprotective effect of antioxidant enzymes such as catalase and superoxide dismutase. The

choice of these enzymes is due to the existence of studies reporting an alteration in their activity in Parkinson's disease patients, thus suggesting their involvement in the onset.

As result of our study, it was established a value of 6-hydroxydopamine IC_{50} of 200nM for rat brain mitochondria and a value of 100µM for cellular cultures of human neuroblastoma cells. Our data showed that the 6-hydroxydopamine toxicological mechanism involves a decrease in both complex I-linked metabolic pathway and ATP synthase activity, meaning that 6-hydroxydopamine neurotoxicity is probably triggered by a decrease on the neurons capacity to generate ATP. Additionally, the study with antioxidant enzymes (catalase and superoxide dismutase) allowed us to describe the reactive oxygen species involved in the neurotoxicological mechanism. Both enzymatic systems showed the ability to protect isolated mitochondria from 6-hydroxydopamine toxicity, suggesting that the molecular mechanism is performed by reactive oxygen species.

However, the neuroprotective effect caused by antioxidant enzymes on SH-SY5Y cells seems to be different when compared with isolated mitochondria. Our data support that superoxide dismutase protect from 6-hydroxydopamine neurotoxicity, while catalase at low concentrations promotes cellular death. This differential effect might be attributed to the decrease in the rate of 6-hydroxydopamine autoxidation when catalase is present, which affects the uptake of

the neurotoxin by dopamine transporters, thus promoting its toxicological activity inside the cell.

Finally, the biochemical mechanisms involved in 6-hydroxydopamine autoxidation (Fig. 5.5) and the differential toxicity under our experimental conditions were evaluated. The activity of SOD may boost the formation of H_2O_2, and consequently the formation of $^{\cdot}OH$ through the involvement of the Fenton reaction or by oxidation in the absence of Fe^{2+}. As consequence, the rate of $HO_2^{\cdot}$ formation is decreased, thus showing a neuroprotective effect. In addition, catalase reduces the amount of H_2O_2 in the mitochondrial and cellular environment, and consequently, the production of $^{\cdot}OH$ by the Fenton reaction or by oxidation in absence of Fe^{2+}. However, the absence of H_2O_2 in the media may promote the 6-hydroxydopamine autoxidation through use of the molecular oxygen (Fig. 5.5), thus increasing the formation of $O_2^{\cdot-}$ and $HO_2^{\cdot}$ as a derivate product. The differential neuroprotective ability of the enzymatic systems suggests that the compounds formed in the catalase pathway present a higher toxicity than those formed in presence of superoxide dismutase. Therefore, our results highlight the particular contribution of $O_2^{\cdot-}$ to the toxicity of 6-hydroxydopamine and putatively also $HO_2^{\cdot}$ as a derivate product.

In summary, this study demonstrated that the molecular mechanism associated to 6-hydroxydopamine toxicity involves a double effect. On the one hand, this toxin shows a direct interaction with the complex I metabolic pathway and an inhibition of ATP synthase. On the other hand, 6-hydroxydopamine autoxidation exhibits the formation of reactive oxygen species, being $O_2^{\cdot-}$ and $HO_2^{\cdot}$ the most relevant for the neurotoxicity.

7.3 Aluminium effect on mitochondrial bioenergetics

Al^{3+} is ubiquitous and the third most abundant metal in the Earth crush. Its oxidative state is invariable (3+), and consequently, is not involved in redox processes. Nevertheless, Al^{3+} might work as a Lewis acid and react with some chemical compounds, like other metals, to form chemical complexes with variable properties. Although, Al^{3+} has not been relate with any biological function (Yokel 2002a), its presence in the brain is suppose to promote neurological disorders. In fact, Al^{3+} exposition has been related with the onset of Alzheimer's disease (Kawahara & Kato-Negishi, 2011), behavioural alterations (Kumar *et al*., 2009), learning impairment, osteomalacia (Becaria *et al.*, 2002), lateral amyotrophic sclerosis (Shaw & Tomljenovic, 2013), and Parkinson's disease (Hirsch *et al*., 1991; Yasui *et al.*, 1992). Indeed, neurotoxicological studies found the presence

of high Al^{3+} concentrations in elder brain, thus constituting a pathological risk (House *et al*., 2012).

The mechanism underlying Al^{3+} toxicity has not been fully clarified, but the post-mitotic nature of neurons makes them especially fragile to its exposition. Also, brain is extremely sensible to oxidative stress that might be caused by either an overproduction of free radicals or a decrease in the antioxidant enzymes activity, as it has been previously reported with Al^{3+} (Sánchez-Iglesias *et al.*, 2007). One of the most important mechanisms that promote oxidative stress is the easy reaction of Al^{3+} with superoxide anion to generate the aluminium superoxide anion. This compound presents stronger redox properties than the anion superoxide itself and promotes the formation of H_2O_2 and $HO_2^{\cdot}$. Evidently, the increase in free radicals species contributes to the oxidation of the molecular environment and consequently induces oxidative stress.

Mitochondrion is able to regulate the oxidative status of the cell, but an increase in the rate of ROS formation may induce alterations on the organelle function. Several studies highlighted that the rise of ROS, the release of Ca^{2+} from biological reservoirs, and the disturbance of mitochondrial functions are relevant events for the molecular mechanism underliying cellular death induced by Al^{3+} (Jonson *et al*., 2005; Savory *et al.*, 2003; Brenner, 2002; Kumar *et al*., 2008). However, the molecular mechanism for Al^{3+} toxicity involving mitochondria and the impairment on its metabolic functions has not

been fully established. The third part of this Thesis (Chapter 6) was developed as an Al^{3+} exposition study using *in vitro* and *in vivo* models. The main goal in this study was to understand the effects caused by Al^{3+} in coupled, uncoupled, and non-coupled mitochondrial bioenergetics. Our results in both models studied (*in vitro* and *in vivo*) showed a toxicological effect that promotes mitochondrial dyscoupling and neuronal death.

Al^{3+} toxicity has been also related with its ability to interact directly with biological membranes. In 2000, Tonitello *et al*. reported the ability of Al^{3+} to bond the mitochondrial inner membrane and open the permeability transition membrane pore. According to this effect on membrane, our results showed an increase on proton leak, which agree with the variation in the coupling index L/E and, under *in vitro* experimental conditions, with a membrane potential dissipation. Although, the opening of the permeability transition membrane pore is usually associated with the swelling of the organelle, our electron micrographs supported that the swelling process is not necessary for an alteration of mitochondrial parameters. The observed difference between the *in vitro* and *in vivo* treatments might be attributed to a differential exposition to the metal. In fact, cells contain several protein systems (e.g. ferritin, transferring, etc.) that may work as natural chelants and consequently to buffer the toxic effect of this metal.

Furthermore, the Al^{3+} effect on the enzymes activities of the electron transport system was assessed, showing a decrease in the activity of complex III and V. Other authors related a similar observation with an increase in oxidative stress (Mailloux *et al.*, 2006; Kumar *et al*., 2008) and a direct action of Al^{3+} on the enzymes that constitute the trycarboxylic acid cycle. In our study, the metal lack of direct interaction with the complex II. In addition, the described inhibition for the non coupled respiration suggest that the metal toxicity occurs in the Krebs cycle, probably by acting at the level of aconitase, as t has been previously hypothesized by Zatta *et al*. (2000).

Finally, in the present study it was found a significant decrease in oxidative phosphorylation under *in vitro* conditions, that was also accompanied by a non significant decrease of this variable *in vivo.* Additionally, the obtained P/E control ratio indicated a lost in the efficiency of mitochondrial respiration affecting both models. These results suggested a decrease in the mitochondrial capacity to modulate and control its respiration from the phosphorylative system. This is particularly relevant given that dopaminergic neurons depend strongly on its bioenergetic ability to meet the high energy demands of their metabolism. The lost on the respiratory modulation involves a decrease on the response rate to energetic changes and, through its effect on coupling degree, as well as on the amount of ATP synthesized on each respiratory cycle. This effect might also

trigger the oxidative stress, which would target directly on the electron transport system. Therefore, if we take also into account the previously reported decreased activity of antioxidant enzymes due to Al^{3+} exposition, we can understand how this metal contributes to the progression of neurodegenerative processes such as Parkinson's disease.

In conclusion, Al^{3+} disrupts mitochondrial bioenergetics and promotes the dyscoupling of the organelle in a dose-dependent manner. Our data suggest that both *in vivo* and *in vitro* treatments promote mitochondrial leakiness, alters ETS_{max} complex II-linked respiratory pathway, and decreases in both cases the activity of complexes III and V. Moreover, our *in vitro* study also showed that the direct action of Al^{3+} includes other additional toxic effects such as an alteration in $\Delta\psi$ and a decrease in OXPHOS capacity. The lack of respiratory efficiency together with both an enhancement in oxidative stress and a decrease in the activity of the major antioxidant enzymes (Sánchez-Iglesias *et al.*, 2009) may contribute to the progression of neurodegenerative disorders as Parkinson's disease.

Conclusions

USC
UNIVERSIDADE
DE SANTIAGO
DE COMPOSTELA

1. The presence of chelants in the procedures for mitochondria isolation modifies the bioenergetics of the mitochondria. This is attributed to the different ability of chelants to form coordinate bonds with metals released during isolation, such as Ca^{2+}. However, the use of 3mM EDTA in the isolation buffer causes the minimal alterations in both mitochondria structure and function. For this reason, we adopted the use of the reported concentration of EDTA in the isolation medium for differential centrifugation in order to obtain an enriched and well preserved mitochondrial pellet.

2. The 6-hydroxydopamine alters mitochondrial respiration in a dose-dependent way, being its IC_{50} of 200nM. This effect has been attributed to the interaction of 6-hydroxydopamine with both the metabolic pathway linked to complex I and an inhibition of the ATP synthase activity. The bioenergetics analysis demonstrated that the most altered respiratory steady-state was the active respiration, resulting in a mitochondrial coupling decrease. The addition of antioxidant enzymes (catalase and superxoxide dismutase) prevents the mitochondrial impairment, thus suggesting the involvement of oxidative stress in the underlying mechanism.

3. The 6-hydroxydopamine promotes the cell death in the human neuroblastoma SH-SY5Y with an IC_{50} of 100µM. The mechanism underlying the neurotoxicity involves the increase in the oxidative stress promoted by 6-hydroxydopamine. The cellular death can be prevented by superoxide dismutase but not by catalase. This difference on the neuroprotective role of the antioxidant enzymes is attributed to both the decrease in the autoxidation rate of 6-hydroxydopamine and the differential radical species formed in the presence of catalase. This effect contributes to increase the transport of the neurotoxin into the cell and consequently its ability to trigger the cell death.

4. The differential neuroprotective effects found with both catalase and superoxide dismutase suggests that the reactive oxygen species formed in the catalase pathway are more toxic than those formed when superoxide dismutase is present. For this reason, we purpose both the anion radical superoxide and the hydroperoxyl radical as the main radical species involved in the neurotoxic mechanism of 6-hydroxydopamine.

5. Aluminium directly interacts with the electron transport system decreasing the activity of complexes III and V in both models studied (*in vitro* and *in vivo*). Its *in vitro* action showed a dose-dependent toxicity with an IC_{50} ~50nM. The most altered pathway in the mitochondria was the complex II non-coupled respiration, thus highlighting the importance of its direct interaction.

6. Aluminium is also able to modify mitochondrial membrane properties, increasing the proton leak in both models (*in vitro* and *in vivo*) studied. This effect is accompanied by a dissipation of the membrane potential dissipation when the concentration of aluminium in the media is high, as confirmed by our *in vitro* study. However, the potential dissipation is not related with swelling or any other alteration in mitochondrial structure.

7. The study of the aluminium showed a loss in the efficiency of the respiratory capacity. Our results suggest an impaired ability of the mitochondria to modulate the respiration through the phosphorylation system. Evidently, this effect might promote the rise of oxidative stress and consequently metal neurotoxicity.

8. High-resolution respirometry has proven to be a good suited tool to insight in the aetiology of neurodegenerative disorders involving bioenergetics impairment and oxidative stress. The precision of this technique in addition to molecular techniques allowed us to determine the molecular mechanisms underlying the mitochondrial impairment and to localize new possible targets for future pharmacological strategies.

Chapter 8

Bibliography

USC
UNIVERSIDADE
DE SANTIAGO
DE COMPOSTELA

Abubakar, M.G., Taylor, A., Ferns, G.A. (2004). Regional accumulation of aluminium in the rat brain is affected by dietary vitamin E. *Journal of Trace Elements in Medicine & Biology*, 18, 53–59.

Agamanolis, D.P. (2011). Neuropathology-web.org, Chapter 9.

Aikens, J., Dix, J.A. (1991). Perhydroxyl radical (HOO·) initiated lipid peroxidation. The role of fatty acid hydroperoxides. The Journal of Biological Chemistry, 266, 15091-15098.

Alfrey, A.C., Hegg, A., Craswell, P. (1980). Metabolism and toxicity of aluminum in renal failure. The American Journal of Clinical Nutrition, 33, 1509–1516.

Andersen, J.K. (2004). Oxidative stress in neurodegeneration: cause or consequence? *Nature reviews Neuroscience*, S18-25.

Andrási, E., Páli, N., Molnár, Z., Kösel, S. (2005). Brain aluminum, magnesium and phosphorus contents of control and Alzheimer-diseased patients. *Journal of Alzheimer's Disease*, 7, 273-24.

Andreyev, A., Fiskum, G. (1999) Calcium induced release of mitochondrial cytochrome c by different mechanisms selective for brain versus liver. *Cell death and Differentiation*, 6(9), 825-32.

Aon, M.A., Cortassa, S., O'Rourke, B. (2010). Redox-optimized ROS balance: A unifying hypothesis. *Biochimica et Biophysica Acta*, 1797, 865-877.

Asanuma, M., Hirata, H., Cadet, J.L. (1998) Attenuation of 6-hydroxydopamine-induced dopaminergic nigrostriatal lesions in superoxide dismutase transgenic mice. *Neuroscience*, 85, 907-917.

Barkats, M., Millecamps, S., Bilang-Bleuel, A., Mallet, J. (2002) Neuronal transfer of the human Cu/Zn superoxide dismutase gene increases the resistance of dopaminergic neurons to 6-hydroxydopamine. *Journal of Neurochemistry*, 82, 101-109.

Bast-Pattersen R., Drablos P. A., Goffeng L. O., Thomassen Y. and Torres C. G. (1994) Neuropsychological deficit among elderly workers in aluminum production. *American Journal of Industrial Medicine*, 25, 649–662.

Becaria, A., Campbell, A., Bondy, S.C. (2002). Aluminum as a toxicant. *Toxicological and Industrial Health,* 18, 309–320.

Bergmeyer, H.U. (Ed.), Bernt, E., Hess, B. (1965). *Lactate dehydrogenase*. *Methods of enzymatic analysis*. Basel: Verlag Chemie.

Berman, S.B. & Hastings, T.G. (1999). Dopamine oxidation alters mitochondrial respiration and induces permeability transition in brain mitochondria: Implications for Parkinson's disease. *Journal of neurochemistry*, 73, 1127-1137.

Betarbet, R., Sherer, T.B., MacKenzie, G., Garcia-Osuna, M., Panov, A.V., Greenamyre, J.T. (2000). Chronic systemic pesticide exposure reproduces features of Parkinson's disease. *Nature Neuroscience*, 3(12), 1301-6.

Betarbet, R., Sherer, T.B., Donat, A., Di Monte, J., Greenamyre, T. (2002). Mechanistic approaches to Parkinson's disease pathogenesis. *Brain Pathology*, 12, 499-510.

Betarbet, R., Sherer, T.B., Greenamyre, J.T. (2005). Ubiquitin-proteasome system and Parkinson's disease. *Experimental neurology*, 191 Suppl.1, S17-27.

Biswas, S.C., Ryu, E., Park, C., Malagelada, C., Greene, L.A. (2005). PUMA and p53 play required roles in death evoked in a cellular model of Parkinson's disease. *Neurochemical Research*, 30, 839-845.

Blum, D., Torch, S., Nissou, M.F., Benabid, A-L., Verna, J.M. (2000). Extracellular toxicity of 6-hydroxydopamine on PC12 cells. *Neuroscience Letters*, 283, 193-196.

Blum, D., Torch, S., Lambeng, N., Nissou, M.F., Benabid, A-L., Sadoul, R., Verna, J.M. (2001) Molecular pathways involved in the neurotoxicity of 6-OHDA, dopamine and MPTP: contribution to the apoptotic theory in Parkinson's disease. *Progress in Neurobiology*, 65, 135-172.

Bolam, J.P. & Pissadaki, E.K. (2012). Living on the edge with too many mouths to feed: why dopamine neurons die. *Movement Disorders*, 27(12), 1478-83.

Bolla, K.I., Briefel, G., Spector, D., Schwartz, B.S., Wieler, L., Herron, J., Gimenez, L. (1992). Neurocognitive effects of aluminium. *Archives of Neurology*, 49(10), 1021-6.

Booth, R.F.G., Clark, J.B. (1978). A rapid method for the preparation of relatively pure metabolically competent synaptosomes from rat brain. *Biochemical Journal*, 176, 365-70.

Bové, J., Prou, D., Perier, C., Przedborsky, S. (2005). Toxin-induced models of Parkinson's disease. *NeuroRx*, 2, 484-494.

Bové, J., Perier, C. (2012) Neurotoxin-based models of Parkinson's disease. *Neuroscience*, 211, 51-76.

Boveris, A., Cadenas, E., Stoppani, A.O. (1976) Role of ubiquinone in the mitochondrial generation of hydrogen peroxide. *Biochemical Journal*, 156, 435-444.

Braak, H., Müller, C.M., Rüb, U., Ackermann, H., Bratzke, H., de Vos, R.A.I., Del Tredici, K. (2006). Pathology associated with sporadic Parkinson's disease- where does it end? *Journal of Neural Transmission [Suppl]*, 70, 89-97.

Brady, S.T., Siegel, G.J., Albers, R.W., Price, D.L. (2012). Besic Neurochemsitry. Principles of molecular, cellular, and medical neurobiology. *Academic Press*, 8th Ed.

Brandt, U. (2011). A two-state stabilization-change mechanism for proton-pumping complex I. *Biochimica et Biophysica Acta*, 1807, 1364-1369.

Brusewitz, S. (1984). Aluminum, Vol 203. Stockholm, Sweden, University of Stockholm Institute of Theoretical Physics.

Cadenas, E., Boveris, A., Ragan, C.I., Stopani, A.O. (1977) Production of superoxide radicals and hydrogen peroxide by NADH-ubiquinone reductase and ubiquinol-cytochrome c reductase from beef-heart mitochondria. *Archives of Biochemistry and Biophysics*, 180, 248-257.

Cadenas, E. Mitochondrial free radical production and cell signaling (2004). *Molecular Aspects of Medicine*, 25, 17-26.

Cann, C.E., Prussin, S.G., Gordan, G.S. (1979). Aluminum uptake by the parathyroid gland. *The Journal of Clinical Endocrinology and Metabolism*, 49, 543–545.

Carlsson, A., Falck, B., Hillarp, N.A. (1962). Cellular localizations of brain monoamines. *Acta Physiologica Scandinavica. Supplementum*, 56(196), 1-28.

Chance, B., Williams, G.R. (1955). Respiratory enzymes in oxidative Phosphorylation. I kinetics of oxygen utilization. *Journal of Biological Chemistry*, 217, 383-393.

Choi, W-S., Yoon, S-Y., Oh, T.H., Choi, E-J., O'Malley, K.L., Oh, Y.J. (1999) Two distinct mechanisms are involved in 6-hydroxydopamine- and MPP^+-induced dopaminergic neuronal cell death: role of caspases, ROS, and JNK. *Journal of Neuroscience Research*, 57, 86-94.

Clark, J.B., Nicklas, W.J. (1970). The Metabolism of Rat Brain Mitochondria. *Journal Biological Chemistry*, 245, 4724-31.

Clark, J.B., Bates, T.E., Boakye, P., Kuimov, A., Land, J.M. (1997). *Investigation of mitochondrial defects in brain and skeletal muscle.* In A.J. Turner, J. Bachelor (Eds.), A practical approach to the investigation of metabolic disease. Oxford: IRL Press at Oxford University Press.

Cohen, G., Farooqui, R., Kesler, N. (1997). Parkinson disease: A new link between monoamine oxidase and mitochondrial electron flow. *Proceedings of the National Academy of Sciences*, 94, 4890-4.

Constantini, S. & Giordano, R. (1991). Aluminium determination in complex matrixes. *Aluminum in Chemistry, Biology and Medicine*, (Nicolini M., Zatta P. F. and Corain B., eds), pp. 21–29. *Raven Press*, New York.

Dawson, T.M. & Dawson, V.L. (2003a). Rare genetic mutations shed light on the pathogenesis of Parkinson's disease. *The Journal of Clinical Investigation*, 111 (2), 145-151.

Dawson, T.M. & Dawson, V.L. (2003b). Molecular pathways of neurodegeneration in Parkinson's disease. *Science*, 302, 819-822.

Dauer, W. & Przedborski, S. (2003). Parkinson's disease: mechanisms and models. *Neuron*, 39, 889-909.

Deng, Z., Coudray, C., Gouzoux, L., Mazur, A., Rayssiguier, Y., Pepin, D. (1998). Effect of oral aluminum and aluminum citrate on blood level and short-term tissue distribution of aluminum in the rat. *Biological Trace Elements Research*, 63, 139–147.

De Lau, L.M. & Breteler, M.M. (2006). Epidemiology of Parkinson's disease. *The Lancet Neurology*, 5(6), 525-535.

De Marchi, U., Mancon, M., Battaglia, V., Ceccon, S., Cardellini, P., Tonitello, A. (2004). Influence of reactive oxygen species production by monoamine oxidase activity on aluminium-induced mitochondrial permeability transition. *Cellular and Molecular Life Sciences*, 61, 2664-2671.

Devlin, T.M. (2004). Bioquímica. Libro de texto con aplicaciones clínicas. Ed. Reverté, 4ª Ed.

Dieteren, C.E., Willems, P.H., Vogel, R.O., Swarts, H.G., Fransen, J., Roepman, R., Crienen, G., Smeitink, J.A., Nijtmans, L.G., Koopman, W.J. (2008). Subunits of mitochondrial complex I exists as part of matrix- and membrane-associated subcomplexes in living cells. *Journal of Biological Chemistry*, 283(50), 34753-61.

Doty, R.L. (2012). Olfaction in Parkinson's disease and related disorders. *Neurobiology of Disease*, 46(3), 527-52.

Dua, R. & Gill, K.D. (2004). Effect of aluminium phosphide exposure on kinetic properties of cytochrome oxidase and mitochondria energy metabolism in rat brain. *Biochimica et Biophysica Acta*, 1674(1), 4-11.

Duchen, M.R. (2004). Mitochondria in health and disease: perspectives on a new mitochondrial biology. *Molecular Aspects of Medicine*, 25, 365-451.

Ebert, A.D., Beres, A.J., Barber, A.E., Svendsen, C.N. (2008). Human neural progenitor cells over-expressing IGF-1 protect dopamine neurons and restore function in a rat model of Parkinson's disease. *Experimental Neurology*, 209(1), 213-23.

Enochs, W.S., Sarna, T., Zecca, L., Riley, P.A., Swartz, H. M. (1994). The roles of neuromelanin, binding of metal ions, and oxidative cytotoxicity in the pathogenesis of Parkinson's disease: a hypothesis. *Journal of Neural Transmission*. 7, 83-100.

Exley, C. (2004). Aluminum in antiperspirants: more than just skin deep. *American Journal of Medicine*, 117, 969–970.

Exley, C. (2013). Human exposure to aluminium. *Enviromental Science: Processes Impacts*, 15: 1807-18016.

Fasching, M. & Gnaiger, E. (2009). Determination of membrane potential with TPP^+ and an ion selective electrode. *Mitochondrial Physiology Network*, 14.5, 1-7.

Fearnley, J.M., Lees, A.J. (1991). Ageing and Parkinson's disease: substantia nigra regional selectivity. *Brain*, 114, 2283-301.

Fernández-Vizarra, E., Ferrín, G., Pérez-Martos, A., Fernández-Silva, P., Zeviani, M., Enríquez, J.A. (2010). Isolation of mitochondria for biogenetical studies: An update. *Mitochondrion*, 10, 253-62.

Finel, M. (1998). Organization and evolution of structural elements within complex I. *Biochimica et Biophysica Acta*, 1364(2), 112-21.

Flaten, T.P. (2001). Aluminium as a risk factor in Alzheimer's disease, with emphasis on drinking water. *Brain Research Bulletib*, 55, 187–196.

Fleischer, S., McIntyre, J.O., Vidal, J.C. (1979). Large-scale preparation of rat liver mitochondria in high yield. *Methods in Enzymology*, 55, 32-9.

Frank, S., Wagenknetch, T., McEwen, B.F., Marko, M., Hsieh, C.E., Mannella, C.A. (2002). Three-dimensional imaging of biological complexity. *Journal of Structural Biology*, 138, 85-91.

Frezza, C., Cipolat, S., Scorrano, L. (2007). Organelle isolation: functional mitochondria from mouse liver, muscle and cultured filroblasts. *Nature Protocols*, 2, 287-95.

Frey, T.G. & Mannella, C.A. (2000). The internal structure of mitochondria. *Trends in Biochemical Sciences*, 25, 319-324.

Friederich, T. & Weiss, H. (1997). Modular evolution of the respiratory NADH:ubiquinone oxidoreductase and the origin of its modules. *Journal of Theorical Biology*, 187, 529-540.

Friedman L.G., Lachenmayer M.L., Wang J., He L., Poulose S.M., Komatsu M., Holstein G.R., Yue Z. (2012). Disrupted Autophagy Leads to Dopaminergic Axon and Dendrite Degeneration and Promotes Presynaptic Accumulation of alpha-Synuclein and LRRK2 in the Brain. *Journal of Neuroscience*, 32(22), 7585–7593.

Fu, S., Gebicki, S., Jessup, W., Gebicki, J.M., Dean, R.T. (1995). Biological fate of amino acid, peptide and protein hydroperoxides. *Biochemical Journal*, 311, 821-827.

Gaeta, A. & Hider, R.C. (2005). The crucial role of metal ions in neurodegeneration: the basis for a promising therapeutic strategy. *British Journal of Pharmacology*, 146(8), 1041-1059.

Gaig, C. & Tolosa, E. (2009). When does Parkinson's disease begin? *Movement Disorders*, 24 Suppl. 2, S656-64.

Ganrot, P.O. (1986). Metabolism and possible health effects of aluminum. *Environmental Health Perspectivas*, 65, 363–441.

Garruto, R.M., Fukatsu, R., Yanagihara, R., Gajdusek, D.C., Hook, G., Fiori, C.E. (1984). Imaging of calcium and aluminium in neurofibrillary tangle-bearing neurons in parkinsonism-dementia of Guam. *Proceedings of The National Academy of Sciences of The United States of America*, 81(6), 1875-9.

Gebicki, S. & Gebicki, J.M. (1993). Formation of peroxides in amino acids and proteins exposed to oxygen free radicals. *Biochemical Journal*, 289, 743-749.

Gee, P. & Davison, A.J. (1989). Intermediates in the aerobic aoutoxidation of 6-hydroxydopamine: relative importance under different reaction conditions. *Free Radicals in Biology & Medicine*, 6, 271-284.

Giasson, B.I., Duda, J.E., Murray, I.V., Chen, Q., Souza, J.M., Hurtig, H.I., Ischiropoulos, H., Trojanowski, J.Q., Lee, V.M. (2000a). Oxidative damage linked to neurodegeneration by selective alpha-synuclein nitration in synucleinopathy lesions. *Science*, 290(5493), 985-9.

Giasson, B.I., Jakes, R., Goedert, M., Duda, J.E., Leight, S., Trojanowski, J.Q., Lee, V.M. (2000b). A panel of epitope-specific antibodies detects protein domains distributed throughout human alpha-synuclein Lewy bodies of Parkinson's disease. *Journal of Neuroscience*, 59(4), 528-33.

Glinka, Y., Tipton, K., Youdim, M. (1996). Nature of inhibition of mitochondrial respiratory complex I by 6-hydroxydopamine. *Journal of Neurochemistry*, 66, 2004-2010.

Glinka, Y., Tipton, K.F., Youdim, M.B.H. (1998). Mechanism of inhibition of mitochondrial respiratory complex I by 6-hydroxydopamine and its prevention by desferroxamine. *European Journal of Pharmacology*, 351, 121-129.

Gnaiger, E. (2007). Mitochondrial Pathways and Respiratory Control. OROBOROS MiPNet Publications. 1st Ed., Bluebook.

Gnaiger, E. (2008). Polarographic oxygen sensors, the oxygraph, and high-resolution respirometry to assess mitochondrial function. In: Dyens J, Will Y (eds) Drug-Induced Mitochondrial Dysfunction. John Wiley & Sons, Hoboken, New Jersey, pp 327-352.

Gnaiger, E. (2009). Capacity of oxidative phosphorylation in human skeletal muscle. New perspectives of mitochondrial physiology. *The International Journal of Biochemistry & Cell Biology*, 41, 1837-1845.

Gomez-Lazaro, M., Galindo, M.F., Concannon, C.G., Segura, M.F., Fernández-Gómez, F.J., Llecha, N., Comella, J.X., Prehn, J.H.M., Jordan, J. (2008). 6-hydroxydopamine activates the mitochondrial apoptosis pathway through p38 MAPK-mediated, p53-independent activation of Bax and PUMA. *Journal of Neurochemistry*, 104, 1599-1612.

Graham, D.G., Tiffany, S.M., Bell, W.R., Gutknetch, W.F. (1978). Autoxidation versus convalent binding of quinones as the mechanism of toxicity of dopamine, 6-hydroxydopamine, and related compounds toward C1300 neuroblastoma cells in vitro. *Molecular Pharmacology*, 14, 644-653.

Greger J. L. & Sutherland J. E. (1997). Aluminum exposure and metabolism. *Critical Reviews in Clinical Laboratory Sciences*, 34, 439–474.

Gunter, T.E., Buntinas, L., Sparagna, G., Eliseev, R., Gunter, K. (2000). Mitochondrial calcium transport:mechanisms and functions. *Cell Calcium*, 28,285-96.

Gutteridge, J.M., Quinlan, G.J., Clark, I., Halliwell, B. (1985). Aluminium salts accelerate peroxidation of membrane lipids stimulated by iron salts. *Biochimica et Biophysica Acta*, 835, 441–447.

Halliwel, B., Gutteridge, J.M., Cross, C.E. (1992). Free radicals, antioxidants, and human disease: where are we now? *Journal of Laboratory and Clinical Medicine*, 119, 598-620.

Halliwell, B. (2006). Oxidative stress and neurodegeneration: where are we now? *Journal of Neurochemistry*, 97, 1634-1658.

Hamilton, E.I., Miniski, M.J., Cearly, J.J. (1973). The concentration and distribution of some stable elements in healthy human tissues from the United Kingdom: An environmental study. *Science of the Total Environment*, 1, 341–374.

Hanrott, K., Gudmunsen, L., O'Neill, M.J., Wonnacott, S. (2006). 6-Hydroxydopamine-induced apoptosis is mediated via extracellular auto-oxidation and caspase 3-dependent activation of protein kinase Cdelta. *The Journal of Biological Chemistry*, 281, 5373-5382.

Harris, W.R., Wang, Z., Hamada, Y.Z. (2003). Competition between transferrin and the serum ligands citrate and phosphate for the binding of aluminum. *Inorganic Chemistry*, 42, 3262–3273.

Hattori, N., Tanaka, M., Ozawa, T., Mizuno, Y. (1991). Immunohistochemical studies on complexes I,II,III, and IV of mitochondria in Parkinson´s disease. Annals of Neurology, 30(4), 563-571.

Hawkes, C.H., Del Tredici, K., Braak, H. (2010). A timeline for Parkinson's disease. *Parkinsonism & Related Disorders*, 16, 79-84.

Hermida-Ameijeiras, A., Méndez-Álvarez, E., Sánchez-Iglesias, S., Sanmartín-Suarez, C., Soto-Otero, R. (2004). Autoxidation and MAO-mediated metabolism of dopamine as a potential cause of oxidative stress: role of ferrous and ferric ions. *Neurochemistry International*, 45, 103-116.

Hornykiewicz, O. & Kish, S.J. (1987). Biochemical pathophysiology of Parkinson's disease. *Advances in neurology*, 45, 19-34.

House, E., Esiri, M., Forster, G., Ince, P.G., Exley, C. (2012). Aluminium, iron and copper in human brain tissues donated to the medical research council's cognitive function and ageing study. *Metallomics*, 4(1), 56-65.

Hsieh, C.E., Marko, M., Frank, J., Mannella, C.A. (2002). Electron tomography of frozen-hydrated tissue sections. *Journal of Structural Biology*, 138, 63-73.

Izumi, Y., Sawada, H., Sakka, N., Yamamoto, N., Kume, T., Katsuki, H., Shimohama, S., Akaike, A. (2005). *p*-Quinone mediates 6-hydroxydopamne-induced dopaminergic neuronal death and ferrous iron accelerates the conversion of p-quinone into melanin extracellularly. *Journal of Neuroscience Research*, 79, 849-860.

Jenner, P. (2003). Oxidative stress in Parkinson's disease. *Annals of neurology*, 53 (suppl. 3), S26-S38.

Julka, D., Sandhir, R., Gill, K.D. (1995). Altered cholinergic metabolism in rat CNS following aluminum exposure: implications on learning performance. *Journal of Neurochemistry*, 65, 2157–2164.

Kabuto, H., Yokoi, I., Iwata-Ichikawa, E., Ogawa, N. (1999). EPC-K1, a hydroxyl radical scavenger, prevents 6-hydroxydopamine-induced dopamine depletion in the mouse striatum by up-regulation of catalase activity. *Neurochemical Research*, 24, 1543-1548

Kamboj, S.S. & Sandhir, R. (2011). Protective effect of N-acetylcysteine supplementation on mitochondrial oxidative stress and mitochondrial enzymes in cerebral cortex of streptozotocin-treated diabetic rats. *Mitochondrion*, 11, 214-22.

Kandiah, J. & Kies, C. (1994). Aluminum concentrations in tissues of rats: effect of soft drink packaging. *Biometals,* 7, 57–60.

Kim, S., Nam, J., Kim, K. (2007). Aluminum exposure decreases dopamine D1 and D2 receptor expression in mouse brain. *Human & Experimental Toxicology*, 26, 741–746.

Kitada, T., Asakawa, S., Hattori, N., Matsumine, H., Yamamura, Y., Minoshima, S., Yokochi, M., Mizuno, Y., Shimizu, N. (1998). Mutations in the parkin gene cause autosomal recessive juvenile parkinsonism. *Nature*, 392(6676), 605-608.

Kulich, S.M., Horbinsky, C., Patel, M., Chu, C.T. (2007). 6-hydroxydopamine induces mitochondrial ERK activation. *Free Radicals in Biology & Medicine*, 43, 372-383.

Kumar, V., Amanjit, B., Kiran, D.G. (2008). Impairment of mitochondrial energy metabolism in different regions of rat brain following chronic exposure to aluminium. *Brain research*, 1232, 94-103.

Krüger, R., Kuhn, W., Müller, T., Graeber, M., Kösel, S., Przuntek, H., Schöls, L., Riess, O. (1998). Ala30Pro mutation in the gene encoding alpha-synuclein in Parkinson's disease. *Nature Genetics*, 18(2), 106-8.

Langston, J.W., Irwin, I., Langston, E.B., Forno, L.S. (1984). Pargyline prevents MPTP-induced parkinsonism in primates. *Science*, 225(4669), 1480-2.

Langston, J.W. (2002). Parkinson's disease:current and future challenges. *Neurotoxicology*, 23(4-5), 443-50.

Leblanc, C., Richard, O., Kloareg, B., Viehmann, S., Zetsche, K., Boyen, C. (1997). Origin and evolution of mitochondria: what have we learnt from red algae? *Current Genetics*, 31, 193-207.

Lenaz, G., Bovina, C., D'Aurelio, M., Fato, R., Formiggini, G., Genova, M.L., Giuliano, G., Merlo Pich, M., Paolucci, U., Parenti Castelli, G., Ventura, B. (2002). Role of mitochondria in oxidative stress and aging. *Annals of the New York Academy of Sciences*, 959, 199-213.

Leroy, E., Boyer, R., Auburger, G., Leube, B., Ulm, G., Mezey, E., Harta, G., Brownstein, M.J., Jonnalagada, S., Chernova, T., Dehejia, A., Lavedan, C., Gasser, T., Steinbach, P.J., Wilkinson, K.D., Polymeropoulos, M.H. (1998). The ubiquitin pathway in Parkinson's disease. *Nature*, 395(6701), 451-452.

Lesnefsky, E.J., Hoppel, C.L. (2006). Oxidative phosphorylation and aging. Ageing Research Reviews, 5, 402-33.

Lévesque, L., Mizzen, C.A., McLachlan, D.R., Fraser, P.E. (2000). Ligand specific effects of aluminum incorporation and toxicity in neurons and astrocytes. *Brain Resesearch*, 877, 191–202.

Lin, J.L., Yang, Y.J., Yang, S.S., Leu, M.L. (1997). Aluminum utensils contribute to aluminum accumulation in patients with renal disease. *American ournal of. Kidney Diseases*, 30, 653–658.

Lin, M.T. & Beal, M.F. (2003). The oxidative damage theory of aging. Clinical Neuroscience Research, 2, 305-315.

Linert, W., Herlinger, E., Jameson, R.F., Kienzl, E., Jellinger, K., Youdim, M.B.H. (1996). Dopamine, 6-hydroxydopamine, iron, and dioxygen-their mutual interactions and possible implication in the development of Parkinson's disease. *Biochimica et Biophysica Acta*, 1316, 160-168.

Liss, B., Haeckel, O., Wildmann, J., Miki, T., Seino, S., Roeper, J. (2005). K-ATP channels promote the differential degeneration of dopaminergic midbrain neurons. Nature Neuroscience, 8, 1742–1751.

Lione, A. (1983). The prophylactic reduction of aluminum intake. *Food Chemical Toxicology*, 21, 103–109.

Lione, A. (1984). Aluminum in foods. *Nutrition Reviews,* 42, 31.

Lione, A. (1985). Aluminum toxicology and the aluminum-containing medications. *Pharmacology & Therapeutics*, 29, 255–285.

Mailloux, R.J., Hamel, R., Appanna, V.D. (2006). Aluminium toxicity elicits a dysfunctional TCA cycle and succinate accumulation in hepatocytes. *Journal of Biochemical Molecular and Toxicology*, 20(4), 198-208.

McLachlan, D.R.C. (1995). Aluminum and the risk of Alzheimer's disease. *Environmetrics,* 6, 233–275.

Malkus, K.A., Tsika, E., Ischiropoulos, H. (2009). Oxidative modifications, mitochondrial dysfunction, and impaired protein degradation in Parkinson's disease: how neurons are lost in the Bermuda triangle. *Molecular neurodegeneration*, 4, 24.

Mannella, C.A., Buttle, K., Rath, B.K., Marko, M. (1998). Electron microscopy tomography of rat-liver mitochondria and their interaction with the endoplasmic reticulum. *Biofactors,* Oxford, 8, 225-228.

Marti, M.J., James, C.J., Oo, T.F., Kelly, W.J., Burke, R.E. (1997). Early developmental destruction of terminals in the striatal target induces apoptosis in dopamine neurons of the substantia nigra. *Journal of Neuroscience*, 17, 2030-2039.

Masini, A., Ceccarelli-Stanzani, D., Muscatello, U. (1983). The effect of oligomycin on rat liver mitochondria respiring in state 4. *FEBS Letters*, 160, 137-140.

Mathews, C.K. & Van Holde, K.E. (1999). *Bioquímica*. Mc-Graw Hill/Interamericana. CD.

Mathiesen, C. & Hägerhall, C. (2003). The Antiporter module of respiratory chain complex I includes the MrpC/NuoK subunit-a revision of the modular evolution scheme. *FEBS Letters*, 549, 7-13.

Mazzio, E.A., Reams, R.R., Soliman, K.F.A. (2004). The role of oxidative stress, impaired glycolysis and mitochondrial respiratory redox failure in the cytotoxic effects of 6-hydroxydopamine in vitro. *Brain Research*, 1004, 29-44.

Méndez-Álvarez, E., Soto-Otero, R., Hermida-Ameijeiras, A., López-Martín, M.E., Labandeira-García, J.L. (2001). Effect of iron and manganese on hydroxyl radical production by 6-hydroxydopamine: mediation of antioxidants. *Free Radicals in Biolology and Medicine*, 31, 986-998.

Méndez-Álvarez, E. & Soto-Otero, R. (2004). Dopamine: A double-edged sword for the human brain. *Recent Research Developments in Life Sciences,* 2, 217-246.

Miu, A.C., Andreescu, C.E., Vasiu, R., Oltenau, Al. (2003). A behavioural study and histological study of the effects of long-term exposure of adult rats to aluminium. *International Journal of Neuroscience*, 113(9), 1197-211.

Moore, P.B., Day, J.P., Taylor, G.A., Ferrier, I.N., Fifield, L.K., Edwardson, J.A. (2000). Absorption of 26aluminium in Alzheimer's disease, measured using accelerator mass spectrometry. *Dementia and Geriatric Cognitive Disorders*, 11, 66–69.

Muller, F.L., Lustgarten, M.S., Jank, Y. Richardson, A., Van Remmen, H. (2007). Trends in oxidative stress and aging. *Free Radical in Biology and Medicine*, 43(4), 477-503.

Nicholls, D.G., Ferguson, S.J. (2002). Bioenergetics 3. *Academic Press*, London. 287p.

Nieboer, E., Gibson, B.L., Oxman, A.D., Kramer, J. R. (1995). Health effects of aluminum: a critical review with emphasis on aluminum in drinking water. *Environmental Reviews*, 3, 29–81.

Niu, P.Y., Niu, Q., Zhang, L.P., Wang, S.C., He, T.C., Wu, P., Conti, M., Di Gioacchino, M., Boscolo, P. (2005). Aluminium impairs rat neural cell mitochondria *In vitro*. *International Journal of Inmunology and Pharmacology*, 18(4), 683-689.

Olanov, C.W. & Brundin, P. (2013). Parkinson's disease and alpha synuclein: is Parkinson's disease a prion-like disorder?. *Movement Disorders*, 28(1), 31-40.

Ossola, B., Kääräinen, T.M., Raasmaja, A., Männistö, P.T. (2008). Time-dependent protective and harmful effects of quercetin on 6-OHDA-induced toxicity in neuronal SH-SY5Y cells. *Toxicology*, 250, 1-8.

Oteiza, P.I., Fraga, C.G., Keen, C.L. (1993). Aluminum has both oxidant and antioxidant effects in mouse brain membranes. *Archives of Biochemistry and Biophysics*, 300, 517–521.

Palmeira, C.M. & Oliveira, C.R. (1992). Partitioning and membrane disordering effects of dopamine antagonists: influence of lipid peroxidation, temperature, and drug concentration. *Archives of Biochemistry and Biophysics*, 295, 161–171.

Panov, A. & Scarpa, A. (1996). Mg2+ Control of Respiration in Isolated Rat Liver Mitochondria. *Biochemistry*, 35, 12849-56.

Parker, W.D. Jr., Swerdlow, R.H. (1998). Mitochondrial dysfunction in idiopathic Parkinson disease. *The American Journal of Human Genetics*, 62, 758-762.

Parkinson J. (1817). An essay on the shaking palsy. London: Whittingham and Rowland for Sherwood, Neely, Jones.

Perier, C., Tieu, K., Guégan, C., Caspersen, C., Jackson-Lewis, C., Carelli, V., Martinuzzi, A., Hirano, M., Przedborsky, S., Vila, M. (2005). Complex I deficiency primes Bax-dependent neuronal apoptosis trough mitochondrial oxidative damage. *Proceedings of the National Academy of Sciences of the United States of America*, 102(52), 19126-31.

Perl, D.P., Gajdusek, D.C., Garruto, R.M., Yanagihara, R.T., Gibbs, C.J. (1982). Intraneuronal aluminum accumulation in amyotrophic lateral sclerosis and Parkinsonism-dementia of Guam. *Science*, 217, 1053–1055.

Pryor, W.A. (1986). Oxy-radicals and related species: their formation, lifetimes, and reactions. Annual Review of Physiology, 48, 657-667.

Puka-Sundvall, M., Wallin, C., Gilland, E., Hallin, U., Wang, X., Sandberg, M., Karlsson, J., Blomgren, K., Hagberg, H. (2000). Impairment of mitochondrial respiration after cerebral hypoxia–ischemia in immature rats: relationship to activation of caspase-3 and neuronal injury. Developmental Brain Research, 125, 43-50.

Ravi, S.M., Prabhu, B.M., Raju, T.R., Bindu, P.N. (2000). Long-term effects of postnatal aluminium exposure on acetylcholinesterase activity and biogenic amine neurotransmitters in rat brain. *Indian Journal of Physiology and Pharmacology*, 44, 473–478.

Roberts, E. (1986). Alzheimer's disease may begin in the nose and may be caused by aluminosilicates. *Neurobioliology of Aging*, 7, 561–567.

Robertson, J.A., Felsenfeld, A.J., Haygood, C.C., Wilson, P., Clarke, C., Llach, F. (1983). Animal model of aluminium-induced osteomalacia: role of chronic renal failure. *Kidney International*, 23(2), 327-35.

Rodríguez, M., Barroso-Chinea, P., Abdala, P., Obeso, J., González-Hernández, T. (2001). Dopamine cell degeneration induced by intraventricular administration of 6-hydroxydopamine in the rat: similarities with cell loss in Parkinson's disease. Experimental Neurology, 169, 163-181.

Roestenberg, P., Manjeri, G.R., Valsecchi, F., Smeitnik, J.A., Willems, P.H., Koopman, W.J. (2012). Pharmacological targeting of mitochondrial complex I deficiency: the cellular level and beyond. *Mitochondrion*, 12(1), 57-65.

Rosenthal, R.E., Hamud, F., Fiskum, G., Varghese, P.J., Sharpe, S. (1987). Cerebral ischemia and reperfusion: Prevention of brain mitochondrial injury by lidoflazine. Journal of Cerebral Blood Flow and metabolism, 7, 752-758.

Saito, Y., Nishio, K., Ogawa, Y., Kinumi, T., Yoshida, Y., Masuo, Y., Niki, E. (2007). Molecular mechanisms of 6-hydroxydopamine-induced cytotoxicity in PC12 cells: involvement of hydrogen peroxide-dependent and -independent action. *Free Radicals in Biology and Medicine*, 42, 675-685.

Sampson, V. & Allen, T. (2001). Cytochrome c/cytochrome c oxidase interaction. European Journal of Biochemistry, 268, 6534-6544.

Sánchez-Iglesias, S., Rey, P., Méndez-Álvarez, E., Labandeira-García, J.L., Soto-Otero, R. (2007a). Time-course of brain oxidative damage caused by intrastriatal administration of 6-hydroxydopamine in a rat model of Parkinson's disease. *Neurochemistry Research*, 32(1), 99-105.

Sánchez-Iglesias, S., Soto-Otero, R., Iglesias-González, J., Barciela-Alonso, M.C., Bermejo-Barrera, P., Méndez-Álvarez, E. (2007b). Analysis of brain regional distribution of aluminium in rats via oral and intraperitoneal administration. *Journal of Trace Elements in Medicine and Biology*, 21Suppl 1, 31-4.

Sánchez-Iglesias, S., Méndez-Álvarez, E., Iglesias-González, J., Muñoz-Patiño, A., Sánchez-Sellero, I., Labandeira-García, J.L., Soto-Otero, R. (2009). Brain oxidative stress and selective behaviour of aluminium in specific areas of rat brain: potential effects in a 6-hydroxydopamine-induced model of Parkinson's disease. *Journal of Neurochemistry*, 109(3), 879-88.

Sauer, H. & Oertel, W.H. (1994). Progressive degeneration of nigrostriatal dopamine neurons following intrastriatal terminal lesions with 6-hydroxydopamine: a combine retrograde tracing and immunocytochemical study in the rat. Neuroscience, 59, 401-415.

Schapira, A.H., Cooper, J.M., Dexter, D., Clark, J.B., Jenner, P., Marsden, C.D. (1990). Mitochondrial complex I deficiency in Parkinson's disease. Journal of Neurochemistry, 54, 823–827.

Schapira, A.H.V. (2008a). Mitochondria in the aetiology and pathogenesis of Parkinson's diseae. Lancet Neurology, 7, 97-109.

Schapira, A.H.V. (2008b). Mitochondrial Dysfunction in Neurodegenerative Diseases. Neurochemical Research, 33, 2502-9.

Schnaitman, C., Greenawalt, J.W. (1968). Enzymatic properties of the inner and outer membranes of rat liver mitochondria. Journal of Cell Biology, 38, 158-75.

Sherer, T.B., Betarbet, R., Stout, A.K., Lund, S., Baptista, M., Panov, A.V., Cookson, M.R., Greenamyre, J.T. (2000). An in vitro model of parkinson's disease: linking mitochondrial impairment to altered alpha-synuclein metabolism and oxidative damage. *Journal of Neuroscience*, 22(16), 7006-15.

Simantov, R., Blinder, E., Ratovitski, T., Tauber, M., Gabbay, M., Porat, S. (1996). Dopamine-induced apoptosis in human neuronal cells: inhibition by nucleic acids antisense to the dopamine transporter. *Neuroscience,* 74, 39-50.

Simola, N., Morelli, M., Carta, A.R. (2007) The 6-hydroxydopamine model of Parkinson's disease. *Neurotoxicity Researck*, 11, 151-167.

Sims, N.R. & Anderson, M.F. (2008). Isolation of mitochondria from rat brain using Percoll densitygradient centrifugation. Nature Protocols, 3, 1228-38.

Singleton, A.B., Farrer, M., Johnson, J., Singleton, A., Haque, S., Kachergus, J., Hulihan, M., Peuralinna, T., Dutra, A., Nussbaum, R., Licoln, S., Crawley, A., Hanson, M., Maraganore, D., Adler, C., Cookson, M.R., Muenter, M., Baptista, M., Miller, D., Blancato, J., Hardy, J., Gwinn-Hardy, K. (2003). Alpha-synuclein locus triplication causes Parkinson's disease. *Science*, 302(5646), 841.

Smith, M.P., Cass, W.A. (2007). GDNF reduces oxidative stress in a 6-hydroxydopamine model of Parkinson's disease. *Neuroscience Letters*, 412(3), 259-263.

Sorenson, J.R., Campbell, I.R., Tepper, L.B., Lingg, R.D. (1974). Aluminum in the environment and human health. *Environmental Health Perspectives*, 8, 3–95.

Soto-Otero, R., Méndez-Álvarez, E., Hermida-Ameijeiras, A., Muñoz-Patiño, A.M., Labandeira-Garcia, J.L. (2000). Autoxidation and neurotoxicity of 6-hydroxydopamine in the presence of some antioxidants: potential implication in relation to the pathogenesis of Parkinson's disease. *Journal of Neurochemistry*, 74,1605-1612.

Soto-Otero, R., Méndez-Álvarez, E., Hermida-Ameijeiras, A., López-Real, A.M., Labandeira-García, J.L., (2002). Effects of (-)-nicotine and (-)-cotinine on 6-hydroxydopamine-induced oxidative stress and neurotoxicity: relevance for Parkinson's disease. *Biochemical Pharmacology*, 64, 125-135.

Swegert, C.V., Dave, K.R., Katyare, S.S. (1999). Effect of Aluminium-induced Alzheimer like condition on oxidative stress energy metabolism in rat liver, brain and heart mitochondria. *Mechanisms of Ageing and Development*, 112, 27-42.

Szabadkai, G. & Duchen, M.R. (2008). Mitochondria: The hub of cellular Ca2+ signaling. Physiology, 23, 84-94.

Tang, H.W., Wei, X.M., Zhang, Z.X., Xie, P.Y., Wang, Q.H., Liang, H.R., Pan, Y. (2002). Effect of aluminium on pathology of central nerve system in rats. *Public Health China*, 18,902.

Tatsuta, T. & Langer, T. (2008). Quality control of mitochondria: protection against neurodegeneration and ageing. *EMBO Journal*, 27, 306-314.

Taylor G. A., Moore P. B., Ferrier I. N., Tyrer S. P. and Edwardson J.A. (1998). Gastrointestinal absorption of aluminium and citrate in man. *J.ourna ofl Inorganic Biochemistry*, 69, 165–169.

Tiffany-Castiglioni, E., Saneto, R.P., Proctor, P.H., Perez-Polo, R. (1982). Participation of active oxygen species in 6-hydroxydopamine toxicity to a human neuroblastoma cell line. *Biochemical Pharmacology*, 31, 181-188.

Tipton, I.H. & Cook, M.J. (1963). Trace elements in human tissue. Part II. Adult subjects from the United States. *Health Physiology*, 9, 103–145.

Tonitello, A., Clari, G., Mancon, M., Tognon, G., Zatta, P. (2000). Aluminium as inducer of the mitocondrial permeability transition. *Journal of Biolological Inorganic Chemistry*, 5, 612-623.

Trapp, G.A. (1980). Studies on aluminium interaction with enzymes and proteins-the inhibition of hexokinase. *Neurotoxicology*, 1, 89-100.

Tsunoda, M. & Sharma, R.P. (1999). Altered dopamine turnover in murine hypothalamus after low-dose continuous oral administration of aluminium. *Journal of Trace Elements in Medicine & Biology*, 13(4), 224-31.

Turrens, J.F., Boveris, A. (1980). Generation of superoxide anion by the NADH dehydrogenase of bovine heart mitochondria. *Biochemical Journal*, 191, 421-427.

Van der Walt, J.M., Nicodemus, K.K., Martin, E.R., Scott, W.K., Nance, M.A., Watts, R.L., Hubble, J.P., Haines, J.L., Koller, W.C., Lyons, K., Pahwa, R., Stern, M.B., Colcher, A., Hiner, B.C., Jankovic, J., Ondo, W.G., Allem Jr., F.H., Goetz, C.G., Small, G.W., Mastaglia, F., Stajich, J.M.,cLaurin, A.C., Middelton, L.T., Scott, B.L., Schmechel, D.E., Pericak-Vance, M.A., Vance, J.M. (2003). Mitochondrial Polymorphisms significantly reduce the risk of Parkinson's disease. American Journal of human genetics, 72(4), 804-11.

Valente, E.M., Bentivoglio, A.R., Dixon, P.H., Ferraris, A., Lalongo, T., Frontali, M., Albanese, A., Wood, N.W. (2001). Localization of a novel locus for autosomal recessive early-onset parkinsonism, PARK6, on human chromosome 1p35-p36. *American Journal of Human Genetics*, 68(4), 895-900.

Vercesi, A.E., Kowaltowski, A.J., Grijalba, M.T., Meinicke, A.R., Castilho, R.F. (1997). The role of reactive oxygen species in mitochondrial permeability transition. *Bioscienece Reports*, 17, 43-52.

Walker, V.R., Sutton, R.A., Meirav, O., Sossi, V., Johnson, R., Klein, J., Fink, D., Middleton, R. (1994). Tissue disposition of 26aluminum in rats measured by accelerator mass spectrometry. *Clinical & Investigative Medicine*, 17, 420-425.

Walton, J.R. (2006). Aluminum in hippocampal neurons from humans with Alzheimer's disease. *Neurotoxicology*, 27, 385–394.

Whittaker, V.P. (1968). The Morphology of Fractions of Rat Forebrain Synaptosomes Separated on Continuous Sucrose Density Gradients. *The Biochemical Journal*, 106, 412-7.

Yokel, R.A. & McNamara, P.J. (2001). Aluminium toxicokinetics: an updated minireview. *Pharmacology and Toxicology*, 88, 159–167.

Yokel, R.A. (2002). Aluminum chelation principles and recent advances. *Coordination Chemistry Reviews*, 228, 97–113.

Youle, R.J. & Narendra, D.P. (2011). Mechanisms of mitophagy. *Nature Reviews Molecular Cell Biology*, 12(1), 9-4.

Zack, M. M., & Langston, J. W. (1995). Is Parkinson's Disease a single entity with a single cause? A cautionary note, in Etiology of Parkinson's Disease (Ellenberg J. H., Koller W. C. and Langston J. W., eds), pp 55-63. Marcel Dekker, New York.

Zahodne, L.B., Marsiske, M., Okun, M.S., Bowers, D. (2012). Components of depression in Parkinson's disease. *Journal of Geriatric Psychiatry and Neurology*, 25(3), 131-7.

Zatta, P., Lain, E., Cagnolini, C. (2000). Effects of aluminium on activity of Krebs cycle enzymes and glutamate dehydrogenase in rat brain homogenate. *European Journal of Biochemistry*, 267, 3049-3055.

Zatta, P., Kiss, T., Suwalsky, M., Berthon, G. (2002). Aluminium(III) as a promoter of cellular oxidation. *Coordination Chemistry Reviews*, 228, 271–284.

Zatta, P., Lucchini, R., van Rensburg, S.J., Taylor, A. (2003). The role of metals in neurodegenerative processes: aluminum, manganese, and zinc. *Brain Research Bulletin*, 62, 15–28.

Zhang, S., Fu, J, Zhou, Z (2004). In vitro effect of manganese chloride exposure on reactive oxygen species generation and respiratory chain complexes activities of mitochondria isolated form rat brain. *Toxicology in Vitro*, 18, 71-77.

Anexo

USC
UNIVERSIDADE
DE SANTIAGO
DE COMPOSTELA

Resumen

En los últimos años, el estudio de la mitocondria ha mostrado su relevancia como una organela implicada en el desarrollo y aparición de enfermedades neurodegenerativas como el Alzheimer, la ataxia de Friedreich, la esclerosis lateral amiotrófica y la enfermedad de Parkinson entre otras (Duchen, 2004; Schapira, 2008b; Jenner, 2003; Dauer & Pzerdborsky, 2003). El análisis de muestras post-mortem en pacientes que sufrían la enfermedad de Parkinson, ha puesto de manifiesto que en muchos casos son requisitos para su aparición y desarrollo el descenso en la actividad de los complejos respiratorios, el aumento en la formación de radicales libres y la fluctuación en los parámetros metabólicos cerebrales (Schapira, 2008a; Hattori *et al.*, 1991).

Como hemos destacado en el Capítulo 1, en respuesta a la demanda energética celular, la función metabólica mitocondrial es regulada y regula los estados moleculares redox, los gradientes iónicos, el potencial de membrana mitocondrial y el estado fosforilativo del sistema ATP. Asimismo, la mitocondria es el orgánulo encargado de generar la energía celular por la vía aeróbica, regular el ciclo celular, la apoptosis y el estrés oxidativo (Cadenas, 2004). Debido a ello, cualquier alteración en la función mitocondrial puede poner en peligro la homeostasis celular.

Sin embargo, ¿Cuál es el factor que hace que las poblaciones neuronales implicadas en la enfermedad de Parkinson sean especialmente sensibles a cambios bioenergéticos? Las neuronas afectadas por la aparición de la enfermedad son las poblaciones dopaminérgicas, en especial las pertenecientes a la *substantia nigra*. Estas neuronas presentan una serie de características que las diferencia de otras poblaciones. Entre ellas destaca una arquitectura del árbol axonal especialmente ramificado, la falta de mielinización de sus fibras y un número de sinapsis muy elevado en sus terminaciones. Resulta especialmente relevante el número de sinapsis que presentan las neuronas dopaminérgicas de la *SNpc* en el estriado (~200,000-350,000/neurona), hasta dos órdenes de magnitud superior a otros tipos neuronales (Bolam & Pissadaki, 2012). Estos factores imponen una demanda energética muy elevada, llevando a la célula a un punto próximo al límite bioenergético, lo que puede explicar su especial fragilidad a un desequilibrio bioenergético. Bajo circunstancias normales, no se observa un efecto directo de esta alta demanda sobre la neurona. Sin embargo, cualquier situación que perturbe el equilibrio entre la producción de energía y su demanda, como puede ser una disfunción mitocondrial o una situación de estrés oxidativo, puede inclinar la balanza por encima del límite bioenergético, produciéndose de este modo un exceso en la demanda energética, que no podrá ser cubierto. Un balance de energía negativo pone a la neurona en una situación perjudicial que

incluye, entre otros, un aumento en el estrés oxidativo, la aparición de disfunciones mitocondriales, alteraciones en la renovación proteica y modificaciones en los procesos de autofagia. Bolam & Pissadaki (2012) relacionan todos estos factores con la aparición y el desarrollo de la enfermedad de Parkinson. A su vez, se ha constatado que la edad avanzada es clave para la aparición de la enfermedad. Detrás de este hecho también podemos encontrar la bioenergética cerebral, dado que se ve alterada con la edad. Por lo tanto, el estudio del metabolismo mitocondrial mediante análisis bioenergéticos es relevante para avanzar en el conocimiento de la etiología de esta enfermedad.

La presencia de altas concentraciones de metales en el cerebro es otro factor implicado en la aparición de enfermedades neurodegenerativas. Un estudio previo realizado en nuestro grupo de investigación con un modelo de la enfermedad de Parkinson (Sánchez-Iglesias *et al.*, 2009) ha demostrado que el aluminio promueve el aumento del estrés oxidativo y facilita la muerte neuronal. Sin embargo, no se ha determinado el mecanismo concreto que desencadena la aparición del estrés oxidativo y la posible alteración del metabolismo celular. Nuestras hipótesis consideran que si se producen déficits energéticos por exposición a tóxicos, se dan las condiciones favorables para el desarrollo de la enfermedad. En este marco, la presente Tesis se plantea como un estudio

bioenergético en modelos de la enfermedad de Parkinson con la intención de ahondar en el conocimiento de su etiología.

Aislamiento mitocondrial e influencia de los quelatantes en la respiración

La precisión de los análisis bioenergéticos relacionados con las enfermedades neurodegenerativas han mejorado gracias al desarrollo de electrodos de oxígeno más sensibles que los de tipo Clark, utilizados en los estudios metabólicos clásicos (Gnaiger, 2008). Un ejemplo de ello son los electrodos aplicados en la respirometría de alta resolución. Para poder beneficiarnos de esta mejora de la sensibilidad y detectar pequeños cambios en la tasa de oxígeno, cuando se llevan a cabo estos estudios con mitocondrias aisladas, se requiere un alto grado de conservación en la estructura y en las propiedades fisiológicas. Esto hace que la elección de un protocolo de aislamiento apropiado sea un punto clave en el desarrollo de nuestros estudios bioenergéticos.

La presencia de Ca^{2+} libre durante el aislamiento del orgánulo se ha relacionado con la alteración de sus propiedades (Gunter *et al.*, 2000; Szabadkai & Duchen, 2008). Esto se debe a la capacidad tamponadora de la mitocondria frente al Ca^{2+} libre que, si supera unos límites de concentración, facilita la apertura del poro de

transición (Gunter *et al*., 2000). Por este motivo, dado que durante la homogeneización del tejido se rompen mecánicamente los reservorios celulares de Ca^{2+}, los protocolos de aislamiento publicados añaden quelatantes (p.ej. EDTA y EGTA) en alguna de las etapas del aislamiento. Sin embargo, el rango de concentraciones utilizado, el punto concreto en el que se añaden y el método de aislamiento aplicado varían mucho de unos autores a otros (Berman & Hastings, 1999; Puka-Sundavall *et al.*, 2000; Lesnefsky & Hoppel, 2006; Frezza *et al.*, 2007; Sims & Anderson, 2008; Fernández-Vizarra *et al.*, 2010; Kamboj & Sandhir, 2011).

Por otro lado, para que la fosforilación oxidativa tenga lugar y se establezca de modo correcto un gradiente electroquímico, es imprescindible la existencia de Mg^{2+} en el medio (Panov & Scarpa, 1996). Las propiedades químicas del EDTA y el EGTA varían en cuanto a su capacidad para formar enlaces coordinados con Ca^{2+} y Mg^{2+}. En concreto, el EGTA presenta una menor fuerza de unión al Ca^{2+} que el EDTA, pero no altera la disponibilidad del Mg^{2+}. Si utilizáramos en el medio de respiración quelatantes que capturen Mg^{2+}, la mitocondria no podría realizar la fosforilación oxidativa.

Es por este motivo que únicamente hemos llevado a cabo una variación en las concentraciones de quelatantes utilizados en el medio de aislamiento, y no en el medio de respiración.

Por lo tanto, para obtener un protocolo óptimo que cumpliera con las condiciones necesarias para nuestra investigación, se diseñó en la primera parte de la presente Tesis (Capítulo 4) un estudio que nos permitiera analizar la acción de los quelatantes sobre la estructura y función mitocondrial. Para ello, añadimos un amplio rango de concentraciones de EDTA o EGTA al medio de aislamiento para su posterior estudio bioenergético. Nuestros resultados demostraron que la utilización de EGTA permite que la mitocondria pueda sufrir modificaciones en sus capacidades bioenergéticas durante el aislamiento. Sin embargo, la utilización de EDTA mantiene las capacidades respiratorias del orgánulo y evita alteraciones en el grado de acoplamiento. Este hecho puede deberse al control de la concentración de Ca^{2+} libre ejercida por el quelatante, lo cual evita posibles episodios de permeabilidad transitoria que alteren las capacidades bioenergéticas.

Gracias a nuestro protocolo de aislamiento, nuestras fracciones mitocondriales cumplen con los requisitos mínimos necesarios para llevar a cabo la respirometría de alta resolución. Este hecho queda demostrado con los resultados obtenidos en la valoración de la estructura a través de la microscopía electrónica y de la integridad de los diversos compartimentos mitocondriales mediante el análisis bioquímico de marcadores moleculares. El análisis mediante los marcadores bioquímicos resultó de especial

relevancia para caracterizar la población mitocondrial aislada. En último término, nos permiten identificar la ruptura de la membrana externa, la integridad de la membrana interna, la pureza de la fracción mitocondrial aislada y la posible formación de mitosomas.

Para finalizar, los resultados obtenidos pusieron de manifiesto que las mitocondrias aisladas son funcionales y están altamente conservadas durante 4-5 horas. Por lo tanto, como base para el desarrollo de los posteriores estudios bioenergéticos, establecimos un protocolo de aislamiento mediante centrifugado diferencial basado en la utilización de un tampón de aislamiento con una concentración de 3mM de EDTA.

Estudio bioenergético del modelo para Parkinson por estrés oxidativo con 6-hidroxidopamina

El estrés oxidativo se ha descrito como uno de los principales factores implicados en el desarrollo de la patología de la enfermedad de Parkinson (Jenner, 2003; Halliwell, 2006). Debido a esto, gran parte de los modelos experimentales utilizados para el estudio de la enfermedad se han centrado en este aspecto mediante el uso de neurotoxinas (p.ej. MPTP, 6-hidroxidopamina, paraquat, rotenona, etc.). El modelo más utilizado para estudiar el efecto del estrés oxidativo en encéfalo de rata es la 6-hidroxidopamina, donde se ha

constatado la muerte de las neuronas dopaminérgicas mediante procesos apoptóticos (Biswas *et al.*, 2005; Kulich *et al.*, 2007; Gomez-Lazarro *et al.*, 2008). Se ha descrito que en condiciones fisiológicas, la 6-hidroxidopamina se oxida rápidamente a su correspondiente *p-quinona* en presencia de oxígeno molecular (Soto-Otero *et al.*, 2000). Esta serie de reacciones libera especies reactivas de oxígeno como: el anión radical superóxido ($O_2^{\cdot-}$), el peróxido de hidrógeno (H_2O_2), el radical hidroxilo ($OH^{\cdot}$) y el radical hidroperoxilo ($HO_2^{\cdot}$) (Fig. 5.5) (Graham *et al.*, 1978; Gee & Davidson, 1989; Soto-Otero *et al*., 2000; Méndez-Álvarez *et al*., 2001). A pesar de ello, aún se desconoce el mecanismo preciso por el cual este neurotóxico produce la citotoxicidad.

En la segunda sección de la presente Tesis (Capítulo 5) hemos estudiado la acción de la 6-hidroxidopamina sobre la bioenergética mitocondrial y sobre la supervivencia celular en cultivos de neuroblastoma humano (SH-SY5Y). Además, se ha llevado a cabo un análisis sobre la posible neuroprotección mediante enzimas antioxidantes, tales como la catalasa y la superóxido dismutasa. La elección de estos dos enzimas se debe a que se ha descrito una alteración de su actividad en pacientes de Parkinson, lo que sugiere su posible implicación en el desarrollo de la enfermedad.

Como resultado de este estudio describimos una DL_{50} para la 6-hidroxidopamina de 200nM para las mitocondrias provenientes de encéfalo de rata y de 100µM para los cultivos celulares de neuroblastoma humano. Nuestros resultados muestran que el mecanismo de acción que lleva a estas dosis de letalidad implica el descenso en la actividad de las rutas metabólicas ligadas al complejo I y a una pérdida de actividad enzimática de la ATP*sintasa*. Sin embargo, se ha constatado que a las concentraciones utilizadas de 6-hidroxidopamina, la permeabilidad de la membrana a los protones permanece inalterada. Estos resultados nos muestran que uno de los posibles mecanismos para la neurotoxicidad de la 6-hidroxidopamina es el descenso en la capacidad de las neuronas para generar ATP.

El estudio realizado en presencia de enzimas antioxidantes (catalasa y superóxido dismutasa) nos ha permitido evaluar las diferentes especies reactivas de oxígeno presentes en el mecanismo toxicológico. Ambos sistemas antioxidantes han mostrado la capacidad de proteger a la mitocondria frente al daño inducido por la 6-hidroxidopamina, lo que nos pone de manifiesto que el mecanismo de acción promovido por el neurotóxico se genera a través de especies reactivas de oxígeno.

Por otro lado, nuestros datos muestran una acción neuroprotectora en el modelo con células SH-SY5Y diferente al descrito para las mitocondrias aisladas procedentes de encéfalo de

rata. En concreto, la presencia de superóxido dismutasa protege contra la acción de la 6-hidroxidopamina, mientras que la catalasa promueve la neurotoxicidad si se encuentra a bajas concentraciones. Este efecto puede atribuirse al descenso en la auto-oxidación de la 6-hidroxidopamina por la acción de la catalasa. De este modo, se promueve la captación de la neurotoxina por parte de las neuronas dopaminérgicas y su entrada en la célula, facilitando su acción neurotóxica.

Para finalizar, se evaluaron las rutas bioquímicas que subyacen a la auto-oxidación de la 6-hidroxidopamina (Fig. 5.5) y su diferente toxicidad bajo las condiciones experimentales utilizadas en esta investigación. La acción de la superóxido dismutasa promueve la formación de H_2O_2 a partir del $O_2^{\cdot-}$ y, con ello, la formación de $HO^{\cdot}$ mediante la reacción de Fenton o por oxidación de la 6-hidroxidopamina en ausencia de Fe^{2+}. Esto tendría como consecuencia un descenso en la cinética de formación del $HO_2^{\cdot}$, explicando así su acción neuroprotectora. Por otro lado, la acción enzimática de la catalasa hace que disminuya la concentración de H_2O_2 y por lo tanto la formación del $HO^{\cdot}$. Sin embargo, existe la posibilidad de que la ausencia de H_2O_2 en el medio fomente la auto-oxidación de la 6-hidroxidopamina por la vía del oxígeno molecular (ver Fig. 5.5) y, por lo tanto, que aumente la aparición de $O_2^{\cdot-}$ y por consiguiente la formación de $HO_2^{\cdot}$. La diferencia en la capacidad

neuroprotectora entre ambas enzimas sugiere que los compuestos formados cuando la catalasa está presente tienen una mayor capacidad neurotóxica que los formados en presencia de la superóxido dismutasa. Por ello, nuestro estudio nos permite deducir que la especie con mayor implicación en la inhibición de la respiración mitocondrial es el $O_2^{\cdot-}$, y como consecuencia de ello, también el $HO_2^{\cdot}$ formado a partir de él.

Así, podemos concluir que el mecanismo molecular asociado a la neurotoxicidad de la 6-hidroxidopamina implica una doble acción del neurotóxico. La primera de ellas es la acción directa sobre la ruta metabólica del complejo I y la inhibición de la ATP*sintasa*. La segunda se debe a la formación de especies reactivas de oxígeno, siendo el $O_2^{\cdot-}$ y el $HO_2^{\cdot}$ las de mayor capacidad neurotóxica.

Acción del aluminio sobre la bioenergética mitocondrial

El aluminio (Al^{3+}) es el tercer metal en abundancia en la corteza terrestre. Su estado oxidativo no es variable (+3), por lo que no se ve implicado en reacciones oxidación-reducción. A pesar de ello, es capaz de comportarse como un ácido de Lewis y reaccionar con otros compuestos, entre ellos otros metales, para formar complejos con propiedades variables. Hasta el momento, no se ha descrito ninguna función biológica para este metal y su acumulación

en el cerebro se ha relacionado con la aparición de enfermedades neurológicas. De este modo, la exposición continuada al Al^{3+} se ha relacionado con la incidencia de la enfermedad de Alzheimer (Kawahara & Kato-Negishi, 2011), cambios en el comportamiento (Kumar *et al.*, 2009), problemas de aprendizaje, osteomalacia (Becaria *et al.*, 2002), esclerosis lateral amiotrófica (Shaw & Tomljenovic, 2013) y la enfermedad de Parkinson entre otros (Hirsch *et al.*, 1991; Yasui *et al.*, 1992). Asimismo, estudios neurotoxicológicos recientes muestran la presencia de cantidades elevadas de Al^{3+} en cerebro de pacientes de avanzada edad, lo que puede constituir un riesgo patológico (House *et al*., 2012).

La razón de la toxicidad del Al^{3+} aún no está establecida, pero se ha determinado que el sistema nervioso, debido a que sus células son de carácter post-mitótico, es muy vulnerable a su acción. Además, el cerebro es especialmente sensible a situaciones de estrés oxidativo debido al aumento de radicales libre y al descenso en los sistemas enzimáticos antioxidantes que conlleva la intoxicación con Al^{3+} (Sánchez-Iglesias *et al.*, 2007). Uno de los mecanismos más comunes para la aparición del estrés oxidativo es la formación de complejos Al-anión superóxido. Estos complejos presentan características reactivas superiores al del propio anión superóxido y promueven la formación de peróxido de hidrógeno y radicales

hidroperoxilo. Este efecto contribuye a la oxidación del ambiente molecular inmediato y a la formación de estrés oxidativo.

La mitocondria está altamente implicada en la regulación del estrés oxidativo celular y el aumento en su tasa de formación se halla ligado a alteraciones en sus funciones fisiológicas. Numeroso estudios han destacado que la generación de estrés oxidativo, la liberación de Ca^{2+} desde los reservorios celulares y la perturbación de la mitocondria son etapas importantes en los mecanismos que subyacen a la muerte celular inducida por Al^{3+} (Jonson *et al.*, 2005; Savory *et al.*, 2003; Brenner, 2002; Kumar *et al.*, 2008). Sin embargo, los mecanismos moleculares que tienen lugar en la mitocondria y la alteración en su función metabólica no han sido establecidos con precisión.

En la presente Tesis (Capítulo 6) desarrollamos un estudio bioenergético *in vitro* y en *in vivo* para analizar la acción del Al^{3+} sobre el metabolismo mitocondrial en condiciones de acoplamiento, desacoplamiento y no acoplamiento. Nuestros resultados en los dos modelos estudiados (*in vitro* e *in vivo*) muestran un efecto toxicológico que promueve el desacoplamiento de la respiración mitocondrial y la muerte neuronal.

La acción del metal se hace efectiva principalmente por su acción directa sobre las membranas biológicas. En el año 2000, Tonitello *et al*. describieron la capacidad del Al^{3+} para unirse a la membrana mitocondrial interna y su correlación con la apertura del poro de transición de permeabilidad de la membrana. Acordes con esta acción sobre la membrana, nuestros resultados muestran un aumento en el goteo de protones. Esta acción se expresa como una variación en el índice de acoplamiento L/E y, en condiciones *in vitro*, como la disipación del potencial de membrana. La apertura del poro de transición de permeabilidad de membrana suele estar asociada con procesos de *swelling*. Sin embargo, nuestras micrografías de microscopía electrónica demuestran que no es necesario este proceso para que los parámetros mitocondriales se vean alterados. La diferencia entre el tratamiento *in vitro* e *in vivo* puede atribuirse a una exposición diferencial para ambos modelos. De hecho, las células poseen varios sistemas proteicos (p. ej. ferritina, transferrina, etc.) que pueden actuar como quelatantes naturales y, de este modo, tamponar en la mediad de lo posible la acción tóxica de los metales.

Por otro lado, el análisis de la acción directa del Al^{3+} sobre los complejos respiratorios del sistema de transporte electrónico desveló un descenso en la actividad enzimática de los complejos III y V. A su vez, se observa una especial interacción con la ruta metabólica ligada al complejo II. Otros autores han relacionado esta acción concreta del

Al^{3+} con un aumento en la producción del estrés oxidativo (Mailloux *et al*., 2006; Kumar *et al*., 2008) y a la acción sobre los enzimas que componen el ciclo de los ácidos tricarboxílicos. En nuestro caso, la falta de interacción directa con el complejo II y la inhibición descrita para la respiración no acoplada sugieren que la toxicidad del metal se produce en el ciclo de Krebs, probablemente a nivel de la aconitasa, tal como se han descrito anteriormente Zatta *et al.* (2000).

Por último, describimos un descenso significativo en la tasa de respiración ligada a la fosforilación oxidativa para el modelo *in vitro*, y una tendencia descendente no significativa para la acción del Al^{3+} *in vivo*. Al mismo tiempo, el análisis del índice de control respiratiorio P/E muestra una pérdida de eficiencia en la respiración mitocondrial en ambos modelos. Estos resultados sugieren un descenso en la capacidad de la mitocondria para modular y controlar su respiración desde el sistema fosforilativo. Este hecho es de especial importancia dado que las neuronas dopaminérgicas dependen en gran medida de una buena capacidad bioenergética para dar respuesta a la gran demanda energética que presentan. La pérdida en el grado de modulación implica un descenso en la velocidad de respuesta y, dado que también afecta al grado de acoplamiento, en la cantidad de ATP sintetizado en cada ciclo respiratorio. Este efecto puede facilitar a su vez la aparición de altos niveles de estrés oxidativo, que tendrían una acción directa sobre el sistema de transporte electrónico. Por lo

tanto, si a esto le unimos el descenso en la capacidad del sistema enzimático antioxidante citado en trabajos previos, podemos ver una posible contribución del Al^{3+} a la progresión de desórdenes neurodegenerativos, tales como la enfermedad de Parkinson.

De este modo, podemos concluir que el Al^{3+} afecta a la bioenergética mitocondrial y promueve el desacoplamiento de la organela de un modo dosis dependiente. Nuestros datos sugieren en ambos modelos estudiados una alteración en la ruta metabólica ligada al complejo respiratorio II, un aumento en el goteo de protones y/o electrones y un descenso en la actividad enzimática de los complejos III y V. Al mismo tiempo, nuestro estudio *in vitro* muestra que la acción directa del metal incluye otros mecanismos toxicológicos como una alteración en el potencial de membrana y un descenso de la capacidad respiratoria OXPHOS. Por lo tanto, la falta de eficiencia respiratoria junto al aumento del estrés oxidativo y al descenso en la actividad de los enzimas antioxidantes descritos en un trabajo previo (Sánchez-Iglesias *et al*., 2009), sugieren que el Al^{3+} puede contribuir a la progresión de procesos neurodegenerativos como la enfermedad de Parkinson.